Siloxane supported hydrolysis catalysts

Beckett, Sean

Award date:
2002

Awarding institution:
University of Bath

SILOXANE SUPPORTED HYDROLYSIS CATALYSTS

Submitted by **Sean Beckett**

for the degree of PhD of the University of Bath, 2002

ProQuest LLC
789 East Eisenhower Parkway
P.O. Box 1346
Ann Arbor, MI 48106-1346

Acknowledgements

At last, the final version is written and 6 years of 'gentle reminders' from everyone I know can come to an end. It almost didn't happen, and my sincere thanks must go to Professor Brian Brisdon for enabling me to finish my work off, for the generous support I received during my time at Bath and especially over the last year, even interrupting his retirement.

I could not have done this without the support of those around me, especially Janice. The last year has been one of great change and without her encouragement and understanding I would have missed this opportunity. Also many thanks to my family who have been passing on their reminders through Janice, but who are blissfully unaware of how close I am now to completing this piece of work. It is only because of their support (personal and financial) that I had the opportunity to be able to start these studies.

I mustn't forget my friends, Algie, Geoffrey and Gracie, who finally resorted to bribes to see me finish. To the Schwooordarians and the Mighty Schwooord of Dobber, who have allowed me to advance the science of drinking, giving me sight beyond sight on many occasions. Thanks also go to John, Chris, Dave, Mike and Mike from many years ago in 4 West, 2.10.

Finally, many thanks to all the other academic staff who helped me to produce all the results in this thesis during my time at Bath and Porton Down, especially Dr Nick Blacker, who made sure that I didn't cause any accidents with some rather dangerous chemicals.

ABSTRACT

The stated aim of this DERA funded research project was **"to prepare and characterise polysiloxane bearing transition metal species that may catalyse the decomposition of chemical warfare agents"**.

A general and facile methodology for preparing metallated organofunctional tri- and polymeric siloxanes has been developed. This has been achieved by a two step procedure involving firstly the modification of a range of readily available bi- and tridentate nitrogen-donor ligands, by the addition of either a 1-propenyl or 1-hexenyl chain. In the second step the modified ligands, and a commercially available alkenylated monodentate ligand, were attached to a siloxane backbone via a platinum catalysed hydrosilylation reaction. All new products were characterised by microanalyses and spectroscopic measurements.

The free ligands, alkenylated ligands, and both model and poly-organofunctional siloxanes have been metallated with copper(II) salts. The crystal and molecular structures of two ligand/copper(II) chloride, four alkenylated-ligand/copper(II) chloride, and one alkenylated-ligand/copper(II) nitrate complexes have been determined by single crystal X-ray crystallography, in order to reveal details of the primary coordination sphere around the metal centre. All of the copper(II) chloride adducts are five-coordinate, with those containing bidentate ligands exhibiting chloride bridges. The copper(II) nitrate complex is six-coordinate.

The catalytic activities of several of the copper(II) complexes prepared in this study, for the hydrolytic decomposition of an organophosphate, have been assessed in facilities provided at the Ministry of Defence establishment, Porton Down, during brief visits in the final year of this programme. Copper(II) complexes of

trimethylethylenediamine and its alkenylated analogues were found to be the most active catalysts. Attachment of a copper containing alkenylated ligand to a trisiloxane moiety resulted in little diminution in catalytic activity, and a polymeric siloxane analogue was also catalytically active.

CONTENTS

ABBREVIATIONS

Å	Angstrom
acac	Acetylacetonate
BPY	2,2'-Bipyridine
b.p.	Boiling point
C.I.	Chemical ionisation
d	Doublet
DEFP	Diethyl fluorophosphate
DFP	Diisopropyl fluorophosphate
DMSO	Dimethyl sulphoxide
GA	N,N-dimethylphosphoroamidocyanidate or Tabun
GB	2-Propyl methylphosphonofluoridate or Sarin
GD	3,3-Dimethyl-2-butylmethylphosphonofluoridate or Soman
HD	2,2'-Dichlorodiethyl sulphide or mustard gas
HEPES	N-2-Hydroxyethylpiperazine-N'-2-ethanesulphonic acid
IR	Infra-red
J	Coupling constant (NMR spectroscopy)
m	Multiplet
NBO	3-N-bromo-4,4'-dimethyl-2-oxazolidinone
N.M.R	Nuclear magnetic resonance
NPIPP	4-Nitrophenyl isopropylphenylphosphinate
NPDPP	4-Nitrophenyl diphenyl phosphate
o-	Ortho
p-	Para

PDMS	Poly(dimethylsiloxane)
PNPP	Para-nitrophenyl phosphate
PNPDPP	Para-nitrophenyl diphenyl phosphate
ppm	Parts per million
s	Singlet
$t_{1/2}$	Half-life
t-	Tertiary
TMS	Tetramethylsilane
VX	O-Ethyl S-2-(diisopropylamino)ethylmethylphosphonothiolate

UNMODIFIED LIGANDS

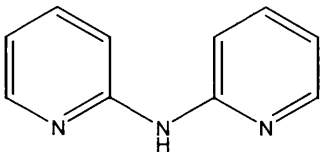

L1

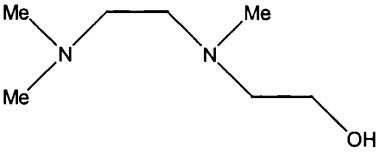

L2

L3

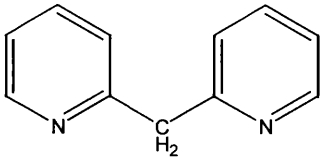

L4

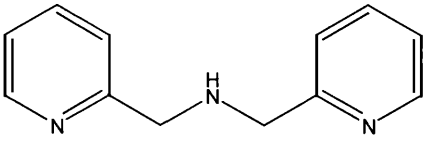

L5

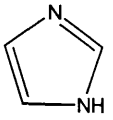

L6

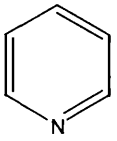

L7

ALKENYLATED LIGANDS

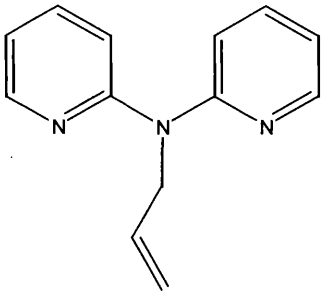

L8

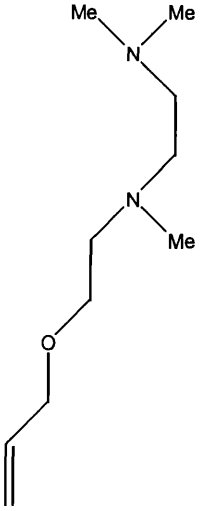

L9

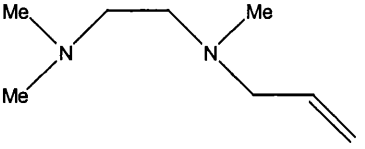

L10

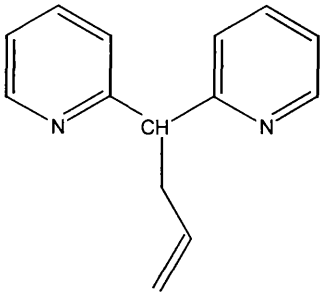

L11

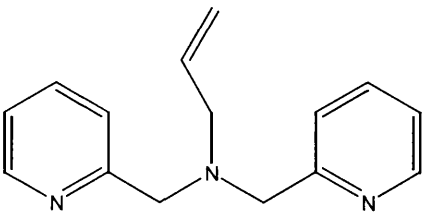

L12

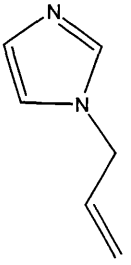

L13

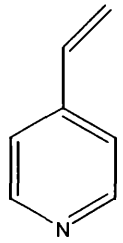

L14

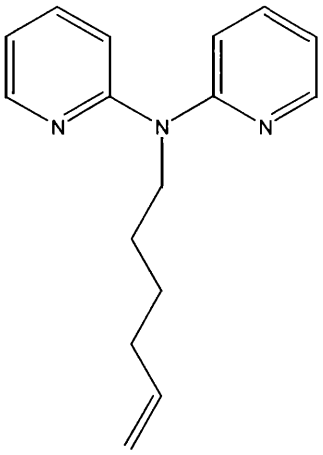

L15

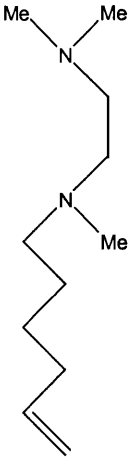

L16

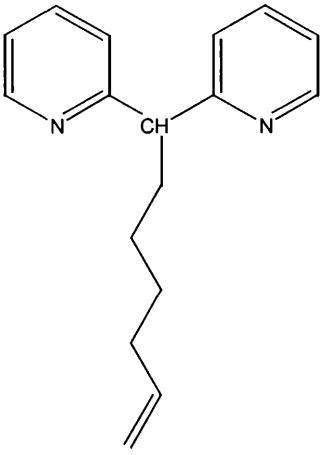

L17

OTHER REACTANT

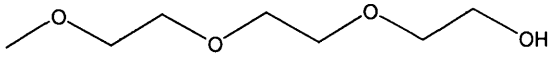

L18

UNMODIFIED TRISILOXANES

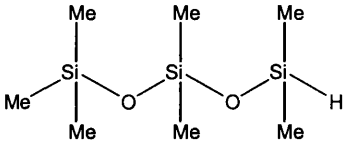

MS1

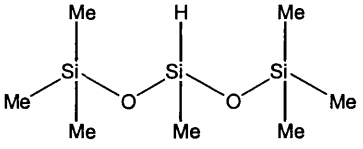

MS2

FUNCTIONALISED TRISILOXANES

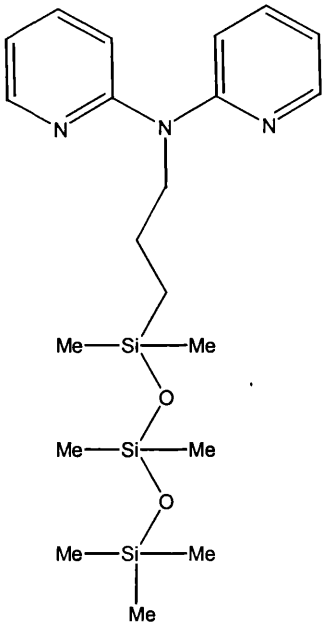

MSL1

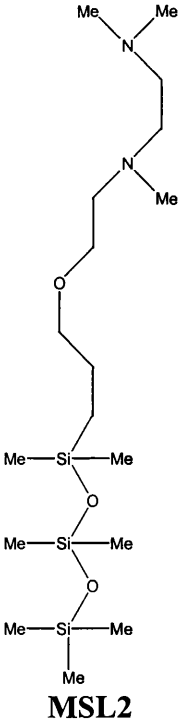

MSL2

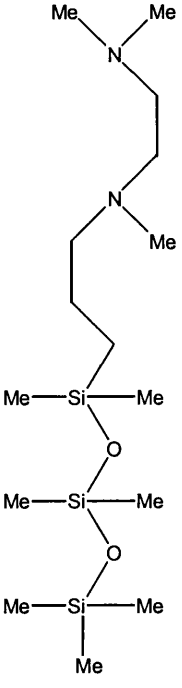

MSL3

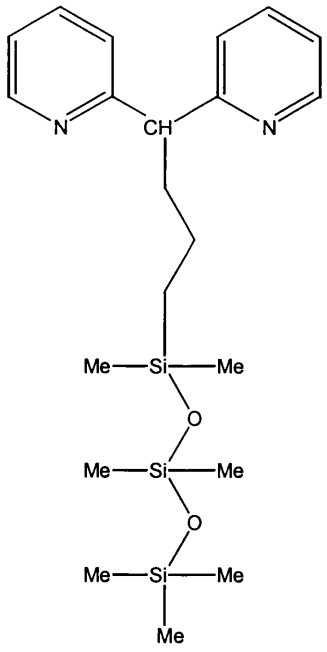

MSL4

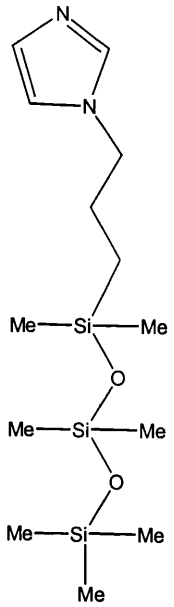

MSL5

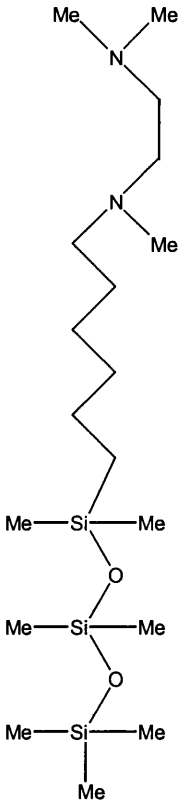

MSL6

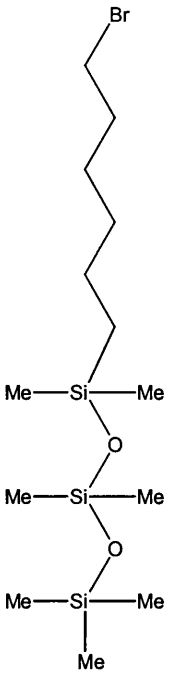

MSL7

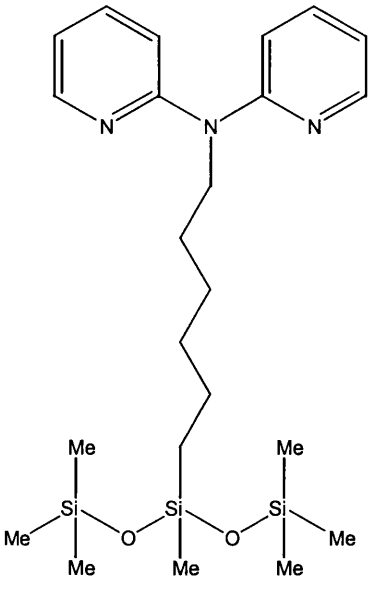

MSL8

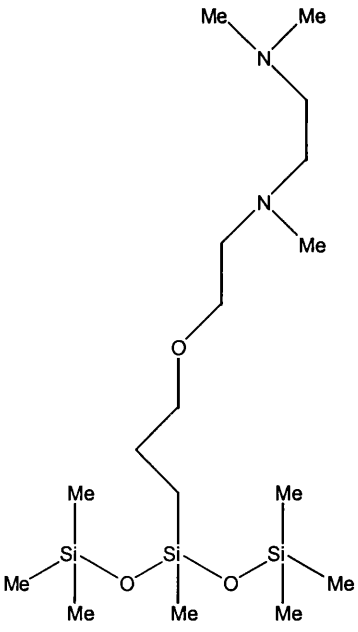

MSL9

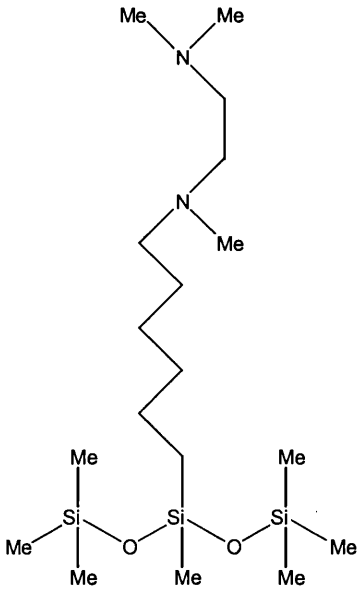

MSL10

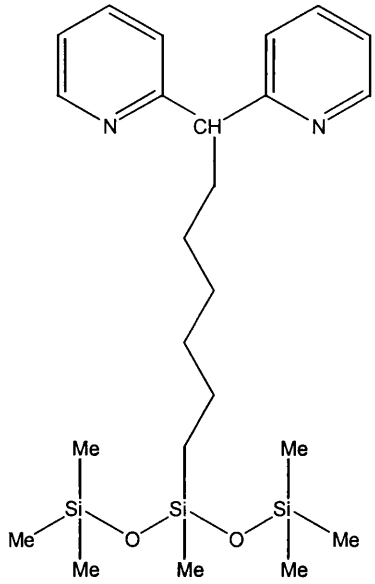

MSL11

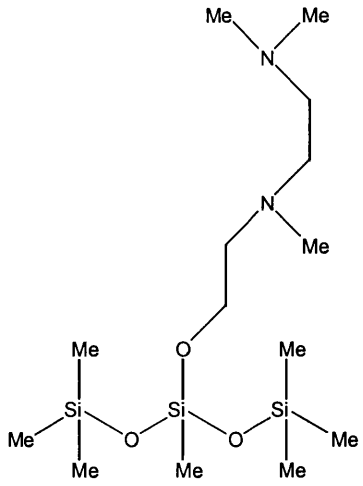

MSL12

UNMODIFIED POLYMERS

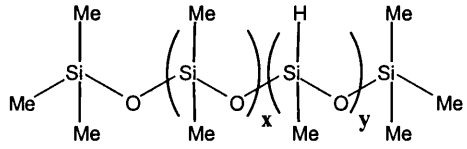

Average values of **x** and **y** for **CP1-3** are below:

CP1 x ~ 172, y ~ 6.7

CP2 x ~ 27.5, y ~ 3.5

CP3 x ~ 19, y ~ 9

FUNCTIONALISED POLYMERS

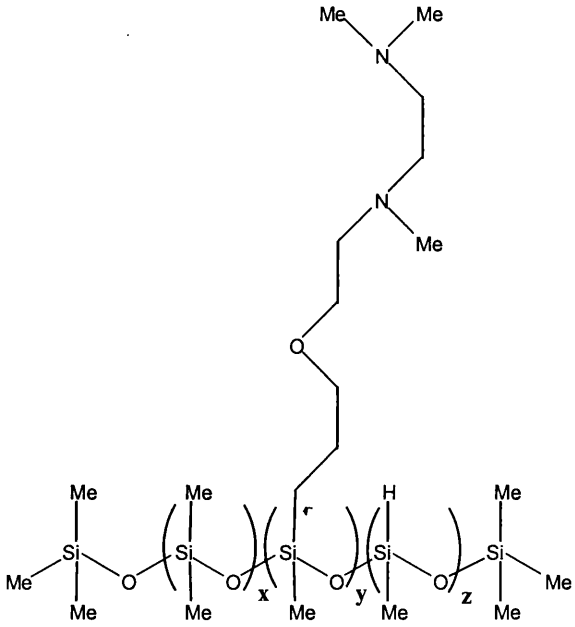

PL1 (x = 172, y = 5, z = 1)
PL3 (x = 27.5, y = 2.6, z = 0.9)

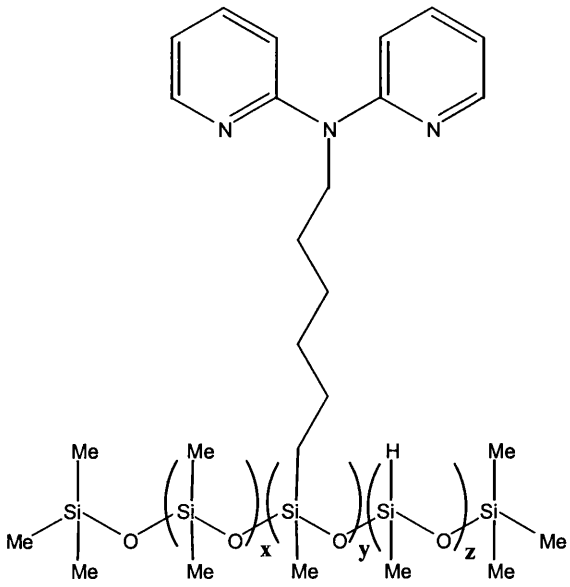

PL2 (x = 172, y = 6.3, z = 0.4)

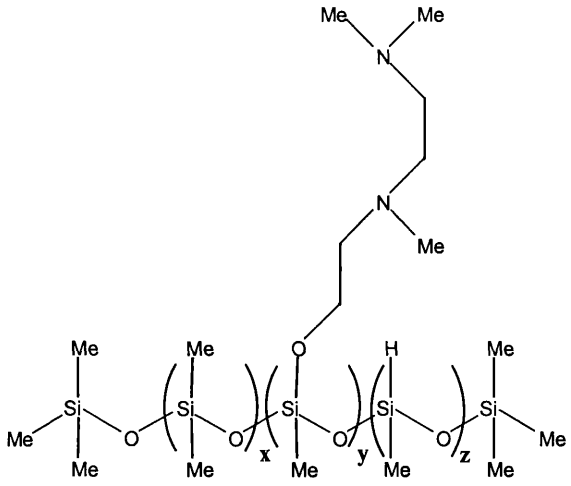

PL4 (x = 27.5, y = 3, z = 0.5)
PL7 (x = 19, y = 4.9, z = 4.1)

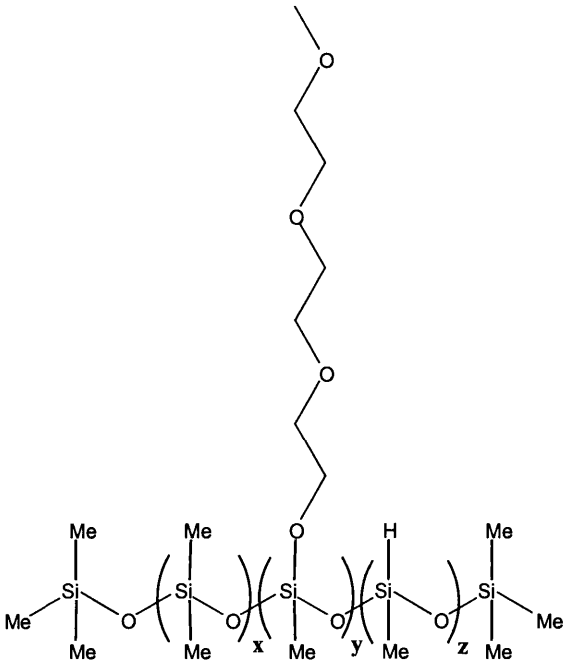

PL5 (x = 27.5, y = 3.2, z = 0.3)
PL8 (x = 19, y = 7.7, z = 1.3)

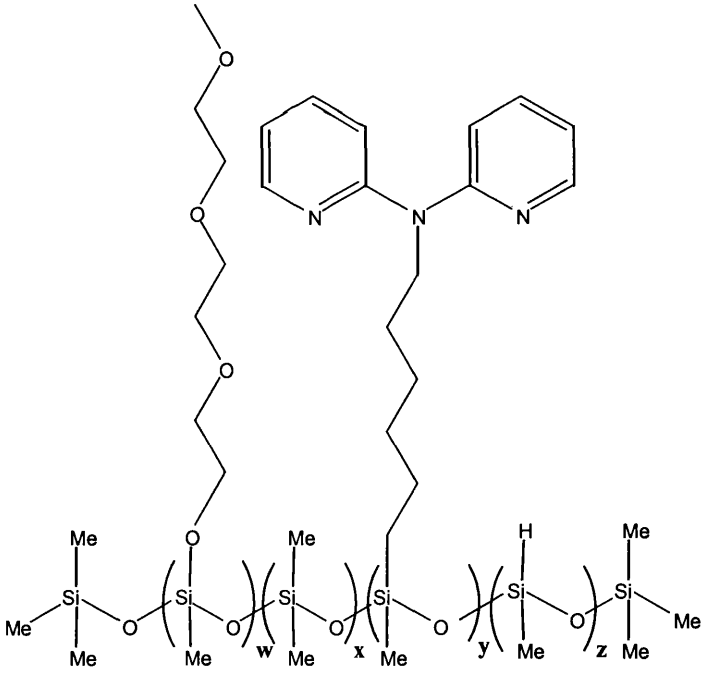

PL6 (w = 1.0, x = 27.5, y = 2.0, z = 0.5)

For Grandma, Mum, Dad, Janice and Karen

and

In memory of Grandad

1. INTRODUCTION

1.1 THE DEVELOPMENT OF CHEMICAL WARFARE AGENTS

Chemical warfare has been used in many forms throughout history, from toxic smokes and caustic solutions[1], to the wide range of nerve agents available to warring parties today. During the 1st World War regular use was made of both chlorine and phosgene to disable the enemy, through the adverse effects of these gases on the respiratory system and the eyes. As with some of the earliest agents, these non-persistent gases were blown away or dissipated in the air fairly quickly. However, protection from inhalation and contact with the eyes was essential.

In 1915, mustard gas (2,2'-dichlorodiethyl sulphide, HD (**1**)) was unleashed with devastating effect upon Allied troops at Ypres[2], whereupon the UK acquired a chemical warfare capability to combat this threat and retaliate in kind. HD is a liquid blistering agent (b.p. 217°C[3]) that attacks the mucous membranes and is lethal at high doses, due to its reactivity with protein and DNA[4]. HD is able to penetrate leather and fabrics, inflicting painful burns on the skin after contact. Unlike the gases used previously, HD is a persistent threat until physically removed or made into a non-toxic compound by chemical reaction (chemical decontamination).

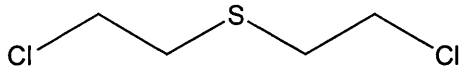

HD (1)

The UK's chemical warfare capability was revived during World War 2 when British forces had access to weapons containing phosgene, HD and a tear gas, bromobenzyl cyanide ($C_6H_5CHBrCN$)[5]. However, neither the Allies nor the Axis Powers deliberately employed chemical weapons during World War 2, despite the accumulation of enormous stockpiles by both sides.

In 1936, during studies of possible pesticides, the German chemist Gerhard Schrader discovered a new chemical warfare agent based on phosphorus(V), Tabun (N,N-dimethylphosphoroamidocyanidate, GA (**2**)). Although never used for fear of retaliation in kind, about 12,000t of GA was produced and stockpiled. Other 'G-Agents', Sarin (2-propyl methylphosphonofluoridate, GB (**3**)) and Soman (3,3-dimethyl-2-butylmethylphosphonofluoridate, GD (**4**)), were also prepared on a much smaller scale. Once this line of research was discovered, the Allied countries, notably the U.K, U.S.A and Russia, extended the range of phosphorus based agents to include O-ethyl S-2-(diisopropylamino)ethylmethylphosphonothiolate, VX (**5**).

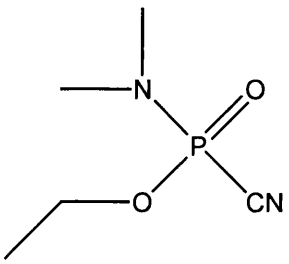

GA (2)

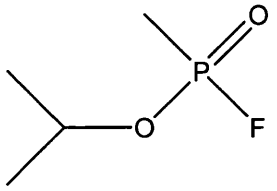

GB (3)

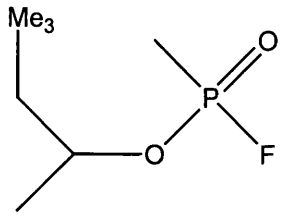

GD (4)

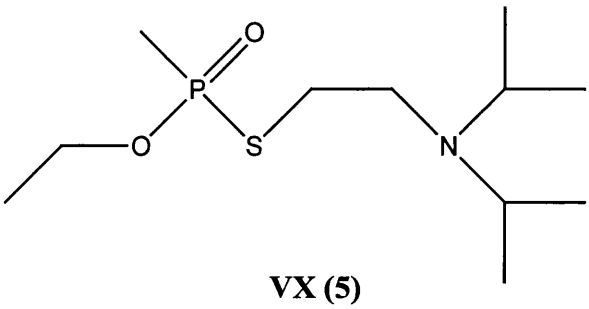

VX (5)

These compounds are orders of magnitude more toxic than HD. Their inhibition of the enzyme acetylcholinesterase causes the respiratory system to fail and death to occur within minutes [6,7].

HD is relatively easy to prepare and huge stockpiles can be quickly built up. The earlier producers of HD favoured the Levinstein Process[8], which involves bubbling dry ethene through sulphur dichloride, allowing the mixture to settle, and distilling the remaining material. More recent production methods involve reaction of thiodiglycol, a relatively common material with a dual use as an ingredient in some inks, with hydrogen chloride[9]. This method, known as the Runcol process, does not result in the solid by-products of the Levinstein Process, and the reactive mixture can be more easily distilled.

$$(HOCH_2CH_2)_2S + 2\,HCl \longrightarrow (ClCH_2CH_2)_2S + 2H_2O$$

A method for the production of GB is from the precursor, methylphosphorus oxodichloride, which is prepared by the reaction of chloromethane with phosphorus trichloride, in the presence of aluminium trichloride and water (Step 1)[10]. Methylphosphorus oxodichloride reacts with hydrogen fluoride to produce an equimolar mixture of methylphosphorus oxodichloride and methylphosphorus oxodifluoride (Step 2), and this mixture is then reacted with isopropyl alcohol to produce GB (Step 3).

Step 1: $CH_3Cl + PCl_3 \longrightarrow CH_3POCl_2 + Cl_2$

Step 2: $CH_3POCl_2 + 2HF \longrightarrow CH_3POCl_2 + CH_3POF_2 + 2HCl$

Step 3: $CH_3POCl_2 + CH_3POF_2 + 2C_3H_7OH \longrightarrow 2C_3H_7O(PO)CH_3F + 2HCl$

Recently large quantities of agents have been declared as being stockpiled in at least two countries, the US (25000 t, the three major agents being HD, GB and VX) and Russia (42000 t)[11].

1.2 DISPOSAL OF CHEMICAL AGENT STOCKPILES

Since the end of the 1st World War, two major treaties have been produced to limit the use, or implement the destruction of chemical weapon stockpiles[12]. The Geneva Protocol, prohibiting use of chemical weapons in warfare, was signed in 1925. Several nations, the United States included, signed with a reservation forswearing only the first use of the weapons and reserved the right to retaliate in kind if chemical weapons were used against them. 132 countries signed the Chemical Weapons Convention in 1993, when it was agreed that all chemical warfare agents should be destroyed within 10 years of ratification of the treaty. 143 States have now ratified the treaty, with the US and Russia, the only open possessors of chemical weapons, ratifying in 1997.

After World War 2 the UK and German stocks of G-agents were, in general, disposed of by incineration or by dumping at sea. By the mid 1950's the UK decided that mustard should also be disposed of by incineration, with the exhaust gases scrubbed by sodium hydroxide solution before being released[13]. In 1982 the US Army also turned to incineration as the preferred method of stockpiled agent disposal[11]. However, in the summer of 1994, in response to public concern and recommendations from the National Research Council, investigations into other methods of disposal were initiated[14].

Therefore other procedures were sought for converting the huge stockpiles of agents into non-toxic products, which could be safely disposed of directly, or post-processed into useful materials. Simultaneously, the means of providing better protection for personnel, who might accidentally or deliberately be exposed to these agents, were sought.

The decontamination of chemical warfare agents is not only a military necessity but is also important in laboratories and pilot plants where chemical agent production, storage and destruction occur. It also has relevance to the detoxification of insecticides and similar residues, which might accumulate in potable water supplies[15].

The agents **1-5** are persistent and hazardous for a considerable time after the initial contamination of a surface. This is especially true for 'thickened' agents, where 5-10% of polymer is mixed with the agent. This type of agent is more viscous and adheres better to a surface than the 'neat' agents, making them more persistent and difficult to remove.

The decontamination of agents can be achieved by either reactive or non-reactive methods. Non-reactive systems involve the physical removal of contaminants including mechanical forces, dissolution, evaporation or absorption. For example, scrubbing, spraying with a soap solution or steam jet, covering with carbonaceous materials or other absorbent powders, such as Fullers Earth. Whilst allowing the agent to be removed from surfaces that are likely to cause an immediate hazard to personnel, the problem is only transferred elsewhere. As a result, reactive systems, which destroy the agent at the site of decontamination, are preferable. Some of the reactive systems that have been developed since 1915 are described in section 1.3 below.

1.3 REACTIVE DECONTAMINANTS

1.3.1 General Decontaminants

The first decontaminants used were bleaching powders, most commonly 2-6 wt % NaOCl in water. As described later in section 1.4, HD reacts with the hypochlorite anion via a series of oxidation and elimination reactions[16], and when used in excess, this oxidant is a very efficient decontaminant for both neat and thickened HD. By 1939, superchlorinated bleaches, such as those in Table 1, were the most commonly used decontaminants[15].

Table 1: Hypochlorite Decontaminants

DECONTAMINANT	COMPOSITION	APPLICATION
Bleach	2-6 wt% NaOCl in water	Skin and equipment
HTH (high test hypochlorite)	$Ca(OCl)Cl + Ca(OCl)_2$ as a solid powder or a 7% aqueous slurry	Equipment and terrain
STB (super tropical bleach)	$Ca(OCl)_2 + CaO$ as a solid powder or as 7, 13, 40, 70 wt% aqueous slurries	Equipment and terrain
Dutch powder	$Ca(OCl)_2 + MgO$	Skin and equipment
ASH (activated solution of hypochlorite)	0.5% $Ca(OCl)_2$ + 0.5% sodium dihydrogen phosphate buffer + 0.05% detergent in water	Skin and equipment
SLASH (self-limiting activated solution of hypochlorite)	0.5% $Ca(OCl)_2$ + 1.0% sodium citrate + 0.2% citrate acid + 0.05% detergent in water	Skin and equipment

Following the discovery of the G-agents, new decontamination processes were required. Bleach solutions, suitable for HD destruction, rapidly detoxify the G-agents through a chlorine-catalysed hydrolysis reaction in aqueous solution[17], and were also found to react with VX[18]. It would appear that a single solution to the general problem of

decontamination had been found. However, alkaline bleach solutions have several important disadvantages:

a) the active chlorine content of most bleach solutions gradually decreases with storage time so that a fresh solution has to be prepared prior to each use;

b) large amounts of bleach are required as a large excess is required;

c) bleaches are corrosive to many surfaces and harmful to personnel;

d) bleach solutions are much less effective at low temperature; and,

e) undesirable and toxic by products are formed with some agents.

Due to these problems, the search for new decontaminants began. Developments initiated in 1951 resulted in the adoption of the new general purpose decontaminant, DS2, in 1960[19]. This is a polar, non-aqueous liquid, composed of 70% diethylenetriamine, 28% ethylene glycol monomethyl ether and 2% sodium hydroxide (w/w). It is a ready to use decontaminant, with long-term storage stability and a large operating temperature range of between –26°C and 52°C. At ambient temperatures it reacts very quickly with all the agents mentioned.

Whilst DS2 is a highly effective decontaminant and non-corrosive to most metal surfaces, damage can be caused to paints, plastics, rubber, and leather goods, and it is also corrosive to skin. In order to minimise these problems, the contact time with paints is kept to 30 minutes and then the surface is washed with water. Personnel handling DS2 are required to wear respirators, eye shields and protective gloves, in order to avoid skin contact and ingestion. It was also found that long exposure to air, or relatively large amounts of water, degrade the decontaminant. Although not perfect, DS2 and STB are still the major general decontaminants used by the military today.

1.3.2 Decontaminants for Skin and Personal Equipment

The search for better personal decontaminants has been ongoing. The first such decontaminants were bleaches, used in dry form, in which the hydrochlorite salt was diluted with an inert solid such as silica. Later, personal decontaminant kits, reputed to be very efficient against thickened GD, were developed in the Soviet Union. These were copied by the Americans to produce the M258 system in 1974, which was updated in the 1980's to the M258A1 and M280 systems[15].

These kits consist of two sealed packets, the first containing a towelette prewetted with a solution of 72% ethanol, 10% phenol, 5% NaOH, 0.2% ammonia, and about 12% water by weight. The other contains a towelette impregnated with chloramine-B, $PhS(O)_2NClNa$, and a sealed glass ampule filled with a solution of 5% $ZnCl_2$, 45% ethanol, and 50% water by weight. Towelette 1 is effective against G-agents and towelette 2, after breaking the ampule and wetting it immediately prior to use, against HD and VX. The two towelettes are used consecutively to wipe the skin and personal items such as masks, hoods, gloves, overboots and weapons.

1.4 THE CHEMISTRY OF DECONTAMINATION

As noted above, both DS2 and STB feature prominently in current decontamination technology, despite their health hazards, and further investigation into new decontaminant systems for personal and battlefield use is required. If a system can be developed that is effective for both uses, then this will be a bonus.

The McKay criterion defines an effective decontamination system as one where destruction of an agent occurs within a cigarette break[20]. Thus the half-life of reaction ($t_{1/2}$) for an effective system, the time taken for the concentration of agent to fall to half the original value, would be expected to be in the order of two minutes or less. When developing a new decontamination procedure, the nature and reactivity of the agents, the effects of the decontaminant on the surroundings, and factors such as cost, ease of production and stability, as well as rate of reaction, are also important considerations.

Many reactions can be used to detoxify agents, but only a few are feasible for practical decontamination. Nucleophilic substitution (including hydrolysis) and oxidation are the two preferred chemical reactions that can detoxify most agents under ambient conditions, as discussed below. These reactions are attractive for conversion to catalytic processes, and they have formed the basis of the investigations reported herein. Electrophilic oxidation is important in the decontamination of agents such as HD and VX, which contain sulphur(II) centres. Hydrolysis is conveniently used for the decontamination of G-agents, but it may also be used for some other agents.

As all the agents have different properties, solubilities and reactivites, the media in which the reaction takes place is important. Aqueous systems are cheap, water is generally readily available and is convenient for mixing with powdered decontaminants. However, not all the common agents are water miscible, especially thickened agents, and micelles and micro-emulsion technologies are being developed to overcome this problem. All common agents are readily soluble in organic solvents, but many of these solvents tend to be expensive and/or flammable and toxic, and they are not readily available under all circumstances. Although homogeneous reactions are preferred, two phase systems,

with the agent as the organic phase and ionic reactants in the aqueous phase, are also worthy of investigation.

The sections below highlight some of the decontamination reactions of agents, with particular respect to oxidation and hydrolysis.

1.4.1 Oxidation Reactions

1.4.1.1 Oxidation of HD

Under oxidising conditions, the sulphur(II) centre in HD may be readily oxidised, initially to the +4 (sulphoxide, (**6**)) state, and then to the +6 (sulphone, (**7**)) state. The sulphoxide of HD is the chemical goal for its oxidative decontamination because of its low toxicity. However, the sulphone is itself a vesicant, although it is less harmful than HD, as it is a solid that poses no vapour hazard[21].

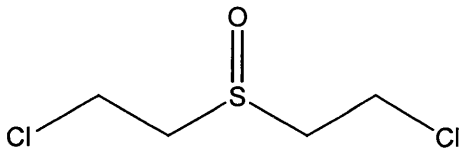

(6)

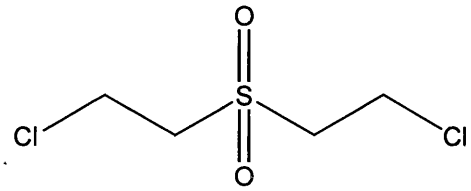

(7)

The first decontaminants, bleaching powders, react very vigorously with HD, both in the neat and thickened form. HD is converted into a series of oxidation and elimination products as shown in the reaction scheme below[16]. The major oxidation products are the sulphoxide and sulphone:

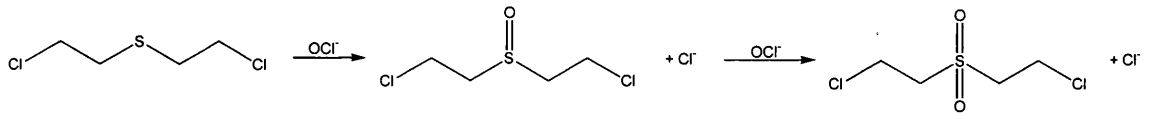

Other oxidation and elimination products include:

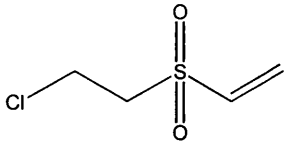

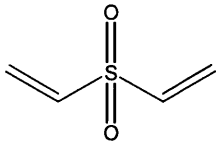

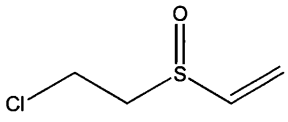

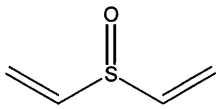

The sulphoxide (**6**) forms first followed by the sulphone (**7**), both of which can undergo HCl elimination in the strongly basic medium to afford the monovinyl and divinyl sulphoxides and sulphones above. This is not an ideal method of decontamination as the oxidation process is difficult to control and results in some sulphone formation.

Although quantitative oxidation of HD to the sulphoxide can be achieved under ambient conditions with some oxidants, e.g. concentrated HNO_3[21], many such reagents are completely unsuitable for practical decontamination purposes.

The oxidative process occurring between HD and the personal decontamination systems M280 and M258A1, mentioned in 1.3.2, are outlined below[22]. Chloramine-B, on the towelette, dissolves in the water added from the ampule and $ZnCl_2$ buffers the solution to between pH5-6. The sulphur in HD is susceptible to electrophilic attack by (**8**), and reacts rapidly to form the sulphimide (**9**), which may be hydrolysed by water to form the sulphoxide. A mixture of the sulphimide and sulphoxide is produced, but no sulphone formation is observed[23]. The reaction is not catalytic and so a new set of reactants is required for each decontamination procedure.

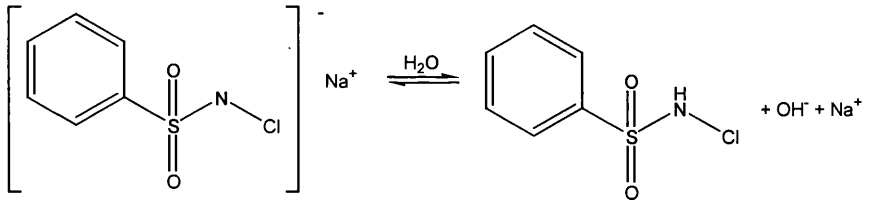

(8)

(9)

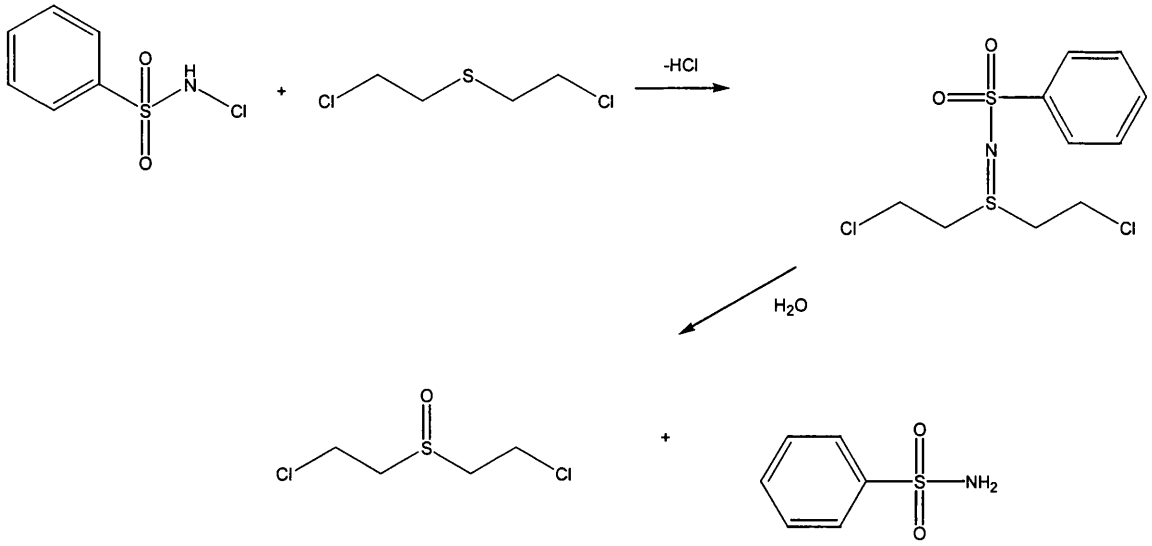

Studies using hydrogen peroxide as oxidant have also been undertaken[24]. The oxidation of HD by this reagent is slow in the absence of a catalyst, but fast in the presence of some metal ions. In a homogeneous solution of 50 vol% *t*-butanol and 0.9M H_2O_2 both oxidation and hydrolysis of HD occurs at the interface, the $t_{1/2}$ for oxidation being 3 hours at 22°C. In a 50/50 mix of water/N-cyclohexyl-2-pyrrolidinone with 1% H_2O_2 at 21°C, HD has a half-life of 6 hours producing the sulphoxide as the only product. However, in the presence of a 0.01M solution of $[VO(acac)_2]$[25,26] in acetonitrile, 1M H_2O_2 completely oxidises $CH_3SCH_2CH_2Cl$ (0.1M) to the sulphoxide in less than two minutes at 20°C. If this result can be replicated with HD, then this system may prove to be very effective for the oxidative decontamination of HD.

The commercial oxidant Oxone is a mixture of three salts, $2KHSO_5/KHSO_4/K_2SO_4$, which produce the active ingredient $[HSO_5]^-$ in aqueous solution[24], and it is a much stronger oxidant than H_2O_2. However, although it first oxidises HD rapidly at the interface to the sulphoxide, the sulphone is the only final product.

The brominating agent NBO (3-N-bromo-4,4'-dimethyl-2-oxazolidinone) **(10)** is effective as a mild oxidising agent, producing the sulphoxide from HD as the predominant product. However this reagent is soluble to the extent of only 0.5% in aqueous solution, which is a major problem for its use[27].

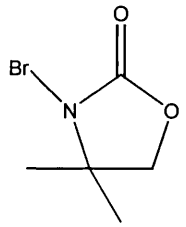

(10)

Other organic oxidising agents, including dimethyl sulphoxide (DMSO), have been found to oxidise HD. The mechanism for DMSO oxidation is shown below[28].

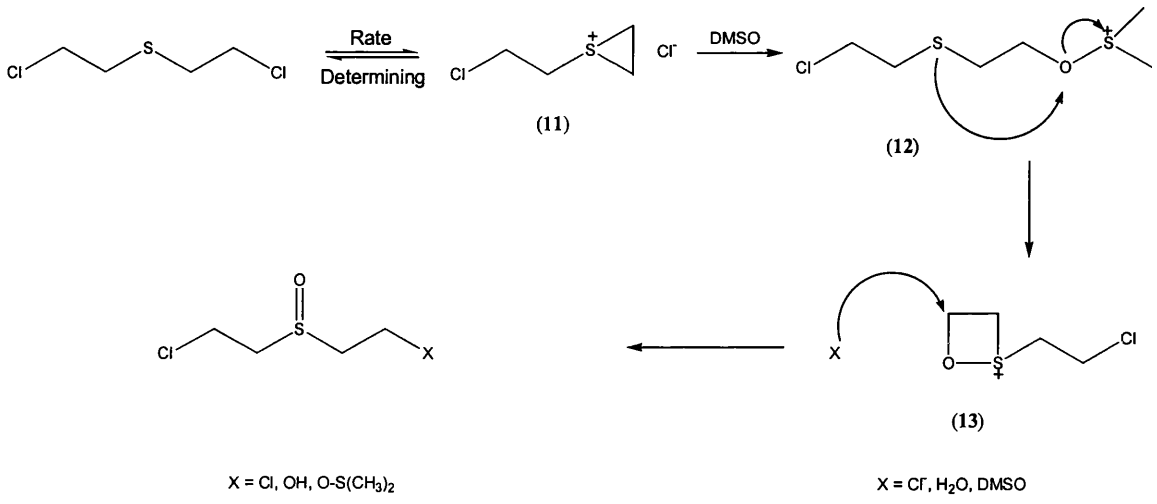

This $S_N1$process is very slow and even after 30 days unreacted HD is present. The first step of the mechanism involves the sulphur(II) centre in HD internally cleaving a C-Cl bond and forming a transient cyclic ethylenesulphonium ion (**11**), which then reacts with DMSO to form **12**. Subsequent sulphur assisted displacement of dimethyl sulphide occurs in **12** to form the four-membered ring in **13**. Due to ring strain this compound reacts rapidly with any nucleophile present, such as chloride ion or water, to produce a sulphoxide. DMSO is effective as an oxidant in this case because of its ability to act as a nucleophile, and the importance of **11** in further nucleophilic substitution reactions is explained in section 1.4.2.

In experiments using half-mustard, an oil in water microemulsion, containing a 2-fold excess of hypochlorite, oxidised the sulphide to the sulphoxide exclusively. It was found that as much as 1 ml of sulphide could be oxidised by 15 ml of microemulsion, and that reaction times were less than 15 seconds[29]. The microemulsion used was stabilised by a long-chain surfactant, and an alcohol cosurfactant (**14**). It is thought that an alkyl hypochlorite forms at the oil / water interface where the cosurfactant is known to reside. Subsequent oxidation then proceeds in or on the droplets as in **14a** below.

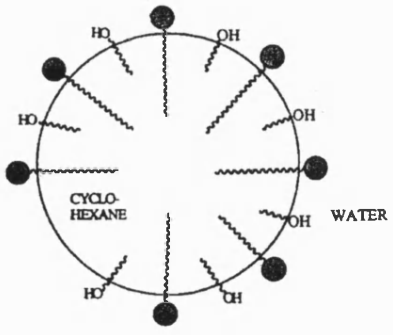

(14)

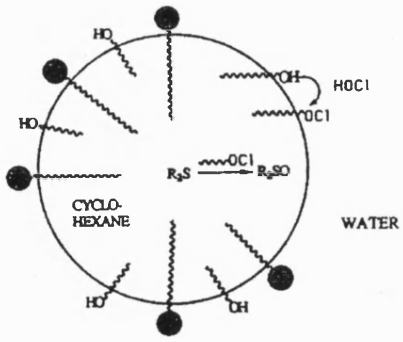

(14a)

The speed of the reaction may be attributable to the huge contact area available, and the system is very promising, as it is cheap, stable and readily available. However, the system is not catalytic, as hypochlorite is consumed stoichiometrically, and larger scale decontamination experiments caused the formation of 32-45% of the sulphone product.

Another attractive approach is to activate the oxygen in the air via a catalytic process in order to decontaminate HD. However, although there are known catalysts for this process, their activity is insufficient at ambient temperature for rapid HD decontamination[30].

1.4.1.2 Oxidation of VX

VX can also be oxidatively detoxified in aqueous solution. However, for a given oxidant, the sulphoxide of VX forms much more slowly than that of HD. Once formed, the VX sulphoxide immediately hydrolyses in the presence of water to form a mixture of phosphonic and sulphonic acids, as the P-S bond is broken under these conditions. However, VX follows a number of reaction paths depending upon the nature of the solvent present. In anhydrous conditions, e.g. organic solvents, the nitrogen of VX is oxidised at a reasonable rate, but oxidation of sulphur is extremely slow[31]. In acidic solution the nitrogen in VX is protonated and is not readily oxidised. In basic and neutral aqueous conditions, oxidation to the stable N-oxide occurs more rapidly than oxidation of sulphur. When only nitrogen is oxidised, VX is not detoxified, as the N-oxide product is also toxic.

Aqueous bleaches are very effective at oxidising VX in acid, neutral or alkaline conditions e.g. pH 4 $t_{1/2}$= 1.2 min, pH10 (calcium hypochlorite) $t_{1/2}$= 1.5 min[18]. However,

the reaction is non-catalytic and the corrosive nature of these oxidants mitigates against them being used on skin or metal. At high pH, VX becomes much less soluble than in neutral or acidic solutions, and so acidic conditions are preferred for its oxidation.

Chloramine-B, within towelette II, is only able to react with VX when the solution is sufficiently acidic so that both reactants are protonated. VX does not react with towelette II because the pH of the solution appears to be increased by VX. It is thought that VX is removed from skin simply by the wiping action and solubilisation in the solution[32]. Studies using an unbuffered aqueous solution of 0.2M chloramine-B showed that about 50% of the 0.01M VX was hydrolysed within a few days, however, this reaction is too slow for practical use[33].

VX is not oxidised by H_2O_2 but reacts rapidly with Oxone[31]. The sulphur is first oxidised followed by hydrolysis at the P-S bond, with a $t_{1/2}$ of 1.9 min in 0.1M Oxone at 21°C. Oxone acts as an acidic buffer (pH1.9) and can dissolve large amounts of VX, due to protonation at nitrogen, and only three equivalents of oxidant are required for one equivalent of VX as illustrated below.

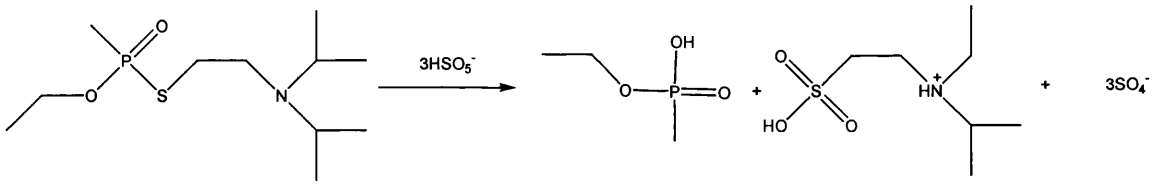

Although this method is better than using bleach, the procedure is still very corrosive and the weight of inert salts present is a major disadvantage in Oxone use. Milder conditions using NBO (**10**) have been attempted at pH 9.6 in a detergent, and $t_{1/2}$ as low as 0.2 min can be obtained. However, 12-18 moles of NBO per 1 mole of VX are needed

for complete reaction, and combined with the low solubility of VX and low stability of the solution this makes for a poor detoxification procedure. The same drawback applies to oxidations using potassium permanganate, in which a 20-fold molar excess is required[35].

Recent studies using ozone as an oxidising agent have been undertaken[36]. VX reacts similarly to a tertiary amine, with oxidation occurring at carbon atoms adjacent to nitrogen. A variety of novel VX derivatives possessing intact P-S bonds is generated, and as such, retain formidable toxicity. Thus, this process is not very suitable for the practical elimination of VX.

1.4.2 Nucleophilic Substitution Reactions

Of the nucleophilic substitution reactions, hydrolysis is the most effective method of decontamination for the G-agents, HD and VX. However, the rate and completeness of this reaction for each agent depends critically upon solubility, structure, pH and temperature.

1.4.2.1 Hydrolysis of G-Agents

GB is completely miscible with water, and GA and GD have solubilities of 7.2 g and 2.1 g per 100 ml of water at 20°C respectively[37]. Hydrolysis under acidic, neutral and basic conditions has been reported, and rate enhancements occur for GB below pH4 and above pH6.5. Thus for GB at 25°C, $t_{1/2}$ = >100 hrs at pH 6.5 and <5 minutes at pH 10[38,39].

The G-agents undergo base-catalysed hydrolysis in water to form their corresponding phosphonic acids and an equivalent of HF (see below for GB) [40]. Hydrolysis is thought to proceed by nucleophilic attack at phosphorus via an S_N2 mechanism[41], and determination

of the rates of hydrolysis at varying pH may be used to indicate any deviations from this simple mechanism[42].

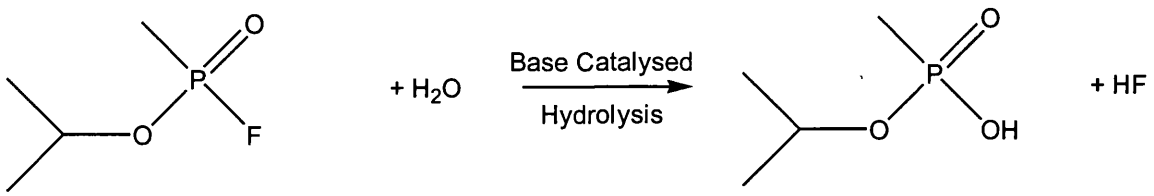

Although further rate enhancements occur under strongly alkaline conditions e.g. NaOH, pH13, $t_{1/2}$= < 1 second, or in the presence of the hypochlorite ion[17], which is found to act as a catalyst for this reaction, these conditions are far too corrosive for use under battlefield conditions.

Slight increases in the rate of hydrolysis were found for two simulants, diisopropyl fluorophosphate (DFP) and diethyl fluorophosphate (DEFP), in the aqueous phase in the presence of imidazole, histidine, pyridine and certain of their derivatives[43]. The half-lives of DFP and DEFP in water are 50 hours and 8 hours respectively. On addition of imidazole, $t_{1/2}$ values are reduced to 2.5 hours and 50 minutes, and with pyridine to >6 hours and 80-100 minutes for mol:mol ratios of 1:7.5 for DFP solutions, and 1:10 for DEFP solutions respectively. More recent studies have shown that the hydrolysis of GB is catalysed by primary amines, particularly ethylenediamine and hydrazine, and that the rate of reaction follows the rate equation below[44].

$$-d[GB]/dt = k_2[GB][amine] + k_{OH}[GB][OH^-]$$

The reactivity shown for mono-protonated 1,2-ethanediamine is thought to arise from intramolecular acid-base catalysis on the bipyramidal transition state of a water co-

ordinated to GB. Concerted proton abstraction from the co-ordinated water by the unprotonated nitrogen of the amine, and hydrogen donation to the equatorial phosphoryl oxygen by the protonated portion occurs, as illustrated below.

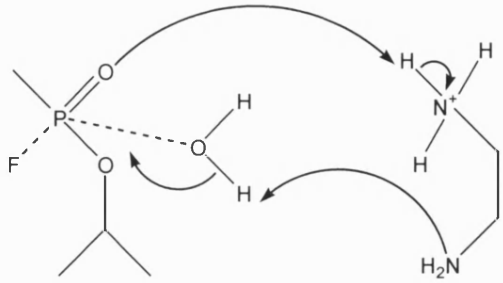

Metal salts, especially those of copper, were found to accelerate the hydrolysis reaction even further. Subsequently copper(II) complexes of various amino acids, imidazole, ethylenediamine and 2,2'-dipyridyl were prepared and shown to be highly active catalysts for the hydrolysis of G-agents[45]. Significant rate enhancements for DFP were noted as shown in Table 2.

Table 2: Comparison of the Rates of Hydrolysis of DFP With Various Catalysts in Bicarbonate-CO_2 Buffer, pH7.6 and at 38°C

COMPLEXING AGENT	HALF-LIFE OF HYDROLYSIS (MINUTES)
No Catalyst	>2500
Ethylenediamine	16
Imidazole	14
2,2'-Dipyridyl	4.5

Many other investigations have taken place into the effect and mechanism of various metal ion systems for the catalytic hydrolysis of nerve agents[46-65], and the most effective catalysts have been shown to be based on copper(II) ions. The observed first order rate coefficient for the catalysed path was determined to follow the relationship given below:

$$k_{obs} = k_2 [OH^-] [M^{n+}] + k_{hyd}$$

where $[M^{n+}]$ = metal ion concentration, $[OH^-]$ = hydroxide ion concentration and k_{hyd} = spontaneous hydrolysis rate coefficient[57]. The mechanism of the copper(II) catalysed hydrolysis of G-agents and their simulants follow a similar scheme to that for the hydrolysis of a phosphate ester by the copper(II) nitrate/2,2'-bipyridine (BPY) complex, as shown below[58-61].

$$[Cu(BPY)(H_2O)_2]^{2+} + OH^- \underset{}{\overset{-H_2O}{\rightleftharpoons}} [Cu(BPY)OH(H_2O)]^+$$

(15) **(16)**

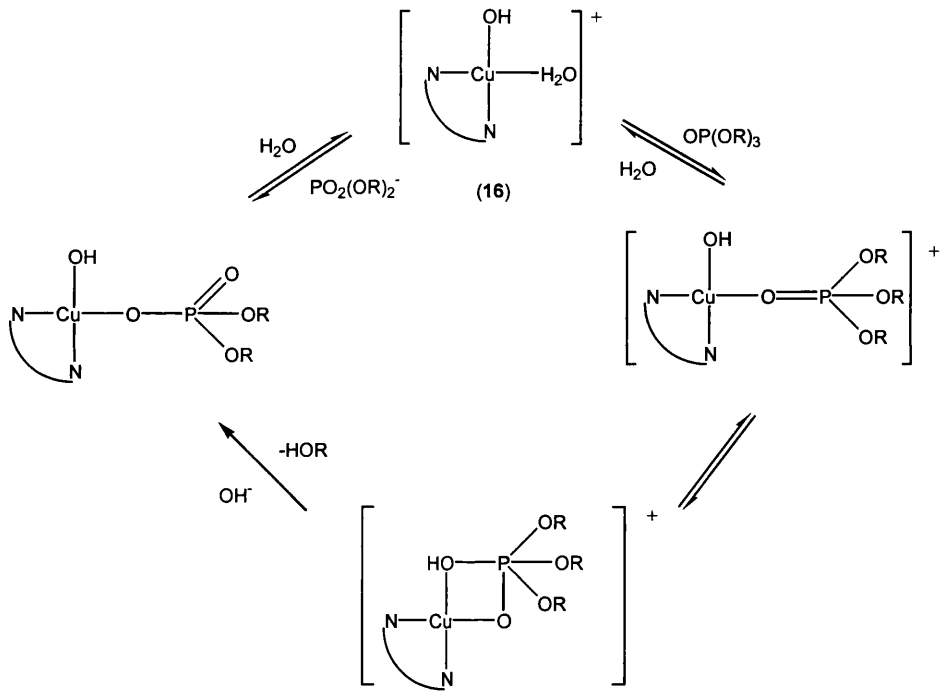

On dissolution of the copper(II) nitrate/2,2'-bipyridine complex in water it forms the diaqua complex (**15**) and is in equilibrium with the active hydroxo-aqua species (**16**), which in turn is in equilibrium with the dihydroxo-bridged dimer (**17**, see below). **17** is inactive in the hydrolysis reaction[62], and reduces the rate of agent hydrolysis as its

concentration in solution increases[63]. The hydrolysis reaction is a 'push-pull' type of mechanism, in which the copper(II) ion polarises the P=O bond by its Lewis acid effect to give a phosphorane intermediate, and the copper(II) then delivers a coordinated hydroxide ion in an intramolecular reaction. Decay to the products then occurs by loss of OR^- here, or F^- when agent is used.

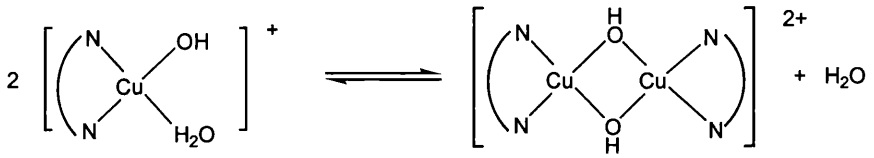

(16) **(17)**

The effects of ligand type and number, overall charge, steric effects, and complex stability have all been investigated in order to define the mechanism of copper(II) catalysed agent hydrolysis and to determine the relative activities of a series of copper(II) complexes[64]. It was found that chelating diamines form the most active copper(II) species, that neutral bidentate ligands induce more activity than tridentate and quadridentate ligands, and that a 1:1 mole ratio of bidentate ligand to copper(II) produces better catalytic activity.

Maximum catalytic activity is favoured for metal chelates in which the copper(II) centre has maximum electropositivity. The more positive the metal ion in the chelate, the greater will be its tendency to hydrolyse to give the active hydroxo-aqua species and its residual affinity for polarising the P=O bond from the phosphate group.

In order to facilitate the process of intramolecular attack of M-OH on a co-ordinated phosphodiester, it has been postulated that two cis-oriented coordination sites must be available on the metal[65]. For tri- and especially quadridentate ligands, this may not be

possible, and so rates are low. Overall, the tetramethylethylenediamine/copper(II) combination has been found to be one of the most effective metal catalysts of this type.

The process of metal ion catalysed hydrolysis has been developed in a number of different directions, in particular through the production of metallomicelles and metal loaded polymers. A long chain chelate of the cupric ion, Atlanta-2 (**18**), has been prepared[66], and when dissolved in water above its critical micelle concentration it forms metallomicelles. In these the Stern region is filled with cupric ion and consists of approximately 40 molecules.

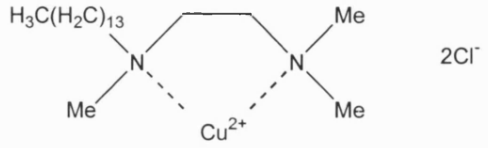

(18)

It is thought that the agent binds to the surface of the micelle where the active species are concentrated. This allows reaction via the mechanism described above, and for GD at 25°C and pH 7, $t_{1/2}$ is 0.85 minutes as opposed to 60 hours without the catalyst.

Similar long chain diamines have been made such that the chain facilitates attachment to a polymer support[20,67], as in the example below (**19**). Polystyrene has been frequently used as the support material and catalytic turnovers were observed for these polymer catalysts, with $t_{1/2}$ = 2.7 minutes at pH8.0 and 25°C for the most active system.

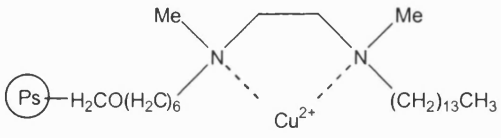

(19)

A long chain near the active centre has been shown to facilitate activity, and a 6-carbon spacer chain accelerates hydrolysis of the GD simulant, 4-nitrophenyl diphenyl phosphate (NPDPP), 8-fold compared to the analogue in which the diamine is attached to the polystyrene support through just one carbon atom. This is an important consideration in respect of the supported catalysts that were to be developed in this project.

There has been a great deal of interest shown in the potential of *o*-iodosobenzoic acid as a catalyst for the hydrolysis of G-agents[68-73]. When solubilised, *o*-iodosobenzoic acid is able to exist in its 1-hydroxy-1,2-benziodoxolin-3-one tautomeric form (**20**) and is in equilibrium with 1-oxido-1,2-benziodoxol-3(1H)-one (**20a**), a strong oxygen nucleophile, which rapidly cleaves esters or phosphates with true catalytic turnover. The hydrolysis reaction with the simulant PNPDPP (*p*-nitrophenyl diphenyl phosphate) is summarised below.

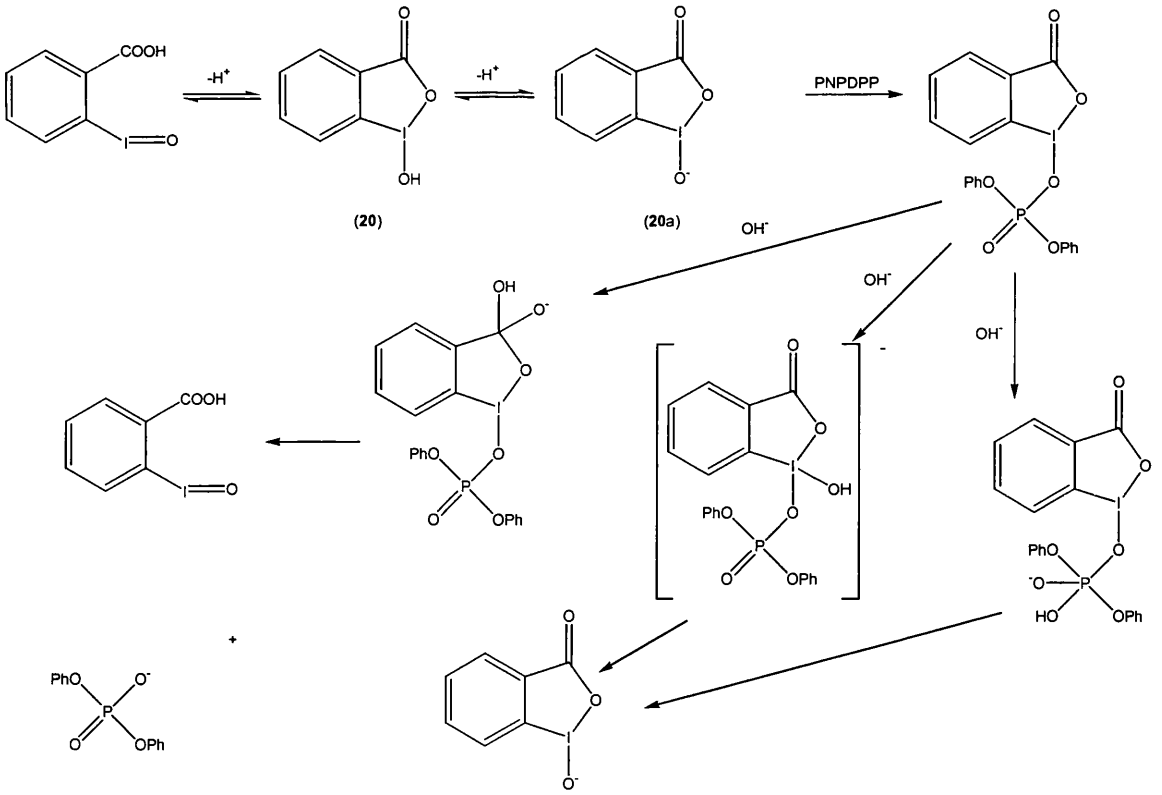

These *o*-iodosobenzoic acid systems are also good catalysts for the hydrolysis of G-agents, reducing $t_{1/2}$ of hydrolysis for GD, GB and GA to minimum values of 29, 51 and 1056 seconds respectively. However, these systems are not effective for VX and are only stoichiometric at sulphur with HD. As *o*-iodosobenzoic acid is relatively easy to modify, micellar[69,70] and solid-supported iodosobenzoate catalysts have also been prepared, including polystyrene and polyacrylate[74], silica[75], titanium dioxide and nylon[76] supported versions, described in 1.5.1.

1.4.2.2 Hydrolysis of HD

HD has a solubility of 0.092 g dm^{-3} in water at 22°C. It dissolves in water at a rate of 1.2 x 10^{-5} g cm^{-2} $minute^{-1}$ [77], and it is the rate of mass transfer that controls the rate of hydrolysis. Although HD has been reported to have $t_{1/2}$ of 5 minutes at 25°C in water, with hydrolysis occurring via an S_N1 mechanism[78], the rate of mass transfer is so slow that HD cannot be detoxified by treatment with water alone. The chemical goal for decontamination by reaction with water is the thiodiglycol (**21**) below.

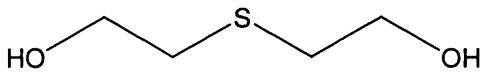

(**21**)

HD will react at the water interface to form a complicated set of products that diffuse rapidly into the bulk water phase, as below[79].

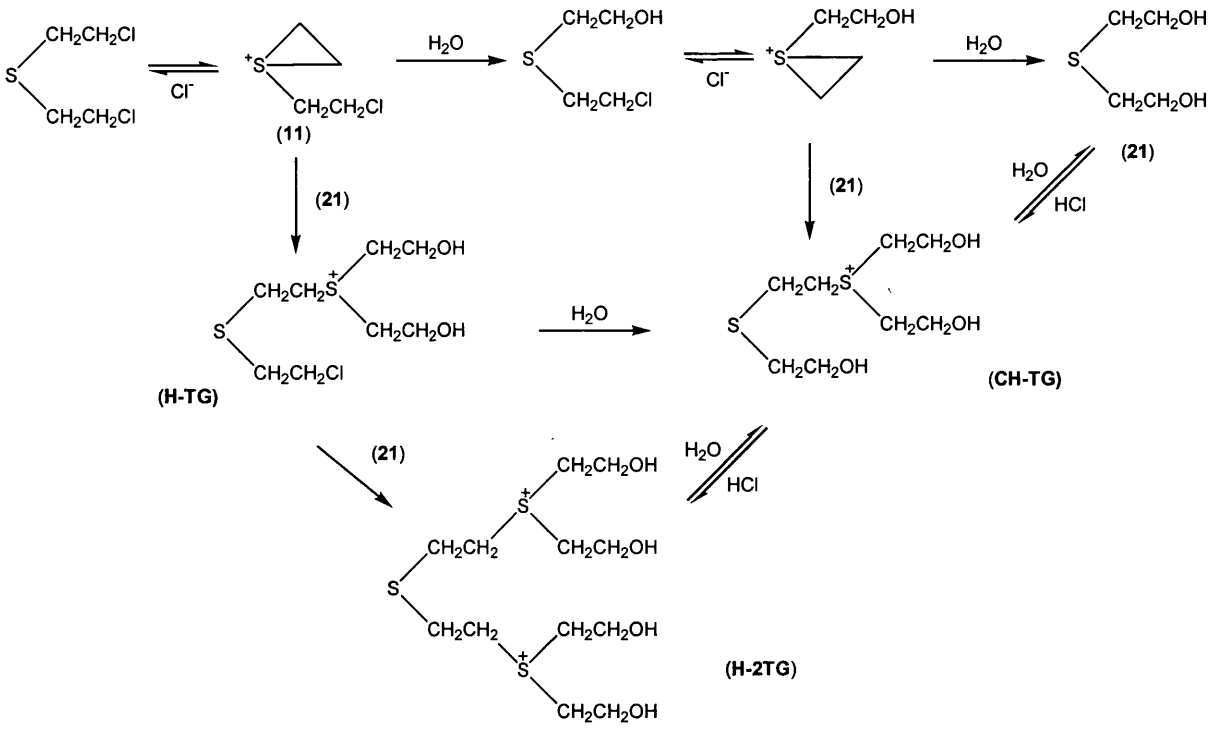

The formation of the ethylenesulphonium ion (**11**) is the key intermediate for the initial stages of the reaction, as it is in the oxidation reaction with DMSO. This ion may then react further to form **21**, which itself reacts further forming the other products. The final products HTG, CH-TG and H-2TG are stable in water but HTG is believed to be quite toxic[80].

The ethylenesulphonium ion also reacts easily with nucleophiles[81], and this forms the basis of other decontamination reactions e.g. with micellar oximes[82]. However, it is noted that the formation of the ethylenesulphonium ion is greatly reduced in less polar solvents, reducing the rate of reaction[83]. Further investigations using detergents, such as alkyl sulphonates, and micelles have shown similar reductions in the rate of reaction[84].

1.4.2.3 Hydrolysis of VX

VX has a solubility of 3% by weight in water and dissolves at a rate of 4 x 10^{-5} g cm^{-3} min^{-1}, with the addition of detergents seemingly ineffective at increasing this rate[77]. The mechanism of hydrolysis is dependent on the pH of the solution, with hydrolysis far slower between pH 7-10, e.g. under the same conditions $t_{1/2}$= 2900 minutes at pH 9.5 and 140 minutes at pH 12. Hydrolysis of the P-S bond is the desired route for decontamination of VX. However, hydrolysis can occur via P-O or C-S bond cleavage, where cleavage of the P-O bond gives a product that is still deadly[85], as below.

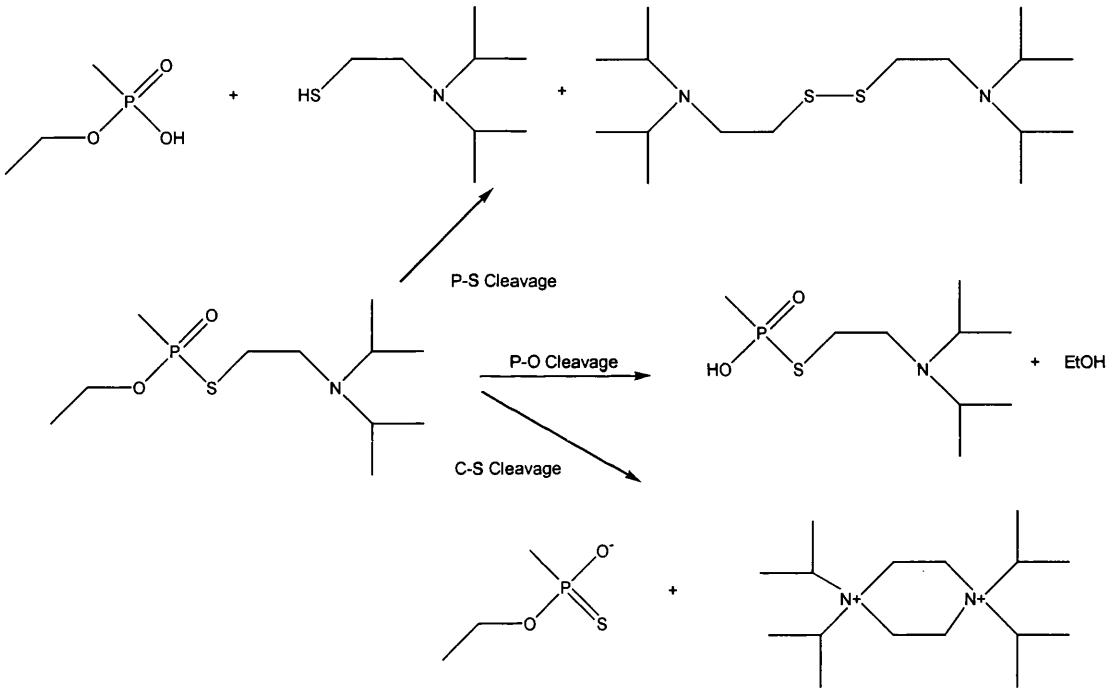

Reaction of excess hydroxide ion (aqueous 0.1 M NaOH) with 0.01 M VX has $t_{1/2}$ of 31 minutes at 22°C, with products from both P-S cleavage (87%) and P-O cleavage (13%)[86]. Speed of reaction, the caustic nature of the solutions used, and the products formed by this process mean that this method cannot be used as a useful decontamination process for VX.

Due to the associated problems of P-O bond cleavage in the above reactions, the peroxyhydrolysis of VX has been studied as an alternative method of decontamination[34]. Peroxyhydrolysis of VX with $[HO_2]^-$ involves quantitative P-S cleavage at rates, 30 to 40 times quicker than that with $[OH]^-$, where $t_{1/2}$ = 0.75 minutes for $[HO_2]^-$ reaction. No evidence of P-O bond cleavage was found. Only the phosphonate and sulphonate ions, and the neutral disulphide are formed as shown below. This is an excellent method for decontamination of VX, however the reaction is not catalytic.

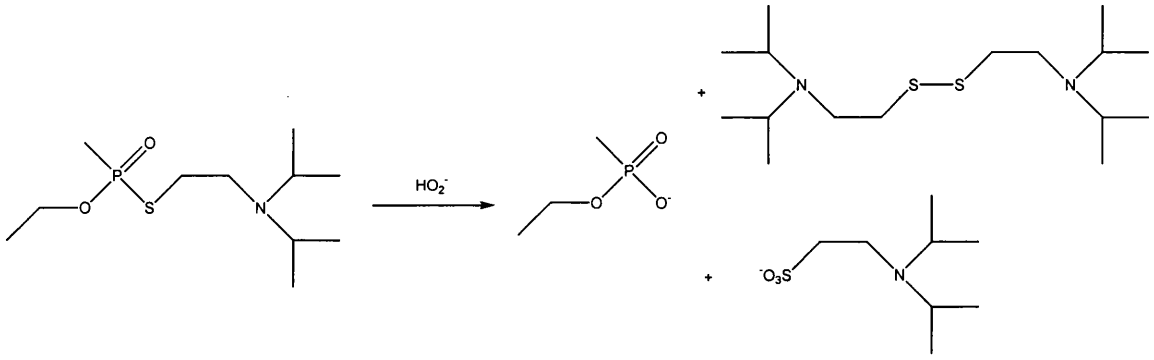

1.4.3 Other Nucleophilic Substitution Reactions

The G-agents have been found to undergo non-catalytic nucleophilic reactions with phenols[87], catechols[88], oximes[89] and hydroxamic acids[90]. Investigations of reactions between HD, VX and micellar oxime systems[35,82] have also been investigated. However, as this study concentrates on catalytic reactions, these will not be discussed here.

1.5 CATALYST SUPPORTS

There are many factors to be taken into consideration when developing new decontaminant systems. The single most important factor is the speed of elimination of

the particular hazard. Further considerations to be taken into account include the cost and ease of production of the decontaminants, their stability, ability to work under a range of climatic conditions, their generality and environmental impact.

The nature of the surface on which the agent may be deposited is also a major consideration. Variables such as the surface contamination density, surface porosity and type must be taken into account. There must be enough decontaminant to eliminate the entire hazard, it must be able to penetrate to where the agent exists, and most importantly the decontaminant must be non-corrosive, so as not to damage the surface.

Most of the systems mentioned earlier in this chapter need a liquid phase in which to react. This will require the transport of large amounts of liquid under field conditions. An ideal decontaminant is one which can be carried and applied to the surface easily, and which uses the minimum of additional solvent to decontaminate all available agents. A catalyst system, which can be attached to a surface to present a preventative shield, is the most desirable therefore, as it would still be effective after the initial use and does not need to be reapplied. Catalytically active species have been incorporated onto silica and also polystyrene supports, for example, because solid decontaminants are easy to handle, potentially fast and efficient, and lend themselves to continuous recycling.

1.5.1 Existing Support / Catalyst Systems

As described above, *o*-iodosobenzoic acid derivatives are active in the decontamination of some agents whilst solubilised in aqueous micellar solutions. Analogues have been attached to polystyrene polymers via quaternary ammonium ion extender units[74].

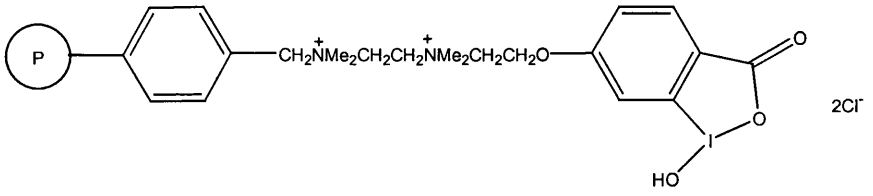

These materials have been found to be active against GD. However, these functional polymers are not easy to prepare, nor are they compatible with the normal aqueous conditions used for agent decontamination.

In contrast, silica based *o*-iodosobenzoic acid catalysts are more polar, wettable, cheaper and easier to prepare via silylation of silica's surface hydroxy groups[75,91].

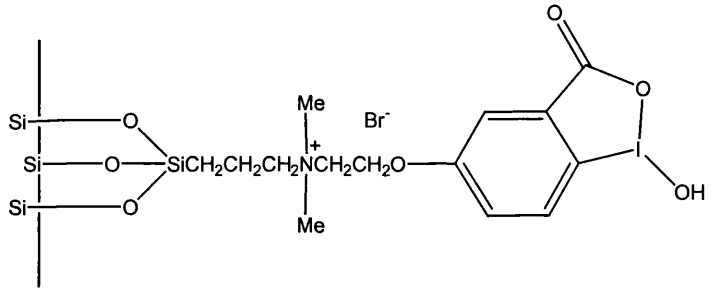

This reagent behaves as a true catalyst turning over in the presence of excess simulant, PNPDPP. It is very active against GD, where $t_{1/2}$ = 4.2 minutes in 0.05M pH8 phosphate buffer, with 5 mmol of GD and 100 mg of supported catalyst. Its activity is about 4 times greater than an analogous polystyrene catalyst and compares to a $t_{1/2}$ of 67 minutes for the simulant in the buffer alone.

This basic idea may be extended to produce a catalytically active coating that can be applied to a surface as a preventative measure. Coatings can be incorporated into appropriate paints, and applied directly onto the surface of the item to be protected. They will also fill the pores and cracks where agents might otherwise not be deactivated.

o-Iodosobenzoic acid reagents have also been immobilised on titanium dioxide (**22**), an important constituent of various paints, and nylon (**23**), a principal element of synthetic fabrics used for clothing[76].

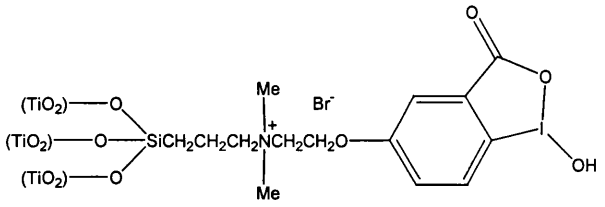

(**22**)

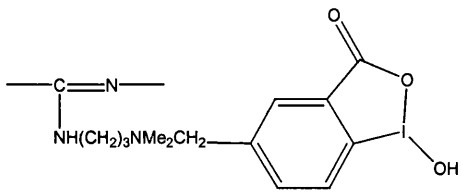

(**23**)

Both reagents are good catalysts for cleavage of the simulant PNPDPP under heterogeneous aqueous conditions at pH8, exhibit turnover capability, and are true catalysts. These catalysts may be washed with buffer, dried and recycled at least four times with little or no loss in their activity.

Polymer attachment has been extended to incorporate the active copper(II)/ligand used in the metallomicellular decontamination reactions described in section 1.4.2.1. Polystyrene polymers incorporating long hydrocarbon chains terminated with an active copper(II)/ethylenediamine derivative have been prepared as outlined below[20].

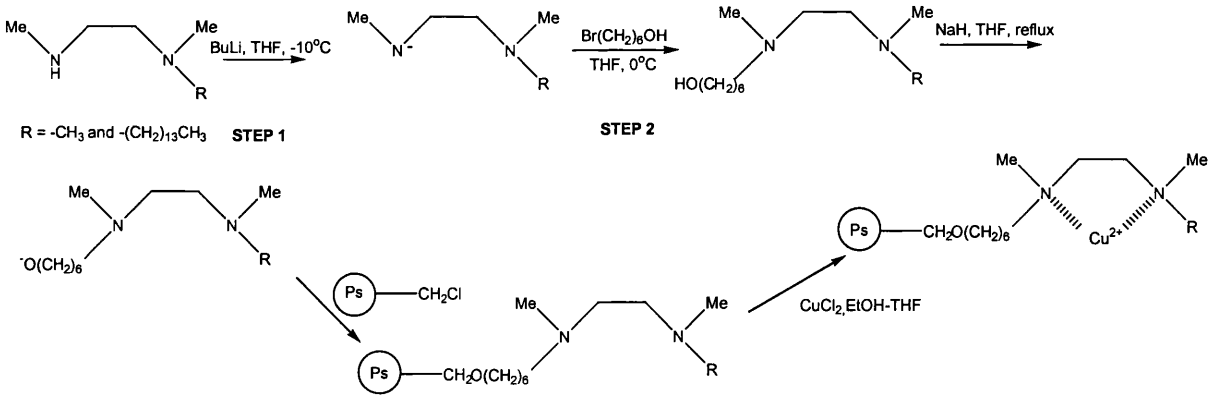

The spacer chain linking the amine to the polystyrene can be varied depending upon the length of the alkyl chain, attached to the alcohol functional group, in step 2. The deprotonated amine, formed by step 1, can also be added directly to the polystyrene support to minimise the chain length. However, it has been shown that a longer spacer chain between support and active metallated amine centre has a positive effect on the rate of hydrolysis as described in section 1.4.2.1[20].

These metallated polymers accelerate the rate of hydrolysis of GD and some simulants. For example the hydrolysis of the simulant NPIPP proceeds 1460 times faster than in the absence of the polymer. It is difficult to compare heterogeneous reactions with the homogeneous metallomicelle catalysed reactions, but if it is assumed that the entire polymer generates an equivalent copper(II) concentration to that in an equivalent amount of the metallomicelle system, the former does not quite achieve the rates obtainable by the latter. However, the solid-state nature of polymeric catalysts permits catalyst removal by filtration, agent decontamination within a flow reactor, and other options unavailable for water soluble catalysts.

Another way of preparing polymer-supported systems is to polymerise a monomeric unit already bearing the desired active group, in order to create a less random polymer. However, only a small number of groups may end up on the polymer surface, the others being effectively buried, so seriously impairing the chemical activity of the polymer. This is a major problem for insoluble polymers lacking porosity. As a result, a synthesis based on the polymerisation of a 'water pool' system[92] has been developed as below. After polymerisation of the product from the procedure below, high surface area polystyrenes, in which most of the reactive sites are on the polymer surface, are produced[67].

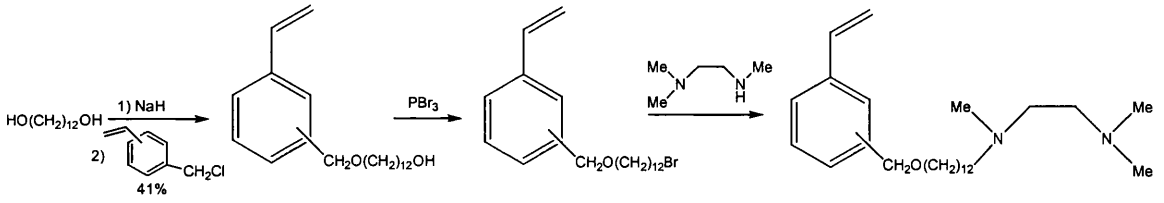

The total content of amine in the resulting polymers may be determined by total nitrogen analysis, and the fraction of amine at the surface can be measured by the polymer's ability to complex copper(II) ions from solution. It was found using the procedure above that 100% amine incorporation occurred, and that after polymerisation some 89% of the diamine groups were exposed at the surface of the polymer. At pH8 and 25°C, an amount of polymer containing 2.5 x 10^{-5} M of copper(II), hydrolysed 2.5 x 10^{-4} M of phosphate ester in aqueous solution with $t_{1/2}$ = 2.5 hours[67].

In more recent studies a range of polymer supported bidentate amine copper(II) complexes has been prepared[93]. These include linear styrene, acrylate and methacrylate polymer structures, and crosslinked resins derived from vinylbenzyl chloride, glycidyl methacrylate and methacrylic acid. Hydrogels based on hydroxyethyl methacrylate, hydroxyethyl acrylate and hydroxypropyl acrylate, each copolymerised with a diamine containing monomer, have also been prepared. All the polymer supported copper(II) complexes showed good catalytic activity, relative to the rate of uncatalysed hydrolysis reactions, based on the measured half-lives for the hydrolysis of GB. The linear polymethacrylate based catalysts were identified as the most active species, where $t_{1/2}$ = 2.6 and 3.2 minutes for the copper(II) chloride and nitrate species respectively.

These examples prove that the addition of a support does not stop the catalyst's ability to promote hydrolysis of agents. The supports also add an extra dimension to the catalysts

in that they can facilitate attachment to a surface, be removed and re-used and, subject to the chemistry of the ligand, allow specific functionality to be controlled and manipulated to suit requirements.

1.5.2 Siloxanes As Catalyst Supports

From many points of view, siloxanes containing the $-[SiR_2(O)]_n-$ repeat unit provide an ideal backbone or support for this type of use:

i) they are relatively cheap and commercially available;

ii) the basic polymers are chemically inert, non-toxic, and have good thermal stabilities;

iii) they are easily functionalised with a wide range of side arm substituents that can be used as property modifiers for use in new applications;

iv) they are highly permeable to gases and vapours;

v) polymers can be prepared in forms as diverse as mobile hydrophobic fluids through to thin, cross-linked elastomeric films that can be immobilised on many surfaces, including natural fibres and inorganic solids; and,

vi) a variety of additives may be incorporated in the polymer in order to improve its performance.

One reason for this unique combination of properties can be traced to the great strength of the Si-O bond, *typically* 480 kJ mol^{-1} according to Emsley[94], which demonstrates the high affinity of silicon for oxygen. Also, the Si-O skeletal bond has a bond length of 1.64Å, whereas the C-C single bond present in most organic homopolymers has a bond length of 1.53Å. The longer Si-O bond tends to reduce steric

hindrance between substituents, although this is partly negated by the larger size of Si compared to C, but not completely. Other reasons include the great flexibility of the Si-O-Si linkage and the very low rotational energy of the Si-C bond. The Si-O-Si bond angle of approximately 143° is much more open than the usual tetrahedral bonding occurring in C-O-C systems. In addition, this bond angle can be greatly deformed without significant loss of bond energy[95].

This combination of properties has a profound effect on the melting point of the polymer (T_m), and poly(dimethylsiloxane), PDMS, has a very low T_m of –40°C. The more flexible a chain, the more it can be cooled before the chains lose their flexibility and mobility. As a result organosiloxanes generally have low glass transition temperatures, for example T_g for PDMS ca –125°C, and so PDMS can be exposed to very low temperatures and not become brittle[96].

Also important in determining T_g is the mobility and size of the side chains attached to the siloxane backbone. Large side groups or polar interactions between side groups will cause the groups to repel or attract each other, so lowering the mobility of the groups and hence increasing T_g. For example the addition of a phenyl side groups increases T_g to –86°C for $(PhSiMeO)_n$ and *ca* 0°C for $(Ph_2SiO)_n$. Variation in the groups can be used as a means of controlling the flexibility of the polymer chains, and thus the physical properties of the materials as required for a large number of uses[97,98].

1.5.3 Preparation of Organofunctional Siloxanes

The simplest and most readily available polymer is polydimethylsiloxane, $Me_3Si(SiMe_2(O))_nOSiMe_2$. Various methods may be used to incorporate a given mole%

of active side-arm substituents onto the siloxane backbone, and produce organofunctional siloxanes of the type, $Me_3SiO(Me_2SiO)_x(MeRSiO)_ySiMe_3$. These methods are exemplified in the sections below.

1.5.3.1 Direct Modification of the Si-Me Group of PDMS

This method is not widely used for the production of organosiloxanes, as the Si-Me group of PDMS is relatively unreactive. The reagents needed to induce reactivity in this group generally cleave a Si-O bond, rather than removing a proton from a Si-Me group, to produce the required intermediate. However, it has been reported that *t*-butyl lithium deprotonates one of the Si-Me groups of hexamethyldisiloxane, and the resultant product reacts with Cp_2ZrCl_2, where Cp = cyclopentadienyl, and Cp^*ZrCl_3, where Cp* = pentamethylcyclopentadienyl, to produce the functionalised siloxanes $Cp_2Zr(CH_2SiMe_2OSiMe_3)_2$ and $Cp^*ZrCl_2(CH_2SiMe_2OSiMe_3)_2$[99], which may prove useful for further synthetic elaboration.

1.5.3.2 Ring Opening Polymerisation

This method involves ring opening copolymerisation of an organofunctional monomer with a cyclodimethylsiloxane ring and a chain terminating agent such as hexamethyl disiloxane[100]. A suitable organofunctional dihalosilane is hydrolysed to form siloxane prepolymers consisting of linear and cyclic materials, which are combined with cyclic dimethylsiloxanes and an end-blocker as illustrated below. The process typically utilises strongly acidic or basic catalysts, which open the cyclic monomers and redistribute the siloxane bonds[101].

$$m(X_2SiMeR) \xrightarrow{H_2O} (MeRSiO)_m + 2mHX$$

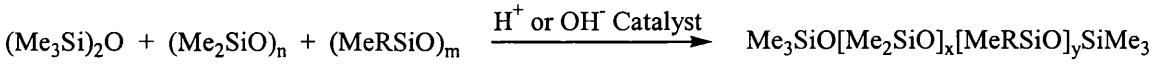

Acid catalysed siloxane polymerisation can be achieved using proton or Lewis acids. The mechanism for this process is described below and starts with the protonation of the oxygen of the highly polar Si-O-Si bond, which subsequently undergoes scission.

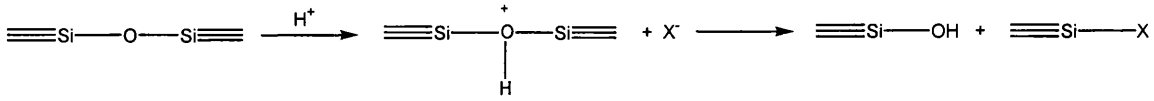

Condensation reactions then reverse the scission by forming new siloxane bonds. This whole process occurs many times to form the final products. The driving force for this reaction is the change in entropy, as the linear polymer has a higher degree of molecular freedom than that of the ring compound. Without the addition of the chain terminators, polysiloxanes with Si-OH and Si-X terminal end groups are formed.

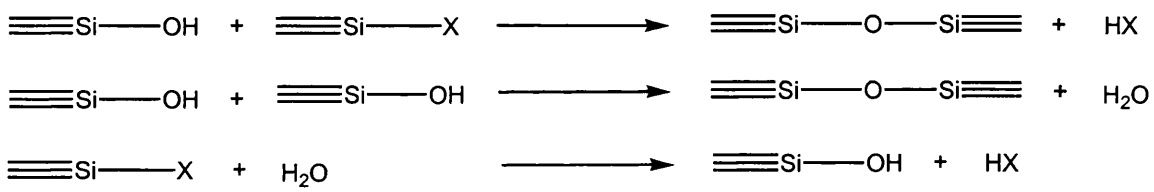

A further reaction may take place to reorganise the siloxane chains. The siloxane oxygen of a non-protonated molecule adds nucleophilically to a protonated species followed by scission and re-formation of Si-O-Si linkages.

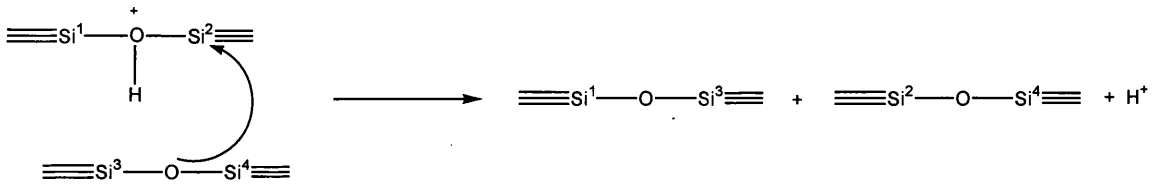

The base catalysed mechanism is promoted by an activated intermediate formed by addition of a hydroxyl group to the siloxane bond, which then cleaves, and the fragments form new Si-O-Si bonds by condensation. The catalyst causes continuous scission and re-formation of the siloxane bond, and thus further growth of the siloxanes.

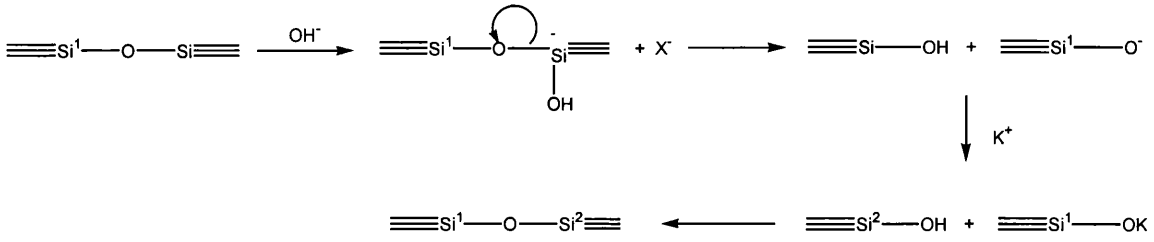

The choice of catalyst is important in order to minimise interaction with the reactive group on the functional monomer. For example, if the final copolymer contains amine groups then the catalyst would normally be a strong base[102,103], and if the final copolymer contains thiol groups, then a strong acid is selected[104]. This process is not limited to the addition of one type of functional group on silicon. Indeed, as long as the chemistry is compatible, then any combination of functional groups is possible, although very difficult to control. This type of reaction gives rise to co-polymers with a wide range of molecular weights with a random distribution of co-monomer units in the polymer chain, and thus this reaction is not suitable for the preparation of specific polymers with defined and reproducible loadings and structure.

1.5.3.3 Reaction of Primary Alcohols with Si-H Moieties

Poly(methylhydrosiloxanes), $(Me_3SiO(MeSi\{H\}O)_x(Me_2SiO)_ySiMe_3)$, are commercially available with a wide range molecular weights and loading of Si-H (ratio of x:y), as are primary alcohols containing other functionalities. The condensation reaction

between Si-H and hydroxyl compounds, such as primary alcohols, takes place in the presence of a variety of metal catalysts to form Si-O-C containing species with elimination of hydrogen. The most commonly used catalysts are zinc octanoate, iron octanoate, and dibutyltin dilaurate1[105,106], but platinum species are also effective.

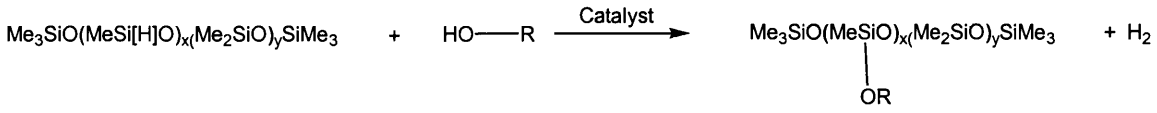

Although high loadings are readily achieved, the resultant poly(organosiloxanes) contain Si-O-C linkages, which are more reactive than Si-C-C linkages formed by the hydrosilylation process outlined below.

1.5.3.4 Hydrosilylation Reactions

Hydrosilylation reactions involve the reaction of a ≡Si-H moiety with a 1-alkenyl group attached to the functional group required, to form silicon-carbon bonds as detailed below[107-109]. The hydrosilylation reaction may be radical or photochemically initiated, or catalysed by one of a number of transition metal complexes. One of the most commonly used catalysts is Speier's catalyst, hexachloroplatinic acid in isopropanol.

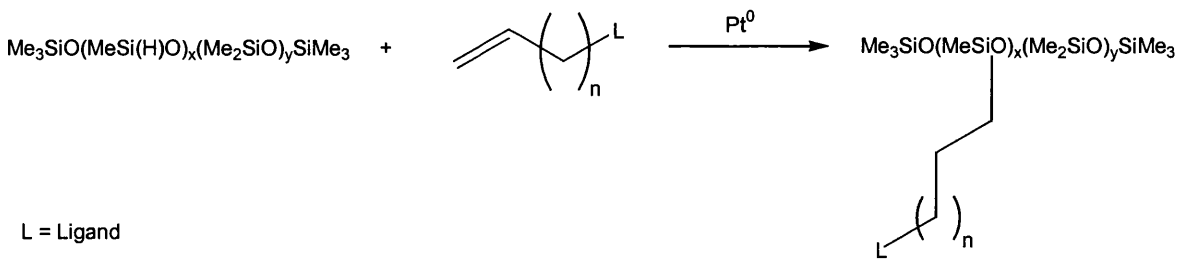

The mechanism of the reaction is not well understood. In the first proposed mechanism, suggested by Harrod and Chalk[110], the reaction was thought to be

homogeneous. However, work by Lewis and Lewis[111] has shown that it is often heterogeneous, with the active platinum species in the colloidal state. This basic cycle involves reduction of Pt(IV) to Pt(0) by the silane, oxidative addition of Si-H to the metal, coordination by the alkene, rearrangement to a σ-bonded alkyl complex, and reductive elimination of the product as outlined below. The isomeric branched silane product is often a minor product in this reaction[109,112,113].

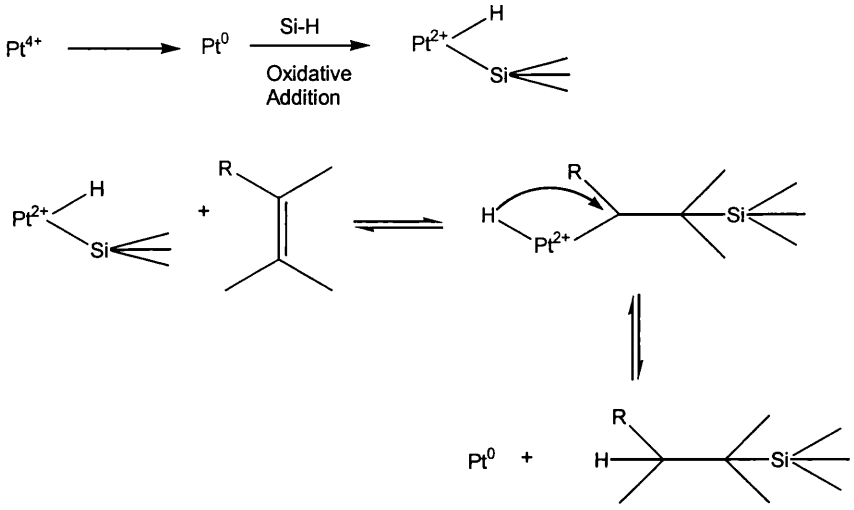

This precious metal catalyst is susceptible to poisoning, difficult to recover or remove, and catalyses secondary reactions involving the solvent, isopropanol. Given the disadvantages of this catalyst, more active platinum catalysts, which are soluble in non-hydroxylic solvents, and contain the metal in the divalent or zero oxidation state, are often preferred and are very efficient.

A range of functionalised model tri- to penta- siloxanes, $Me_3SiO(MeOSiH)_nSiMe_3$ (n = 1 to 3) have been prepared previously using hydrosilylation procedures[114]. The model siloxanes mimic the reactions of polymer species and can be used to explore the best conditions for addition of side chains. Functional side chains added previously include

entities such as perfluoroethers[112,115], $CH=CH_2$, -CN and $-PPh_2$[114]. Some of these have been metallated using metal halide and metal carbonyl moieties, and the products isolated and characterised[116], for example $[(Me_3SiO)_2SiMe(CH_2CH_2PPh_2)]RhCl$ and $[(Me_3SiO)_2SiMe(CH_2CH_2Ph)]Mo(CO)_3$.

As Si-H containing prepolymers, polymers and cyclics are commercially available, well defined organofunctional polymeric siloxanes may be prepared via hydrosilylation reactions. There is a wide range of effective catalysts to choose from[116] and a wide number of organosiloxanes have been produced for many different purposes using this method. Side chain functionalities that have been incorporated onto polysiloxanes include silyl ketene acetals[118], cyclic carbonates[119] crown ethers[120], amines, ethers and esters[121,122].

The physical and chemical properties of organofunctional polymers can be modified further through control of the degree of ligand loading, and incorporation of cross-linking moieties in order to prepare siloxane films. The Si-H groups on the polysiloxanes can be completely converted to functional side chains or, under careful control of the reaction, precise amounts of side chain can be added in order to control the amount of functionality of the polymer. The remaining Si-H groups can be used to add another type of side chain, or more commonly, to prepare cross-linked membranes[121]. Cross-linking can be achieved using long chain silanol terminated poly(dimethylsiloxane), $(HO-[Si(Me)_2-O-]_m-H)$, in the presence of tetraethoxysilane, $(Si[OEt]_4)$, promoted by a dibutyltin dilaurate catalyst for example, to give a membrane as in the diagram below.

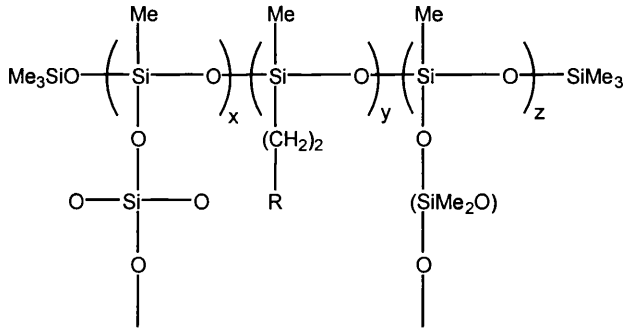

The studies referenced above have shown that after attachment of the required functional groups to a siloxane backbone, metal salts may complexed with the suitable functional side chain, to produce metal containing organosiloxanes that can then be used for further applications. These methods have formed the basis of the procedures used to prepare the organofunctional, and subsequent metallated siloxanes that have been produced in this study.

1.5.3.5 Nucleophilic Attack of Chloroalkyl Functional Siloxanes

A less frequently used method of preparing organofunctional siloxanes involves nucleophilic attack on chloroalkyl functional siloxanes. Chloroalkyl siloxane monomers may be synthesised from the appropriate cyclic precursors via a hydrosilylation reaction. Ring opening copolymerisation may then be used to prepare a chloroalkyl functional siloxane polymer. Displacement of the chloride ion has been accomplished using amines or carboxylates[123,124] for example, and is a potential route to materials that cannot be formed by direct hydrosilylation. However, this method has a major disadvantage in that nucleophilic attack on the siloxane backbone may also occur, resulting in chain scission.

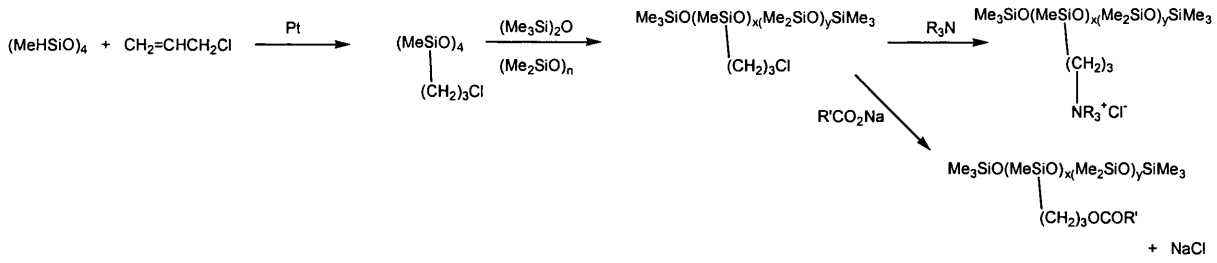

1.5.4 Uses of Polyorganosiloxanes

There are numerous applications of such organofunctional siloxanes. In relation to practical uses in fields related to this research, these polymers have been found to be particularly useful in textile treatments[100], selective liquid extraction[125], and in permselectivity processes[122].

Silicones have been used for many years as a water repellent treatment for clothing. The addition of side chains to the polymer can effectively modify the behaviour of the siloxane. For example, the addition of an amine side chain has been effective in preventing the shrinkage of silicone treated wool during wash cycles[126]. As selective liquid extractants, crown ether containing siloxanes are fluids, and can be made completely miscible with water at high loadings and short polymer chain lengths[125]. Thus, the hydrophobic/hydrophilic balance of a silicone can be modified by side-arm functionalisation.

Paints can be applied to numerous surfaces that require protection, and functional siloxanes may be incorporated into both water or organic solvent based paints, depending on the properties of the functional siloxane polymer. Once incorporated, and the paint applied, an appropriately functionalised polymer may be able to facilitate the decontamination of agents on the paint surface. Alternatively, the functional siloxane polymer catalyst may be dissolved in a solvent, the solution applied to a surface and the

solvent evaporated in order to coat the surface with an active coating. Reactive cross-linked siloxane membranes can also be made. Such membranes will allow gases and liquids to permeate through them, and as organosiloxanes are normally hydrophobic, a toxic agent may be expected to dissolve in the membrane, so bringing it into intimate contact with either a metal catalyst or other decontaminating agent. Alternatively, the organofunctionality of the polymer may be chemically modified to create a surface barrier that repels agents, in order to stop it permeating into a surface and affecting the underlying material.

In summary, the physical properties of siloxane polymers, and the facility with which they can be modified to meet the chemical and physical requirements of chemical warfare agent decontamination procedures, make these systems promising for use as supports for decontamination catalysts. Incorporation, at the molecular level, of the catalyst systems shown to be most active against agents (section 1.4) may produce siloxane polymer systems that are extremely useful in this respect, both on the battlefield and in an industrial setting.

2. EXPERIMENTAL

2.1 SYNTHETIC METHODS AND INSTRUMENTATION

2,2'–Dipyridylmethane (**L4**) was prepared in 58% yield by the reduction of 2,2'–dipyridylketone with hydrazine hydrate and sodium hydroxide. (2,2'–Dipyridyl) methylamine (**L5**) was prepared in 41% yield via the reaction of 2-chloromethylpyridine with 2-aminomethylpyridine following modified literature methods as noted below[127,128].

6-Bromo-1-hexene was purchased from Fluka. Triethylene glycol monomethyl ether (**L18**), platinum divinyltetramethyldisiloxane (**C2**), all model siloxanes and siloxane copolymers were purchased from Fluorochem. All other solid reagents were purchased from Aldrich and used without further purification. Solvents and liquid reagents, including 4-vinyl pyridine (**L14**) and allyl imidazole (**L13**) (from Aldrich), were dried as necessary using molecular sieves. A vinyltrimethylsiloxane platinum(0) catalyst (**C1**) of research quality was obtained from Dow Corning, and dichloro(1,5-cyclooctadiene)platinum(II) (**C3**) was prepared elsewhere at Bath University and used without further purification.

All distillations were carried out under reduced pressure using a Kugelruhr apparatus. Spectra were recorded on the following instruments: Nicolet 510P FT-IR (I.R spectra), JOEL GX270 and EX400 (^{1}H, ^{13}C and ^{29}Si N.M.R spectra) and VG 70-70E (mass spectra). N.M.R spectra were recorded as $CDCl_3$ solutions unless otherwise stated. Chemical shifts are quoted in ppm, relative to TMS = 0. For all ^{29}Si N.M.R samples, [$Cr(acac)_3$] was used as a relaxation agent.

All experimental procedures carried out at Bath were performed only after their potential hazards had been evaluated. Experiments carried out at Porton Down, under the immediate supervision of Dr. N. Blacker, conformed with DERA safety protocols.

Dr. M.F. Mahon carried out all solid-state structure determinations. All data were measured on a CAD 4 automatic four-circle diffractometer in the range $2 \leq \theta \leq 24^{o}$ at room temperature. Data were corrected for Lorentz and polarisation, but not for absorption, in all cases.

2.1.1 Preparation of N-Donor Ligands

2.1.1.1 2,2'-Dipyridylmethane (L4)

2,2'-Dipyridylketone (5.00 g, 27 mmol) was added to a hot solution of potassium hydroxide (3.14 g, 56 mmol) in diethylene glycol (100 ml), giving a dark red solution. Hydrazine hydrate (3.0 ml, 62 mmol) was added, resulting in the solution boiling, and the solution was further heated under reflux for four hours to give a clear orange solution. On cooling, water (100 ml) was added, and the solution extracted with dichloromethane (8 x 20 ml). The extracts were dried over $MgSO_4$ and evaporated under reduced pressure, leaving a yellow liquid. Hydrobromic acid (46-48% aqueous solution, 5 ml) was then added to this residue. On dilution with ethanol (100 ml) and standing, colourless crystals of the dihydrobromide salt of the product formed. The salt was dissolved in water (50 ml), neutralised with potassium carbonate, and extracted with chloroform (8 x 10 ml). The combined extracts were dried over magnesium sulphate, the solvent was then removed, and the resultant oil distilled at 110°C and 0.05 mbar to give 2,2'-dipyridylmethane as a colourless liquid (2.69 g, 58%). Analysis (%): Found (Required for $C_{11}H_{10}N_2$)– C, 77.3 (77.6); H, 5.92 (5.92); N, 16.3 (16.5). I.R (cm^{-1}): ν(pyridine rings), 1589, 1568. N.M.R (ppm) ($CDCl_3$): ^1H, 4.34 (s, 2H, CH_2), 7.08-7.12 (m, 2H, aromatic), 7.24-7.27 (d, J = 7.69 Hz, 2H, aromatic), 7.55-7.61 (m, 2H,

aromatic), 8.53-8.55 (m, 2H, aromatic); ^{13}C, 46.9 (bridging CH_2), 121.2, 123.3, 136.3, 149.0, 159.1 (aromatics). Mass spectrum (70eV C.I. m/z): 170 (M^+).

2.1.1.2 (2,2'-Dipyridyl)methylamine (**L5**)

2-Chloromethylpyridine hydrochloride (10.0 g, 61 mmol) in water (20 ml) was neutralised with a saturated solution of potassium carbonate. The free base was then added to an ethanolic solution (25 ml) of 2-aminomethylpyridine (15.0 g, 140 mmol) and kept at 40-45°C for one hour. The solvent was removed and the remaining oil redissolved in a strong aqueous solution of potassium hydroxide. The solution was then extracted with ether (8 x 10 ml), the extract dried with magnesium sulphate and the solvent removed to leave a red oil. This was distilled at 140°C (0.1 mbar) to produce the required product as a yellow oil (5.00 g, 41%). Analysis (%): Found (Required for $C_{12}H_{13}N_3$)- C, 71.4 (72.3), H, 6.47 (6.58), N, 20.9 (21.1). I.R (cm^{-1}): ν(N-H) 3122; ν(pyridine rings) 1591, 1570. N.M.R (ppm) ($CDCl_3$): ^1H, 2.74 (s, 1H, NH), 3.89-3.98 (m, 4H, CH_2), 7.13 (m, 2H, aromatic), 7.33-7.36 (m, 2H, aromatic), 7.59-7.62 (m, 2H, aromatic), 8.54 (m, 2H, aromatic); ^{13}C, 54.6 (N-CH_2), 121.7, 122.0, 136.2, 149.1, 159.6 (aromatics). Mass spectrum (70eV C.I. m/z): 199 (M^+).

2.1.2 Ligand Alkenylation Reactions

An N– or C– alkenyl group (1–propenyl or 1–hexenyl) was introduced into the following ligands so that the products could be used in hydrosilylation reactions.

2.1.2.1 Alkenylation of 2,2'-Dipyridylamine (**L1**)

L1 (1.71 g, 10 mmol) was added to a solution of potassium *t*-butoxide (1.12 g, 10 mmol) in THF (50 ml) and the mixture stirred at room temperature for one hour. Allyl bromide (0.95 ml, 11 mmol) was then added, and the solution stirred for a further hour,

during which time a suspension of potassium bromide in a bright yellow solution formed. The suspension was filtered off, the solvent removed, and the remaining solution chromatographed on a silica gel (70-230 mesh) column using a 9:1 (v/v) mixture of 60^{o}-80^{o} petroleum ether and ethyl acetate as elutant. The product was isolated from the first fraction as a light yellow liquid and was identified as the required N–alkenylated compound, **L8**, (0.74 g, 35%). Analysis (%): Found (Required for $C_{13}H_{13}N_3$)- C, 73.9 (73.9); H, 6.36 (6.20); N, 19.6 (19.9). I.R (cm^{-1}): ν(C=C), 1643. N.M.R (ppm) ($CDCl_3$): ^{1}H, 4.85-4.89 (m, 2H, N-CH_2), 5.07-5.21 (m, 2H, CH=C$\underline{H}_2$), 5.97-6.06 (m, 1H, C$\underline{H}$=CH_2), 6.83-6.86 (m, 2H, aromatic), 7.14-7.17 (m, 2H, aromatic), 7.49-7.55 (m, 2H, aromatic), 8.32-8.34 (m, 2H, aromatic); ^{13}C, 50.0 (N-CH_2), 115.4 (CH=$\underline{C}H_2$), 134.5 ($\underline{C}$H=CH_2), 114.2, 116.7, 136.8, 147.8, 156.7 (aromatics). Mass spectrum (70eV E.I. m/z): 211 (M^+).

The N–hexenyl substituted dipyridylamine analogue, **L15**, was prepared via a similar experimental method using 6-bromo-1-hexene (10 mmol) instead of allyl bromide. Yield, 0.71 g, 28%. Analysis (%): Found (Required for $C_{16}H_{19}N_3$)- C, 76.4 (75.9); H, 7.77 (7.56); N, 16.6 (16.6). I.R (cm^{-1}): ν(C=C), 1639. N.M.R (ppm) ($CDCl_3$): ^{1}H, 1.39-1.50 (m, 2H, CH_2), 1.66-1.78 (m, 2H, CH_2), 2.03-2.11 (m, 2H, CH_2), 4.16-4.22 (m, 2H, N-CH_2), 4.89-5.00 (m, 2H, CH=C$\underline{H}_2$), 5.70-5.86 (m, 1H, C$\underline{H}$=CH_2), 6.80-6.85 (m, 2H, aromatic), 7.06-7.09 (d, J = 8.43 Hz, 2H, aromatic), 7.46-7.52 (m, 2H, aromatic), 8.32-8.34 (m, 2H, aromatic); ^{13}C, 26.3, 27.7, 33.5 (CH_2), 48.0 (N-CH_2),114.3 (CH=$\underline{C}H_2$), 136.9 ($\underline{C}$H=CH_2), 114.6, 116.7, 138.8, 148.2, 157.4 (aromatics). Mass spectrum (70eV E.I. m/z): 253 (M^+).

2.1.2.2 Alkenylation of 2-{[2-(Dimethylamino)ethyl]methylamino}ethanol (**L2**)

Potassium *t*-butoxide (1.12 g, 10 mmol) was dissolved in THF (50 ml) and **L2** (1.46 g, 10 mmol) was added slowly, and the reaction mixture left stirring under a dinitrogen

atmosphere for two hours. Allyl bromide (0.95 ml, 11 mmol) was then added, causing the precipitation of potassium bromide. After stirring for a further hour at room temperature, the suspension was filtered off and the solvent removed from the filtrate to leave an orange liquid. The liquid was then purified by column chromatography, on a deactivated alumina column, using a mixture of acetone and 60°-80° petroleum ether (1:9 v/v). After removal of the solvent the required allylether, **L9**, was obtained as a yellow liquid (1.23 g, 66%). Analysis (%): Found (Required for $C_{10}H_{22}N_2O$)- C, 64.4 (64.5); H, 12.0 (11.9); N, 14.1 (15.0). I.R (cm^{-1}): ν(C=C), 1647. N.M.R (ppm) ($CDCl_3$): ^1H, 2.23-2.25 (m, 6H, N-Me_2), 2.30-2.33 (m, 3H, N-Me), 2.38-2.43 (m, 2H, N-C$\underline{H}_2$$CH_2$-N), 2.51-2.56 (m, 2H, N-CH_2C$\underline{H}_2$-N), 2.60-2.65 (m, 2H, N(Me)C$\underline{H}_2$), 3.52-3.59 (m, 2H, CH_2C$\underline{H}_2$-O), 3.97-4.00 (m, 2H, C$\underline{H}_2$-CH=CH_2), 5.14-5.30 (m, 2H, CH=C$\underline{H}_2$), 5.84-5.98 (m, 1H, C$\underline{H}$=CH_2); ^{13}C, 42.9 (N-Me), 45.6 (N-Me_2), 55.8 (CH_2-N-$\underline{C}H_2$), 57.1 (N-$CH_2$$\underline{C}H_2$-N), 68.1 ($CH_2$$\underline{C}H_2$-O), 71.8 ($CH_2$-O-$\underline{C}H_2$), 116.6 (CH=$\underline{C}H_2$), 134.6 ($\underline{C}$H=$CH_2$). Mass spectrum (70eV C.I. m/z): 186 (M^+).

2.1.2.3 Alkenylation of Trimethylethylenediamine (**L3**)

To a solution of **L3** (1.53 g, 15 mmol) in diethyl ether (50 ml), *n*-butyllithium, 1.6M in hexanes, (9.5 ml, 15 mmol) was added drop wise at 0°C under a dinitrogen atmosphere. After stirring for 15 minutes, allyl bromide (1.4 ml, 16 mmol) was added and the mixture left stirring for three hours at room temperature. Lithium bromide was filtered off and the solvent removed from the filtrate leaving an orange liquid, which was purified on a deactivated alumina column using a 2% solution of methanol in dichloromethane. The product, **L10**, was isolated from the first fraction as a yellow liquid after the solvent was removed (0.79 g, 37%). Analysis (%): Found (Required for $C_8H_{18}N_2$)- C, 66.6 (67.6); H, 13.0 (12.8); N, 18.7 (19.7). I.R (cm^{-1}): ν(C=C), 1643. N.M.R (ppm) ($CDCl_3$): ^1H, 2.24 (s, 9H, N-Me), 2.40-2.46 (m, 4H, NCH_2CH_2N), 3.01-

3.03 (m, 2H, $C\underline{H}_2$-CH=CH_2), 5.10-5.20 (m, 2H, CH=$C\underline{H}_2$), 5.80-5.95 (m, 1H, $C\underline{H}$=CH_2); ^{13}C, 42.3, 45.7 (N-Me) 54.8, 57.4, (N-CH_2CH_2-N), 61.4 ($\underline{C}H_2$CH=CH_2), 117.3 (CH=$\underline{C}H_2$), 135.6 ($\underline{C}$H=CH_2). Mass spectrum (70eV C.I. m/z): 142 (M^+).

The N–hexenyl derivative of **L3** was prepared by a similar method using 6-bromo-1-hexene (15 mmol) instead of allyl bromide, and purification was achieved by distillation at 130°C and 0.05 mbar to yield **L16** (1.55 g, 56%). Analysis (%): Found (Required for $C_{11}H_{24}N_2$)- C, 71.3 (71.6); H, 13.3 (13.1); N, 15.2 (15.2). I.R (cm^{-1}): ν(C=C), 1641. N.M.R (ppm) ($CDCl_3$): ^{1}H, 1.38-1.49 (m, 4H, CH_2), 2.05-2.07 (m, 2H, CH_2), 2.23-2.25 (m, 9H, N-Me), 2.32-2.47 (m, 6H, CH_2, N-$(CH_2)_2$-N), 4.91-5.03 (m, 2H, CH=$C\underline{H}_2$), 5.72-5.85 (m, 1H, $C\underline{H}$=CH_2); ^{13}C, 26.5, 26.7, 33.5, 55.5 (CH_2), 57.4, 58.1 (N-CH_2-CH_2-N), 42.5, 45.7 (N-Me), 114.3 (CH=$\underline{C}H_2$), 138.6 ($\underline{C}$H=CH_2). Mass spectrum (70eV E.I. m/z): 184 (M^+).

2.1.2.4 Alkenylation of 2,2'-Dipyridylmethane (**L4**)

A 1.8 molar solution of phenyllithium in cyclohexane:ether (7:3 v/v) (5.6 ml, 10 mmol) was added slowly to a solution of **L4** (1.70 g, 10 mmol) in dry diethyl ether (50 ml) under a dinitrogen atmosphere at 0°C causing orange crystals of the lithium salt to separate. After stirring for thirty minutes, allyl bromide (1.0 ml, 11 mmol) was added drop-wise and the mixture stirred for a further four hours at room temperature, during which time the solution became lighter, with a red-orange tint. Water (20 ml) was added and the organic layer extracted with dilute hydrochloric acid (8 x 5 ml). The acidic liquor was neutralised with potassium carbonate and then extracted with ether (8 x 10 ml). The combined extracts were dried over magnesium sulphate and then the solvent removed to leave a yellow oil, which was purified by column chromatography on a silica gel (70-230 mesh) column using a mixture of ethyl acetate and 60°-80° petroleum ether (1:4 v/v). The product, **L11,** was isolated as a yellow oily liquid from the first

fraction from the column (1.37 g, 65%). Analysis (%): Found (Required for $C_{14}H_{14}N_2$)- C, 79.1 (80.0); H, 6.68 (6.71); N, 13.6 (13.3). I.R (cm^{-1}): ν(C=C), 1641. N.M.R (ppm) ($CDCl_3$): ^1H, 3.00-3.05 (m, 2H, CH-C$\underline{H}_2$), 4.36-4.40 (t, J = 7.81 Hz, 1H, CH bridge), 4.90-5.05 (m, 2H, CH=C$\underline{H}_2$), 5.69-5.79 (m, 1H, C$\underline{H}$=CH_2), 7.07-7.10 (m, 2H, aromatic), 7.32-7.34 (m, 2H, aromatic), 7.55-7.60 (m, 2H, aromatic), 8.55-8.56 (m, 2H, aromatic); ^{13}C, 38.3 (CH_2), 55.6 (CH bridge) 116.3 ($\underline{C}H_2$=C), 136.2 ($\underline{C}$H=CH_2), 121.4, 123.0, 136.3, 149.1, 162.0 (aromatics). Mass spectrum (70eV C.I. m/z): 210 (M^+).

The C–hexenyl substituted derivative of **L4** (**L17**) was prepared in the same manner using 6-bromo-1-hexene (10 mmol) instead of allyl bromide, and purified by distillation at 135°C and 0.05 mbar. Yield, 1.72 g, 68%. Analysis (%): Found (Required for $C_{17}H_{20}N_2$)- C, 80.2 (80.9); H, 8.26 (7.99); N, 11.3 (11.1). I.R (cm^{-1}): ν(C=C), 1639. N.M.R (ppm) ($CDCl_3$): ^1H, 1.21-1.38 (m, 2H, CH_2), 1.41-1.49 (m, 2H, CH_2), 1.96-2.04 (m, 2H, CH_2), 2.21-2.30 (m, 2H, CH_2), 4.23-4.29 (t, J = 7.79 Hz, 1H, CH bridge), 4.85-4.97 (m, 2H, CH=C$\underline{H}_2$), 5.67-5.82 (m, 1H, C$\underline{H}$=CH_2), 7.05-7.10 (m, 2H, aromatic), 7.31-7.36 (m, 2H, aromatic), 7.53-7.60 (m, 2H, aromatic), 8.54-8.56 (m, 2H, aromatic); ^{13}C, 27.2, 28.7, 33.4, 34.2 (CH_2), 56.0 (CH bridge), 114.1 (CH=$\underline{C}H_2$), 138.7 ($\underline{C}$H=CH_2), 121.3, 122.9, 136.2, 149.1, 162.8 (aromatics). Mass spectrum (70eV C.I. m/z): 252 (M^+).

2.1.2.5 Alkenylation of 2,2'-(Dipyridylmethyl)amine (**L5**)

L5 (1.20 g, 6.0 mmol) was dissolved in THF (20 ml) and added to a solution of potassium *t*-butoxide (0.68 g, 6.1 mmol) in THF (20 ml), turning the solution dark purple. After stirring for an hour, allyl bromide (0.55 ml, 6.4 mmol) was added and the solution left stirring for a further 2 hours. The grey precipitate formed was filtered off to leave an orange filtrate. This was then dissolved in 40°-60° petroleum ether (5 ml) and purified on a deactivated alumina column using a mixture of 40°-60° petroleum ether:

ethyl acetate (3:2 v/v). The product, **L12**, was collected as a yellow oil from the first fraction. Yield, 0.80 g, 56%. Analysis (%): Found (Required for $C_{15}H_{17}N_3$)- C, 75.0 (75.3); H, 7.41 (7.16); N, 17.0 (17.6). I.R (cm^{-1}): ν(C=C), 1643. N.M.R (ppm) ($CDCl_3$): ^1H, 3.18-3.20 (d, J = 6.23 Hz, 2H, N-C$\underline{H}_2$CH=CH_2), 3.83 (s, 4H, CH_2-N-CH_2), 5.15-5.27 (m, 2H, CH=C$\underline{H}_2$), 5.87-5.99 (m, 1H, C$\underline{H}$=CH_2), 7.12-7.16 (m, 2H, aromatic), 7.53-7.56 (m, 2H, aromatic), 7.62-7.68 (m, 2H, aromatic), 8.51-8.53 (m, 2H, aromatic); ^{13}C, 57.1 (N-$\underline{C}H_2$CH=CH_2), 59.7 (CH_2-N-CH_2), 117.8 (CH=$\underline{C}H_2$), 135.2 ($\underline{C}$H=CH_2), 121.7, 122.7, 136.3, 148.8, 159.5 (aromatics). Mass spectrum (70eV C.I. m/z): 239 (M^+).

2.1.3 Siloxane Functionalisation via Hydrosilylation Reactions

Hydrosilylation reactions between alkenylated ligands and trisiloxanes, containing either a terminal or central Si-H group, were carried out in sealed vessels, in an inert atmosphere, and under rigorously anhydrous conditions. Products were purified by distillation. Hydrosilylations involving Si-H containing co-polymers were carried out similarly. The degree of functional group loading of each product polymer was determined by proton N.M.R and elemental analysis.

2.1.3.1 Reactions of Ligands with 1,1,1,3,3,5,5-Heptamethyltrisiloxane (MS1)

A mixture of **MS1** (0.84 g, 3.75 mmol), the alkenylated substrate (3.75 mmol) and toluene (2 ml) were put in a flame dried tube under a dinitrogen atmosphere. Two drops of the platinum catalyst, **C1**, were added, and the tube was then sealed. The mixture was heated at 80°C for 24-48 hours. For long reactions, an additional aliquot of catalyst was added after 24 hours. The solvent and unreacted volatiles were removed by rotary evaporation, and the remaining crude products of the reactions were purified as follows:

(a) Reaction with **L8** – The product was distilled at 175°C and 0.05 mbar to yield **MSL1**, as a clear liquid (0.88 g, 54%). Analysis (%): Found (Required for $C_{20}H_{33}N_3O_2Si_3$)- C, 55.5 (55.4); H, 8.35 (8.13); N, 9.70 (9.69). I.R (cm^{-1}): δ(Si-O-Si), 1047. N.M.R (ppm) ($CDCl_3$): ^1H, -0.03 (s, 6H, O-Si(Me)$_2$-O), 0.04 (m, 15H, Si-Me$_3$, Si(Me)$_2$-CH$_2$), 0.55-0.60 (m, 2H, Si-CH$_2$), 1.68-1.76 (m, 2H, Si-CH$_2$-CH$_2$), 4.12-4.16 (m, 2H, CH$_2$-N), 6.79-6.82 (m, 2H, aromatic), 7.06-7.08 (d, J = 8.55 Hz, 2H, aromatic), 7.46-7.50 (m, 2H, aromatic), 8.31-8.32 (m, 2H, aromatic); ^{13}C, 0.00, 1.04, 1.63 (Si-Me), 15.2, 21.7, 51.1 (CH$_2$ chain), 114.5, 116.6, 136.8, 148.1, 157.3 (aromatics); ^{29}Si, 7.49 (Si-Me$_3$), 7.15 (Si(Me)$_2$-CH$_2$), -20.79 (-O-Si(Me)$_2$-O-).

(b) Reaction with **L9** – The product was distilled at 135°C and 0.075 mbar to yield a clear liquid as the required product, **MSL2**, (1.40 g, 91%). Analysis (%): Found (Required for $C_{17}H_{44}N_2O_3Si_3$)- C, 49.5 (49.9); H, 11.1 (10.8); N, 6.60 (6.85). I.R (cm^{-1}): δ(Si-O-Si), 1047. N.M.R (ppm) ($CDCl_3$): ^1H, -0.07 (s, 6H, O-Si(Me)$_2$-O), -0.01 (s, 6H, Si(Me)$_2$-CH$_2$), 0.00 (s, 9H, Si-Me$_3$), 0.41-0.47 (m, 2H, Si-CH$_2$), 1.45-1.60 (m, 2H, Si-C-CH$_2$), 2.15 (s, 6H, N-Me$_2$), 2.21 (s, 3H, N-Me), 2.32-2.35 (m, 2H, CH$_2$-N-CH$_2$), 2.43-2.54 (m, 4H, N-CH$_2$-CH$_2$-N), 3.31-3.33 (t, J = 6.05 Hz, 2H, CH$_2$-O-CH$_2$), 3.43-3.47 (t, J = 7.14 Hz, 2H, CH$_2$-O-CH$_2$); ^{13}C, -0.05, 1.09, 1.65 (Si-Me), 14.1, 23.3 (Si-CH$_2$-CH$_2$), 43.0, 45.7 (N-Me), 56.0 (N-CH$_2$CH$_2$-O), 57.2, 57.3 (N-CH$_2$-CH$_2$-N), 68.8, 76.5 (CH$_2$-O-CH$_2$); ^{29}Si, 7.45 (Si-Me$_3$), 6.96 (Si(Me)$_2$-CH$_2$), -21.02 (O-Si(Me)$_2$-O).

(c) Reaction with **L10** – The product was distilled at 130°C and 0.05 mbar to yield the required product, **MSL3**, as a clear liquid (0.86 g, 63%). Analysis (%): Found (Required for $C_{15}H_{40}N_2O_2Si_3$)- C, 48.7 (49.4); H, 11.2 (11.1); N, 7.55 (7.68). I.R (cm^{-1}): δ(Si-O-Si), 1049. N.M.R (ppm) ($CDCl_3$): ^1H, -0.01-0.06 (m, 21H, Si-Me), 0.44-0.49 (m, 2H, Si-CH$_2$), 1.40-1.49 (m, 2H, Si-CH$_2$-CH$_2$), 2.15-2.21 (s, 9H, N-Me), 2.30-2.45 (m,

6H, CH_2-N-$(CH_2)_2$-N); ^{13}C, 0.00, 1.13, 1.66 (Si-Me), 15.7, 20.8, 55.5 (CH_2 chain), 42.4, 45.7 (N-Me), 57.4 (N-$\underline{C}H_2$ -CH_2-N) ,61.8 (N-CH_2 -$\underline{C}H_2$-N); ^{29}Si, 7.49 (Si-Me_3), 7.15 (Si$(Me)_2$-CH_2), -20.8 (O-Si$(Me)_2$-O-).

(d) Reaction with **L11** – The product was distilled at 160°C and 0.07 mbar to yield the required product, **MSL4**, as a yellow tinted oil (1.09 g, 67%). Analysis (%): Found (Required for $C_{21}H_{36}N_2O_2Si_3$)- C, 57.8 (58.3); H, 8.40 (8.38); N, 6.50 (6.47). I.R (cm^{-1}): δ(Si-O-Si), 1047. N.M.R (ppm) ($CDCl_3$): ^1H, -0.07 (s, 6H, O-Si$(Me)_2$-O), -0.01 (s, 6H, Si$(\underline{Me})_2$-CH_2), 0.03 (m, 9H, Si-Me_3), 0.57-0.61 (m, 2H, Si-CH_2), 1.24-1.32 (m, 2H, Si-CH_2-$C\underline{H}_2$), 2.23-2.30 (m, 2H, $C\underline{H}_2$-CH), 4.27-4.31 (t, J = 7.78 Hz, 1H, CH bridge), 7.05-7.08 (m, 2H, aromatic), 7.33-7.35 (m, 2H, aromatic), 7.53-7.58(m, 2H, aromatic), 8.52-8.54 (m, 2H, aromatic); ^{13}C, 0.05, 1.12, 1.73 (Si-Me), 18.1, 21.4, 38.2 (CH_2 chain), 55.9 (CH bridge), 121.3, 122.9, 136.3, 149.1, 162.9 (aromatics); ^{29}Si, 7.19 (Si-Me_3), 7.07 (Si$(Me)_2$-CH_2), -20.94 (-O-Si$(Me)_2$-O-).

(e) Reaction with **L13** – The product was distilled at 130°C and 0.05 mbar to yield the required product, **MSL5**, as a clear liquid (0.79 g, 64%). Analysis (%): Found (Required for $C_{13}H_{30}N_2O_2Si_3$)- C, 47.3 (47.2); H, 9.41 (9.15); N, 8.30 (8.47). I.R (cm^{-1}): δ(Si-O-Si), 1049. N.M.R (ppm) ($CDCl_3$): ^1H, -0.05-0.05 (m, 21H, Si-Me), 0.40-0.45 (m, 2H, Si-CH_2), 1.72-1.78 (m, 2H, Si-CH_2-$C\underline{H}_2$), 3.83-3.87 (m, 2H, N-CH_2), 6.84 (m, 1H, ring), 6.99 (m, 1H, ring), 7.40 (s, 1H, ring); ^{13}C, 0.00, 1.17, 1.74 (Si-Me), 15.0, 25.3, 49.7 (CH_2 chain), 118.6, 129.2, 137.0 (ring); ^{29}Si, 7.34 (Si-Me_3), 6.92 (Si$(Me)_2$-CH_2), -20.48 (-O-Si$(Me)_2$-O-).

(f) Reaction with **L16** – This reaction was carried out in the same fashion as those above, this time using **C2** as the catalyst. Distillation at 130°C and 0.04 mbar yielded **MSL6** as a clear liquid (1.03 g, 68%). Analysis (%): Found (Required for

$C_{18}H_{46}N_2O_2Si_3$)- C, 52.6 (53.1); H, 11.5 (11.4); N, 6.80 (6.89). I.R (cm^{-1}): δ(Si-O-Si), 1049. N.M.R (ppm) ($CDCl_3$): ^1H, -0.10-0.04 (m, 21H, Si-Me), 0.48 (m, 2H, Si-CH_2), 1.27 (m, 6H, Si-$CH_2(C\underline{H}_2)_3CH_2$), 1.41 (m, 2H, Si-$(CH_2)_4C\underline{H}_2$), 2.18-2.19 (m, 9H, N-Me), 2.27-2.29 (m, 2H, N-$C\underline{H}_2(CH_2)_5$), 2.35-2.41 (m, 4H, N-$(CH_2)_2$-N); ^{13}C, 0.00, 1.08, 1.63 (Si-Me), 18.1, 23.0, 27.0, 27.1, 33.2, 55.5 (CH_2 chain), 42.5, 45.7 (N-Me), 57.4, 58.4 (N-$(CH_2)_2$-N); ^{29}Si, 7.42 (Si-Me_3), 7.03 (Si$(Me)_2$-CH_2), -21.1 (O-Si$(Me)_2$-O).

(g) An analogous reaction was carried out between 6-bromo-1-hexene and **MS1**, using **C3** as catalyst. The required product, **MSL7**, was isolated after distillation at 175°C and 0.02 mbar as a clear liquid (1.33 g, 92%). Analysis (%): Found (Required for $C_{13}H_{33}BrO_2Si_3$)- C, 40.8 (40.5); H, 8.85 (8.63). I.R (cm^{-1}): δ(Si-O-Si), 1049. N.M.R (ppm) ($CDCl_3$): ^1H, 0.02 (s, 6H, O-Si$(Me)_2$-O), 0.06 (s, 6H, Si$(Me)_2$-CH_2), 0.09 (s, 9H, Si-Me_3), 0.52-0.56 (m, 2H, Si-CH_2), 1.32-1.36 (m, 4H, chain Si-$CH_2(C\underline{H}_2)_2$), 1.42-1.45 (m, 2H, Si-$(CH_2)_3$-$C\underline{H}_2$), 1.82-1.89 (q, J = 7.10 Hz, 2H, Si-$(CH_2)_4C\underline{H}_2$), 3.39-3.42 (t, J = 6.87 Hz, 2H, CH_2-Br); ^{13}C, 0.00, 1.10, 1.63 (Si-Me), 18.0, 22.9, 27.7, 32.3, 32.6, 33.8 (chain CH_2); ^{29}Si, 7.34 (Si-Me_3), 7.11 (Si$(Me)_2$-CH_2), -20.94 (-O-Si$(Me)_2$-O-).

2.1.3.2 Reactions of Ligands with 1,1,1,3,5,5,5-Heptamethyltrisiloxane (**MS2**)

A mixture of **MS2** and alkenylated substrate, in 1:1 mole ratio, toluene (3 ml) and **C2** (4 drops) were put in a flame dried sealed tube under a dinitrogen atmosphere and heated at 80°C for up to 48 hours. Another portion of catalyst was added after 24 hours if all Si-H had not reacted (monitored by I.R spectroscopy). Once reaction was complete, the solvent was removed and the products purified as follows:

a) Reaction with **L15** (1.30 g, 5.1 mmol) – The product was distilled from the residue at 185°C and 0.05 mbar to yield **MSL8** as a clear liquid (2.06 g, 86%). Analysis (%):

Found (Required for $C_{23}H_{41}N_3O_2Si_3$)- C, 58.3 (58.1); H, 8.80 (8.86); N, 9.04 (8.83). I.R (cm^{-1}): δ(Si-O-Si), 1047. N.M.R (ppm) ($CDCl_3$): ^1H, -0.03 (s, 3H, Si-Me), 0.07 (s, 18H, $Si-Me_3$), 0.40-0.44 (m, 2H, $Si-CH_2$), 1.31 (m, 6H, $Si-CH_2(C\underline{H}_2)_3$), 1.66-1.68 (m, 2H, $Si-(CH_2)_4C\underline{H}_2$), 4.14-4.18 (m, 2H, $N-CH_2$), 6.81-6.84 (m, 2H, aromatic), 7.06-7.08 (m, 2H, aromatic), 7.47-7.51 (m, 2H, aromatic), 8.32-8.34 (m, 2H, aromatic); ^{13}C, 0.00, 2.16 (Si-Me), 17.9, 23.4, 27.1, 28.5, 33.3, 48.7 (chain CH_2), 115.0, 117.1, 137.3, 148.6, 157.8 (aromatic); ^{29}Si, 6.92 ($Si-Me_3$), -21.13 (Si-Me).

b) Reaction with **L9** (1.12 g, 6 mmol) – The product was distilled at 120°C and 0.05 mbar to give **MSL9** as a clear liquid (1.76 g, 72%). Analysis (%): Found (Required for $C_{17}H_{44}N_2O_3Si_3$)- C, 49.0 (49.9); H, 10.7 (10.8); N, 6.75 (6.85). I.R (cm^{-1}): δ(Si-O-Si), 1039. N.M.R (ppm) ($CDCl_3$): ^1H, -0.06-0.05 (m, 21H, Si-Me), 0.39 (m, 2H, $Si-CH_2$), 1.53 (m, 2H, $Si-CH_2C\underline{H}_2$), 2.17-2.20 (m, 6H, $N-Me_2$), 2.23-2.25 (m, 3H, N-Me), 2.35 (m, 2H, $N-C\underline{H}_2(CH_2)_2$), 2.47-2.56 (m, 4H, $N-(C\underline{H}_2)_2-N$), 3.31-3.33 (m, 2H, $O-C\underline{H}_2CH_2=CH$), 3.47-3.48 (m, 2H, $C\underline{H}_2-O-(CH_2)_2$); ^{13}C, 0.00, 2.25 (Si-Me), 14.0, 23.6 ($Si-(CH_2)_2$), 43.6, 46.3 (N-Me), 56.5 ($N-CH_2CH_2-O$), 57.8 ($N-(CH_2)_2-N$), 69.3, 74.3 (CH_2-O-CH_2); ^{29}Si, 7.15 ($Si-Me_3$), -21.6 (Si-Me).

c) Reaction with **L16** (1.14 g, 6.2 mmol) - **MSL10** was distilled at 120°C and 0.04 mbar as a clear liquid (1.35 g, 54%). Analysis (%): Found (Required for $C_{18}H_{46}N_2O_2Si_3$)- C, 52.6 (53.1); H, 11.3 (11.4); N, 6.80 (6.89). I.R (cm^{-1}): δ(Si-O-Si), 1049. N.M.R (ppm) ($CDCl_3$): ^1H, -0.06-0.04 (m, 21H, Si-Me), 0.40 (m, 2H, $Si-CH_2$), 1.26 (m, 6H, $Si-CH_2(C\underline{H}_2)_3$), 1.41 (m, 2H, $Si-(CH_2)_4C\underline{H}_2$), 2.19-2.20 (m, 9H, N-Me), 2.30-2.31 (m, 2H, $N-C\underline{H}_2(CH_2)_5$), 2.36-2.40 (m, 4H, $N-(CH_2)_2-N$); ^{13}C, 0.00, 2.14 (Si-Me), 17.9, 23.3, 27.5, 27.6, 33.5, 55.9 (CH_2 chain), 42.9, 46.2 (N-Me), 57.8, 58.8 ($N-(CH_2)_2-N$); ^{29}Si, 6.84 ($Si-Me_3$), -21.3 (Si-Me).

d) Reaction with **L17** (0.48 g, 1.9 mmol) - **MSL11** was distilled at 135°C and 0.01 mbar, and was isolated as a yellow liquid (0.74 g, 83%). Analysis (%): Found (Required for $C_{24}H_{42}N_2O_2Si_3$)- C, 60.6 (60.7); H, 8.93 (8.92); N, 5.99 (5.90). I.R (cm^{-1}): δ(Si-O-Si), 1049. N.M.R (ppm) ($CDCl_3$): ^1H, -0.18-0.06 (m, 21H, Si-Me), 0.31-0.34 (m, 2H, Si-CH_2), 1.12-1.25 (m, 8H, Si-$CH_2(C\underline{H}_2)_4$), 2.13-2.18 (q, J = 7.63 Hz, 2H, $Si(CH_2)_5C\underline{H}_2$), 4.16-4.20 (t, J = 7.63 Hz, 1H, bridging CH), 6.98-7.01 (m, 2H ,aromatic), 7.26-7.28 (d, J = 7.63 Hz, 2H, aromatic), 7.47-7.51 (triplet of doublets, J = 1.83 Hz (doublets), J = 7.63 Hz (triplet), 2H, aromatic), 8.46-8.47 (m, 2H, aromatic); ^{13}C, 0.00, 2.14 (Si-Me), 17.8, 23.3, 28.1, 29.6, 33.4, 34.9 (chain CH_2), 56.5 (bridging CH), 121.7, 123.3, 136.6, 149.5, 163.3 (aromatic); ^{29}Si, 6.84 (Si-Me_3), -21.1 (Si-Me).

e) An analogous reaction between **L2** (1.46 g, 10 mmol) and **MS2** (2.23 g, 10 mmol), using **C3** as catalyst, stirred together in a flame dried flask at 90°C for 24 hours, yielded **MSL12** as the product after distillation at 95°C and 0.04 mbar (3.18 g, 87%). Analysis (%): Found (Required for $C_{14}H_{38}N_2O_3Si_3$)- C, 45.9 (45.9); H, 10.6 (10.4); N, 7.75 (7.64). I.R (cm^{-1}): δ(Si-O-Si), 1055. N.M.R (ppm) ($CDCl_3$): ^1H, -0.03-0.09 (m, 21H, Si-Me), 2.13-2.17 (m, 6H, N-Me_2), 2.22-2.23 (m, 3H, N-Me), 2.31-2.34 (m, 2H, N-$C\underline{H}_2CH_2$-O), 2.45-2.52 (m, 4H, N-$(CH_2)_2$-N), 3.68-3.71 (m, 2H, CH_2-O); ^{13}C, -3.90, 1.58 (Si-Me), 43.1, 45,7 (N-Me), 56.1, 57.3, 59.5, 60.0 (CH_2); ^{29}Si, 8.30 (Si-Me_3), -56.9 (Si-Me).

2.1.3.3 Reactions of Ligands with (3-4%)-Methylhydro-(96-97%)-dimethylsiloxane Copolymer (CP1)

Using ^1H N.M.R and microanalysis, it was found that **CP1** required 6.7 equivalents of ligand for complete reaction. Reactions between **CP1** and **L9** and **L15** were carried out using the general procedure below. Microanalysis and ^1H N.M.R spectroscopy were

used to determine the loading and degree of Si-H replacement of the functionalised polymer product.

A mixture of **CP1** (1.33 g, 0.4 mmol), alkenylated ligand (2.8 mmol), toluene (4 ml) and 5 drops of **C2** were heated together for 48 hours in a flame dried sealed tube, under a dinitrogen atmosphere at 80°C. Addition of extra catalyst took place after 24 hours. The toluene was removed using a rotary evaporator, and the remaining polymer/ligand mix was washed with a large excess of cold methanol. Filtration of the polymer through celite removed any remaining platinum and any traces of solvent were finally removed by pumping. This yielded the products **PL1** and **PL2** as below:

a) The reaction with **L9** produced a viscous clear liquid, **PL1**, which was found to have 75% of the available reactive Si-H sites replaced. From ^{1}H N.M.R and microanalysis, the polymer was shown to be loaded with 2.8 mol% of **L9**. Analysis (%): Found (Required for 75% replacement)- C, 34.3 (34.6); H, 8.47 (8.46); N, 1.00 (1.00). I.R (cm^{-1}): δ(Si-O-Si), 1008. N.M.R (ppm) ($CDCl_3$): ^{1}H, 0.04-0.09 (m, Si-Me), 0.45-0.51 (m, Si-CH_2), 1.58 (m, Si-$CH_2C\underline{H}_2$), 2.23 (s, N-Me_2), 2.39 (s, N-Me), 2.40-2.43 (m, N-$C\underline{H}_2CH_2$-O), 2.51-2.62 (m, (N-$(CH_2)_2$N), 3.34-3.39 (m, CH_2-O), 3.50-3.54 (m, O-CH_2); ^{13}C, 1.03 (Si-Me), 13.5, 23.3 (Si-$(CH_2)_2$), 43.2, 45.8 (N-Me), 56.0, 57.4 (N-CH_2-CH_2-N), 69.0, 73.9 (CH_2-O-CH_2); ^{29}Si, -21.86 (O-Si$(Me)_2$-O), -21.56 (O-Si(Me)(CH_2)-O), 7.34 (Si-Me_2).

b) The reaction with **L15** produced a viscous yellow liquid, **PL2**, which had 94% of the available Si-H sites replaced, based on the ^{1}H N.M.R and microanalysis results. The polymer contained 3.5 mol% functionalisation. Analysis (%): Found (Required for 94% replacement)- C, 36.8 (37.3); H, 8.15 (8.16); N, 1.83 (1.82). I.R (cm^{-1}): δ(Si-O-Si), 1016. N.M.R (ppm) ($CDCl_3$): ^{1}H, -0.03-0.02 (m, Si-Me), 0.42 (m, Si-CH_2), 1.25 (m, Si-

$CH_2(C\underline{H_2})_3$), 1.65 (m, Si-$(CH_2)_4C\underline{H_2}$), 4.10 (m, N-CH_2), 6.78 (m, aromatic), 7.01 (m, aromatic), 7.42 (m, aromatic), 8.23 (m, aromatic); ^{13}C, 1.02 (Si-Me), 17.7, 23.0, 26.8, 28.3, 34.2, 48.4 (chain CH_2), 114.7, 116.8, 137.0, 148.3, 157.6 (aromatics).

2.1.3.4 Reactions of Ligands with (15-18%)-Methylhydro-(82-85%)-dimethylsiloxane Copolymer (**CP2**)

It was found from ^1H N.M.R and microanalysis results, that on average, **CP2** required a 1:3.5 mole ratio of polymer:ligand for complete reaction.

a) A mixture of copolymer (1.5 g, 0.75 mmol), **CP2**, alkenylated ligand, **L9**, (2.7 mmol), toluene (3 ml) and two drops of **C2,** in a flame dried, sealed tube under a dinitrogen atmosphere were heated together at 85°C for 24 hours. All Si-H groups were found to have reacted as indicated by IR monitoring. The toluene was removed by rotary evaporation, and the excess ligand was removed by distillation at 95°C and 0.02 mbar to yield the product, **PL3**, as a clear liquid. This was found to have 74% of the reactive sites replaced, producing a polymer with 7.9 mol% functionalisation. Analysis (%): Found (Required for 74% replacement)- C, 38.3 (38.5); H, 9.17 (9.06); N, 2.65 (2.66). I.R (cm^{-1}): δ(Si-O-Si), 1020. N.M.R (ppm) ($CDCl_3$): ^1H, -0.17-0.07 (m, Si-Me), 0.44-0.50 (m, Si-CH_2), 1.60 (m, Si-$CH_2C\underline{H_2}$), 2.21 (s, N-Me_2), 2.27 (s, N-Me), 2.40-2.48 (m, N-$C\underline{H_2}CH_2$-O), 2.51-2.60 (m, N-$(CH_2)_2$-N), 3.33-3.38 (t, J = 6.96 Hz, CH_2-O), 3.48-3.53 (t, J = 6.06 Hz, O-CH_2).

Reactions between **CP2** and **L2** and **L18** were also carried out whereby a mixture of **CP2** (1.5 g, 0.75 mmol) and ligand (2.7 mmol) were stirred with a catalytic amount of **C3** in a flame dried flask at 90°C for 12 hours, or until the reaction proceeded no

further. The remaining reaction mixture was distilled at 100°C and 0.1 mbar to remove the excess ligand. The residue was then filtered through celite yielding the functionalised products described below.

b) The reaction with **L2** yielded the product, **PL4**, a yellow liquid that analysis showed to contain 86% of the available Si-H groups replaced, producing a 9.1 mol% functionalised polymer. Analysis (%): Found (Required for 86% replacement)- C, 36.5 (37.1); H, 8.98 (8.92); N, 3.15 (3.15). I.R (cm^{-1}): δ(Si-O-Si), 1020. N.M.R (ppm) ($CDCl_3$): ^1H, 0.02-0.08 (m, Si-Me), 2.27 (s, N-Me_2), 2.31 (s, N-Me), 2.34-2.39 (m, N-$C\underline{H}_2CH_2$-O), 2.48-2.58 (m, N-$(CH_2)_2$-N), 3.74-3.79 (m, CH_2-O).

c) The reaction with **L18** produced a clear liquid, **PL5**, which was shown to have had 91% Si-H replacement by **L18,** affording a 9.7 mol% functionalised polymer. Analysis (%): Found (Required for 91% replacement)- C, 36.7 (35.9); H, 8.61 (8.54); N, 0.00 (0.00). I.R (cm^{-1}): δ(Si-O-Si), 1020. N.M.R: ^1H, 0.02-0.09 (m, Si-Me), 3.35 (s, CH_3), 3.53-3.63 (m, CH_2), 3.81 (m, CH_2).

d) A mixture of **CP2** (1.81 g, 0.91 mmol), **L15** (0.47 g, 1.86 mmol), toluene (3 ml) and five drops of **C2** were stirred in a flame dried sealed tube under a dinitrogen atmosphere at 85°C for 24 hours, after which time no alkenylated substrate was detected. The solvent was removed on a rotary evaporator and the resulting mixture was then heated at 90°C with **L18** (excess) in a flame dried flask under a flow of nitrogen until the intensity of the Si-H stretch in the I.R spectrum decreased no further. Excess **L18** was removed by distillation at 95°C and 0.02 mbar, and the yellow product, **PL6**, was found to have reacted at 86% of the available sites of which **L15** occupied 57.1% (6.1 mol%) and **L18** 28.6% (3.0 mol%). Analysis (%): Found (Required for the above replacement)- C, 41.0 (36.5); H, 8.16 (8.69); N, 3.10 (3.10). I.R (cm^{-1}): δ(Si-O-Si),

1016. N.M.R (ppm) ($CDCl_3$): ^1H, 0.10-0.19 (m, Si-Me), **L15**- 0.56 (m, Si-CH_2), 1.41 (m, Si-$CH_2(C\underline{H}_2)_3$), 1.77 (m, Si-$(CH_2)_4C\underline{H}_2$), 4.22-4.28 (t, J = 7.60 Hz, N-CH_2), 6.86-6.97 (m, aromatic), 7.14-7.18 (d, J = 8.43 Hz, aromatic), 7.56-7.61 (t, J = 8.29 Hz, aromatic), 8.41 (m, aromatic), **L18**- 3.47-3.48 (m, CH_3), 3.65-3.74 (m, CH_2), 3.93 (m, CH_2).

2.1.3.5 Reactions of Ligands with (30-35%)-Methylhydro-(65-70%)-dimethylsiloxane Copolymer (**CP3**)

Both ^1H N.M.R and microanalysis results indicated, that on average **CP3** required at least 9 equivalents of ligand for total replacement. Reactions between **L2** and **L18** and **CP3** were carried out, using 6.8 mmol of ligand, following the procedure used for the analogous reactions with **CP2** above.

a) The reaction with **L2** yielded a yellow liquid, **PL7**, as the product, with 54 mol% replacement of Si-H by **L2**, so affording a polymer with 16.3 mol% loading. Analysis (%): Found (Required for 54% replacement)- C, 37.1 (39.1); H, 8.94 (9.23); N, 5.45 (5.43). I.R (cm^{-1}): δ(Si-O-Si), 1032. N.M.R (ppm) ($CDCl_3$): ^1H, 0.04-0.06 (m, Si-Me), 2.19-2.20 (m, N-Me_2), 2.25 (m, N-Me), 2.35-2.37 (m, N-$\underline{C}H_2CH_2$-O), 2.47-2.53 (m, N-$(CH_2)_2$-N), 3.73-3.75 (m, CH_2-O).

b) The reaction with **L18** yielded a clear liquid, **PL8**, as the product that had 86% of the available Si-H groups replaced, so producing a polymer with 25.7 mol% loading of ligand. Analysis (%): Found (Required for 86% replacement)- C, 38.6 (41.0); H, 8.36 (8.77); N, 0.00 (0.00). I.R (cm^{-1}): δ(Si-O-Si), 1022. N.M.R (ppm) ($CDCl_3$): ^1H, 0.05-0.10 (m, Si-Me), 3.36 (m, O-CH_3), 3.63 (m, CH_2), 3.80 (m, CH_2).

2.1.4 Metallation Reactions

2.1.4.1 Metallation of Ligands and Ligand-Functionalised Trisiloxanes

The ligands **L1-L17** and model trisiloxanes **MSL1-MSL6** and **MSL8-MSL11** were metallated with copper(II) chloride, and in some cases copper(II) nitrate, following the general procedure below:

An ethanolic solution of copper(II) salt (5 ml solvent, 10 mmol copper salt) was added to an ethanolic solution of ligand (10 ml solvent, 10 mmol ligand), and the mixture stirred vigorously for 30 minutes. The metallated ligands were then purified as follows:

a) The ligands **L1, L3-L8** and **L10-L17** produced metallated salts that were insoluble in ethanol. They were filtered off, dried and analysed without further purification. Products from the reactions involving **L2** and **L9** were soluble, and so isolation and purification of the products was undertaken as follows.

Dichloromethane was added to the metallated salt of **L2** to precipitate the product, which was filtered off and analysed. (Note: If the metallation reaction is carried out using MeCN as a solvent, then the product may be collected by filtration from the reaction mixture)

The metallated salt of **L9** was redissolved in the minimum amount of methanol and then ether was added to initiate crystallisation. On standing, the pure product that was formed was filtered off and analysed. The analytical data for these products are given in Tables 8 & 9, section 3.1.3.

b) The model siloxanes, **MSL1-MSL6**, **MSL8-MSL11**, gave products that were soluble in ethanol. Ethanol was removed from the reaction medium by rotary evaporation, and the residue treated with excess dichloromethane. Filtration removed any excess copper(II) salt, and evaporation of the filtrate afforded the pure product.

The experimental data for these reactions are summarised in Table 10, section 3.1.3.

2.1.4.2 Metallation of Functionalised Polymers

The functionalised polymers **PL1** and **PL2** were metallated with $CuCl_2$. An ethanolic solution of the polymer (10 ml solvent, 10 mmol equivalent of functionalised ligand) and an ethanolic solution of copper(II) chloride (10 ml solvent, 9 mmol copper(II) chloride) were mixed and stirred for 24 hours in order to produce a metallated polymer with a maximum of 90% of the available ligands metallated. Ethanol was evaporated and the metallated polymer was washed with cold water (3 x 10 ml) to remove any free copper(II) chloride.

2.2 X-RAY CRYSTALLOGRAPHIC STUDIES

Dr. M.F. Mahon, Department of Crystallography, carried out solid-state structure determinations on $CuCl_2$ complexes of **L2, L4, L9, L10, L12, L17** and a $Cu(NO_3)_2$ derivative of **L10** using single crystal X-ray diffraction. Molecular structures are illustrated in section 3.2, Figures 1-7. All data were measured on a CAD 4 automatic four-circle diffractometer in the range $2 \leq \theta \leq 24^{\circ}$ at room temperature and the relevant crystallographic data are presented in Table 4. Data were corrected for Lorentz and polarisation but not for absorption in all cases. The thermal ellipsoids in Figures 1-7 are shown at the 30% probability level.

The structures of **L2, L10, L12**/$CuCl_2$ and **L10**/$Cu(NO_3)_2$ were solved by Patterson methods and **L9, L17**/$CuCl_2$ were solved by Direct methods, all being refined using the SHELX[129,130] suite of programs. The structure of **L4**/$CuCl_2$ was solved using SHELX86[130] and refined using SHELX93[131]. In the final least squares cycles all atoms were allowed to vibrate anistropically. Hydrogen atoms were included for:

L2/$CuCl_2$ - at calculated positions on the carbon atoms, the hydroxyl protons could not be located satisfactorily.

L4/$CuCl_2$ – at calculated positions where relevant, except on the solvent molecule.

L9/$CuCl_2$ - at calculated positions in all cases except for the allylic protons (H9, H101, H102) which were located in the penultimate Difference Fourier and refined at a fixed distance of 1.07 Å from the parent atoms (C9, C10). The chiral integrity of the molecule as presented is considerably greater than 99% based on the Hamiltonian significance test.

L10/$CuCl_2$ - in an advanced Difference Fourier map and refined at a fixed distance (0.98 Å) from the relevant parent atoms.

L10/$Cu(NO_3)_2$ - at calculated positions except in the case of H51, H61 and H62 (attached to C5 and C6 respectively). These protons were located in an advanced Difference Fourier and refined at a distance of 0.96 Å from the relevant parent atoms.

L12/$CuCl_2$ - at calculated positions except for H141, H151 and H152 (attached to olefinic carbons C14 and C15). These protons were located in an advanced Difference Fourier and refined at a distance of 0.96 Å from the relevant parent atoms. The lattice was also contained some residual solvent straddling the centre of symmetry at 0, 0.5, 0.5. Due to disorder, this fragment did not approximate to anything recognisable, and the best results were obtained by 'mopping-up' this electron density as partial isotropic carbon atoms (C1', C2' with occupancies 0.48 and 0.31 respectively).

L17/$CuCl_2$ - at calculated positions in all cases except for C15, C16 and C17. The difference electron density map exhibited some smudging in the C16/C17 region. This was largely due to the disorder in the positions of these 2 atoms with C16a and C17a in the ratio 62:38.

Table 3: Crystallographic Data for Molecular Structures Determined by X-Ray Diffraction

	L2/$CuCl_2$	**L4**/$CuCl_2$	**L9**/$CuCl_2$	**L10**/$CuCl_2$
Empirical Formula	$C_7H_{18}N_2Cl_2OCu$	$C_{11}H_{10}Cl_2N_2Cu.½CH_3OH$	$C_{10}H_{22}N_2OCl_2Cu$	$C_8H_{18}N_2Cl_2Cu$
Formula Weight	280.71	320.67	320.7	276.7
Space Group	$P2_1/a$	P-1 (No.2)	$P2_12_12_1$	$P2_1/n$
Crystal System	Monoclinic	Triclinic	Orthorhombic	Monoclinic
Unit Cell Dimensions				
a (Å)	8.030(3)	8.3490(10)	8.284(1)	8.546(1)
b (Å)	39.480(8)	10.005(2)	11.609(2)	11.992(2)
c (Å)	8.357(2)	15.425(3)	15.042(1)	12.542(2)
α (deg)		99.35(2)		
β (deg)	118.82(3)	89.95(2)		101.61(1)
γ (deg)		99.59(2)		
Volume (Å^3)	2321.3	1253.1(4)	1446.6	1259.1
Z	4	4	4	4
Density (calc,gcm^{-3})	1.60	1.70	1.47	1.46
F(000)	1160	648	668	572
Absorption Coefficient ($\mu(M_0\text{-}K_\alpha)$) (cm^{-1})	23.2 cm	2.149mm^{-1}	18.7	21.3
Goodness of Fit		0.958		
R	0.0680	0.0418	0.0386	0.0388
R_w	0.0700	0.0970	0.0365	0.0381

	L10/$Cu(NO_3)_2$	**L12**/$CuCl_2$	**L17**/$CuCl_2$
Empirical Formula	$C_8H_{18}N_4O_6Cu$	$C_{15}H_{17}N_3Cl_2Cu$	$C_{17}H_{20}N_2Cl_2Cu$
Formula Weight	329.8	373.8	386.8
Space Group	$P2_1/n$	$P2_1/n$	$P2_1/n$
Crystal System	Monoclinic	Monoclinic	Monoclinic
Unit Cell Dimensions			
a (Å)	8.594(2)	9.031(1)	9.753(2)
b (Å)	13.675(3)	13.518(2)	12.414(2)
c (Å)	12.510(3)	13.891(1)	14.520(2)
α (deg)			
β (deg)	105.92(9)	109.307(9)	97.79(2)
γ (deg)			
Volume (Å^3)	1413.8	1650.3	1741.8
Z	4	4	4
Density (calc,gcm^{-3})	1.55	1.50	1.47
F(000)	684	764	796
Absorption Coefficient ($\mu(M_0\text{-}K_\alpha)$) (cm^{-1})	15.7	16.5	15.6
Goodness of Fit			
R	0.0357	0.0322	0.0322
R_w	0.0388	0.0369	0.0348

2.3 KINETIC STUDIES

2.3.1 Initial Studies

An assessment of the potential of a number of the copper(II) complexes for catalysing the hydrolysis of agents was conducted at the Ministry of Defence laboratories at Porton Down, under carefully regulated safety conditions. Dr Nick Blacker undertook all addition of neat agent to reaction mixtures. The activity of these complexes was identified using pH-stat techniques, through measurement of the percentage of a known quantity of GB (sarin) hydrolysed by a given complex in 30 minutes. Sodium hydroxide, of a known concentration, was mechanically titrated against the HF liberated on hydrolysis of GB. The reaction was kept at 20°C and a constant pH of 6.5. The pH-stat equipment used was a Radiometer Titralab with ABU91 autoburette, ref. 201 reference electrode, and G2040B pH electrode.

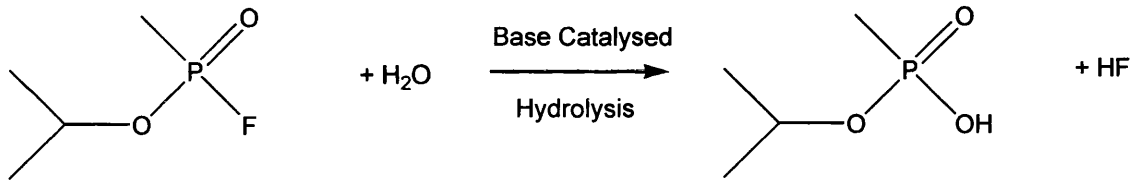

The copper(II) complexes **L1-L11, L13**/$CuCl_2$ and **L8-L11**/$Cu(NO_3)_2$ were prepared as above and used without further purification. The activities of the model metallated siloxane, **L9**/$CuCl_2$ and the copper(II) chloride complexed polymer, **PL1**, were also assessed. A stock solution (3.9×10^{-3} M) of each copper(II) salt was prepared in deionised water and adjusted to pH6.5 in readiness for the hydrolysis reaction, which was carried out using 1 ml of the stock copper(II) solution and an excess (200:1) of agent. The hydrolysis reaction was followed quantitatively for 30 minutes. The results and discussion of these studies are given in section 3.3.1.

2.3.2 Kinetic Studies

Kinetic studies were also conducted as above in the Ministry of Defence laboratories, Porton Down, on the catalytic hydrolysis of GB mediated by a number of siloxane supported copper(II) catalysts. However, studies involving the copper(II) complexes of **MSL8-MSL11** were quickly abandoned when it was discovered that the siloxane-containing materials interfered with the fluoride electrode being used to monitor the reaction. Thus studies using copper(II) complexes of **L9, L15-L17** were carried out in order to assess the rates of decomposition of GB and their relative half-lives of reaction. The equipment used was a ref. 201 reference electrode, PHM95 pH/Ion meter and Radiometer ISE25F fluoride electrode.

Reactions were carried out under similar conditions to those described above, but the pH of the solution was maintained at 6.5 through the use of a buffer. A fluoride electrode was used to determine the amount of liberated fluoride, and the copper(II) complexes were used in approximately 17:1, copper(II) complex:agent molar excess. The hydrolysis reaction was followed quantitatively until all agent had been hydrolysed, or for 30 minutes, whichever was the shorter. The results of these pseudo-first order reaction studies are described in section 3.3.2.

3. RESULTS AND DISCUSSION

The chemistry involved in the decomposition of G-agents (GB, GD, GA) is fairly well defined, and this study concentrated on developing siloxane supported metal catalysts to promote their hydrolysis. If a suitable supported catalyst could be produced for G-agent hydrolysis, then chemical manipulations of the support and/or metal centre might be carried out in a future study to produce catalysts for the decontamination of other agents, such as VX and HD.

Section 1.4.2.1 highlighted copper(II) complexes containing N-donor ligands as being extremely effective catalysts in promoting the hydrolytic decomposition of G-agents and phosphate esters, which are sometimes used as simulants for G- agents[20,42,45-50,57-67]. For example, $t_{1/2}$ for the hydrolysis of the phosphotriester, 2,4-dinitrophenyldiethyl phosphate, is 52 days for a control sample, but only 1.2 minutes in the presence of a copper(II)/2,2'-dipyridylamine catalyst[61]. Table 4 summarises the catalytic effect of various copper(II) catalysts on the $t_{1/2}$ of this phosphotriester.

Table 4: Relative Catalytic Effects of Copper(II) Complexes on the Hydrolysis of 2,4-Dinitrophenyldiethyl Phosphate at 34°C

COMPLEXING AGENT	pH	k_{obs} (s^{-1})	$t_{1/2}$ (min)
N,N,N',N'-tetramethylethylenediamine	7.0	4.48×10^{-3}	2.6
N,N,N'-trimethylethylenediamine (**L3**)	7.0	1.88×10^{-3}	6.1
2,2'-dipyridylamine (**L1**)	7.0	9.21×10^{-3}	1.2
Imidazole (**L6**)	7.0	4.89×10^{-4}	23.6
2,2'-bipyridine	7.0	1.51×10^{-4}	76.5
Control	7.0	1.55×10^{-7}	52 days

As a result, the ligands **L1-L7**, and their copper(II) derivates, were chosen as the basis for the synthetic, structural and catalytic investigations reported in this thesis. For ligands **L1-L5**, facile alkenylation reactions can be carried out on the bridging atoms between the aromatic rings of **L1** (-NH-) and **L4** (-CH_2-), the -OH group of **L2,** and the -NH groups of **L3** and **L5**. Alkenylated forms of **L6** and **L7** can be purchased and used for further synthetic elaboration directly. Alkenylation permits attachment of the ligand to a siloxane support using a hydrosilylation procedure, as described previously.

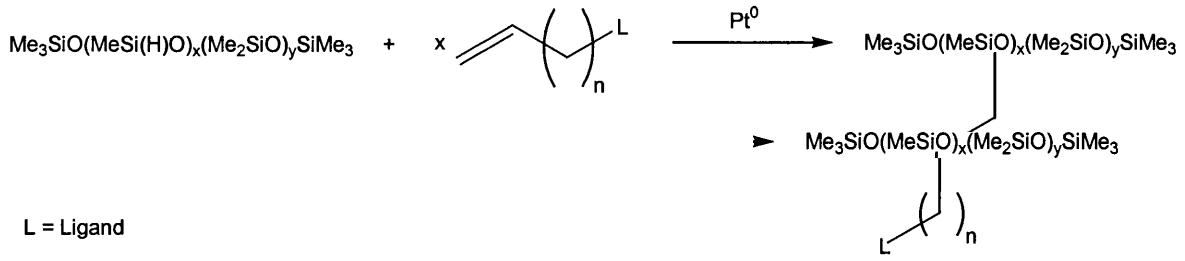

3.1 CATALYST PREPARATION

3.1.1 Alkenylation Reactions of Ligands L1 – L5

Deprotonation of the ligands was achieved using the strong bases, potassium *t*-butoxide, *n*-butyllithium or phenyllithium to remove a proton from -NH (**L1**, **L3**, **L5**), bridging -CH_2- (**L4**), or -OH (**L2**) groups. This was followed by addition of either allyl bromide or 6-bromo-1-hexene to the ligand anion, as described in Chapter 2. The difference in the alkenyl chain length allowed for an investigation into the effects on reactivity of both short (3 carbons) and long (6 carbons) spacer chains, between the ligand and the support. After work-up, the alkenylated products were isolated as stable liquids that were easily purified and handled. Table 5 summarises the analytical data on the products **L8-L12** and **L15-L17**.

Table 5: Analytical Data on Alkenylated Products L8-L12, L15-L17

LIGAND	REACTANTS	YIELD	ν(C=C) (cm^{-1})	^{1}H N.M.R (CH=C$\underline{H}_2$)	^{1}H N.M.R (C$\underline{H}$=CH_2)	^{13}C N.M.R (CH=$\underline{C}H_2$)	^{13}C N.M.R ($\underline{C}$H=CH_2)
L8	**L1** + potassium *t*-butoxide / allyl bromide	35%	1643	5.07 – 5.21	5.97 – 6.06	115.4	134.5
L9	**L2** + potassium *t*-butoxide / allyl bromide	66%	1647	5.14 – 5.30	5.84 – 5.98	116.6	134.6
L10	**L3** + *n*-butyl lithium / allyl bromide	37%	1643	5.10 – 5.20	5.80 – 5.95	117.3	135.6
L11	**L4** + phenyl lithium / allyl bromide	65%	1641	4.90 – 5.05	5.69 – 5.79	116.3	136.2
L12	**L5** + potassium *t*-butoxide / allyl bromide	56%	1643	5.15 – 5.27	5.87 – 5.99	117.8	135.2
L15	**L1** + potassium *t*-butoxide / 6-bromo-1-hexene	28%	1639	4.89 – 5.00	5.70 – 5.86	114.3	136.9
L16	**L3** + *n*-butyl lithium / 6-bromo-1-hexene	56%	1641	4.91 – 5.03	5.72 – 5.85	114.3	138.6
L17	**L4** + phenyl lithium / 6-bromo-1-hexene	68%	1639	4.85 – 4.97	5.67 – 5.82	114.1	138.7

Products were purified by column chromatography, with the exception of **L16** and **L17**, as this technique gave better separation than distillation. Moderate yields of the required products were achieved in most cases, but only low yields of **L8**, **L10**, and **L15**. The low yields of products **L8** and **L15** can be accounted for by multiple product formation from [**L1**-H]$^-$, as both N-alkenylation and C-alkenylation of the aromatic rings is likely, as is apparent from the canonical forms for [**L1**-H]$^-$ shown below.

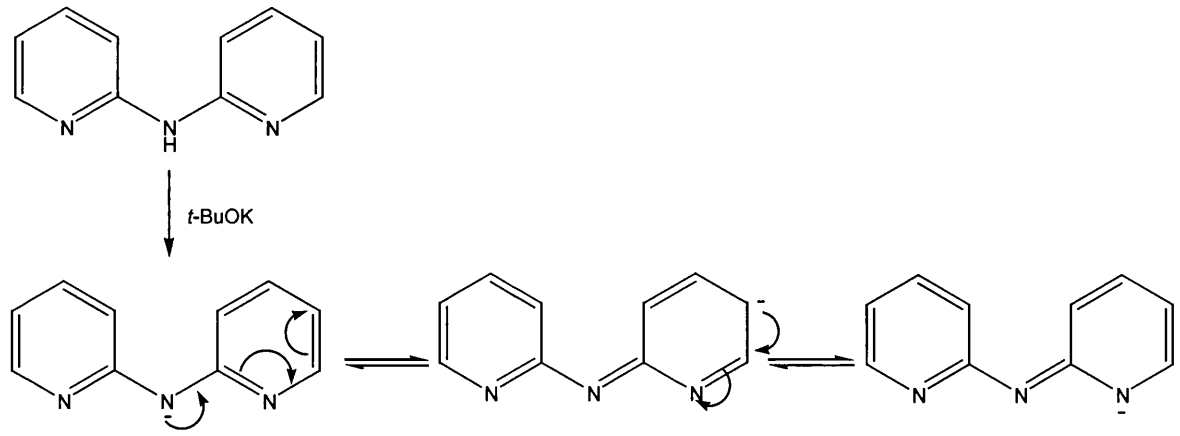

The IR spectrum of all the alkenylated products showed the alkene stretching mode between 1639 and 1647 cm^{-1}, typical of 1-alkenes[132]. The C-H stretching vibration of the alkenylated ligands, which normally occurs in the region 3050 – 3150 cm^{-1} [133], was observed between 3067 – 3080 cm^{-1} in **L8-L17**. Thus, the infrared spectral properties of the alkene group are not affected to any great extent by the ligand terminus.

^{13}C N.M.R spectra of the hexenyl substituted ligands showed -CH=$\underline{C}H_2$ and -$\underline{C}$H=CH_2 resonances with chemical shifts between 114.1-114.3 ppm and 136.2-138.7 ppm respectively, and for the allyl substituted ligands, between 115.4-117.8 ppm and 134.5-136.2 ppm. The equivalent chemical shifts for 1-hexene occur at 114.1 and 139.1 ppm, and for propene at 115.4 and 135.7 ppm[133].

Proton chemical shifts for -CH=C$\underline{H}_2$ and -C$\underline{H}$=CH_2 groups in 1-alkenes occur in the regions 4.6-5.0 ppm and 5.2-5.7 ppm respectively[132]. In comparison to these typical values, variances are observed in the ^1H spectra of the alkenylated ligands. The allyl modified ligands, **L8-L12**, show chemical shifts significantly downfield of the above values i.e. 5.07-5.30 ppm compared to 4.6-5.0 ppm, and 5.80-6.06 ppm compared to 5.2-5.7 ppm. This can be ascribed to the electron withdrawing nature of the nitrogen (**L8, L10, L12**) and oxygen (**L9**) atoms to which the short alkenyl chains are attached. The downfield chemical shifts

for **L11** are smaller as the carbon to which the allyl chain is attached is less electron withdrawing than the heteroatoms in the other ligands.

A similar but much weaker effect is observed in hexenyl-substituted ligands, in which the heteroatoms and $-CH=CH_2$ moieties are separated by a $-(CH_2)_4-$ chain. Changes in electron density on alkenylation of the ligands may also affect the positive charge at the copper(II) centres on complexation. As a result, the activity of complexes derived from alkenylated ligands (particularly those with C_3 chains) may be adversely affected compared with their non-alkenylated analogues, as the most active catalytic systems have the most electropositive metal ions, as described in section 1.4.2.1[64]. Both the steric bulk, and in one case the H-bonding capability, of the alkenylated and non-alkenylated ligands will also differ. These other factors may also play a significant role in modifying the catalytic properties of their copper(II) derivatives.

3.1.2 Siloxane Functionalisation Reactions

Hydrosilylation reactions between the alkenylated ligands and the model trisiloxanes, 1,1,1,3,3,5,5-heptamethyltrisiloxane (**MS1**) and 1,1,1,3,5,5,5-heptamethyltrisiloxane (**MS2**), were successful under carefully controlled conditions, and the products were generally isolated in reasonable yields. All of the model siloxane/ligand products are stable liquids, which are easily stored, handled and are miscible with common organic solvents. A summary of the products, purification methods, and analytical data are given in Table 6.

Yields of between 54% and 67% were achieved in the addition of ligands with a spacer chain length of 3-carbon atoms, with the exception of **MSL12**, which is detailed below. However, with the exception of **L16**, spacer chain lengths of 6-carbon atoms afforded

products in higher yields of 72% - 92%. It is probable that the steric bulk of the ligands, in close proximity to the unsaturation in of the short chain compounds, may impede the hydrosilylation reaction.

Table 6: Summary of the Model Siloxane Hydrosilylation Reactions

PRODUCT (Length of spacer chain)	REACTANTS	PURIFICATION	YIELD	C, H, N ANALYSIS ACTUAL % (EXPECTED %)		
				C	H	N
MSL1 (3)	**MS1+L8**	Distilled at 175°C and 0.05 mbar	54%	55.5 (55.4)	8.35 (8.13)	9.70 (9.69)
MSL2 (6)	**MS1+L9**	Distilled at 135°C and 0.075 mbar	91%	49.5 (49.9)	11.1 (10.8)	6.60 (6.85)
MSL3 (3)	**MS1+L10**	Distilled at 130°C and 0.05 mbar	63%	48.7 (49.4)	11.2 (11.1)	7.55 (7.68)
MSL4 (3)	**MS1+L11**	Distilled at 160°C and 0.07 mbar	67%	57.8 (58.3)	8.40 (8.38)	6.50 (6.47)
MSL5 (3)	**MS1+L13**	Distilled at 130°C and 0.05 mbar	64%	47.3 (47.2)	9.41 (9.15)	8.30 (8.47)
MSL6 (6)	**MS1+L16**	Distilled at 130°C and 0.04 mbar	68%	52.6 (53.1)	11.5 (11.4)	6.80 (6.89)
MSL7 (6)	**MS1+ 6-Bromo-1-Hexene**	Distillation at 175°C and 0.02 mbar	92%	40.8 (40.5)	8.85 (8.63)	0.00 (0.00)
MSL8 (6)	**MS2+L15**	Distilled at 185°C and 0.05 mbar	86%	58.3 (58.1)	8.80 (8.86)	9.04 (8.83)
MSL9 (6)	**MS2+L9**	Distilled at 120°C and 0.05 mbar	72%	49.0 (49.9)	10.7 (10.8)	6.75 (6.85)
MSL10 (6)	**MS2+L16**	Distilled at 120°C and 0.04 mbar	54%	52.6 (53.1)	11.3 (11.4)	6.80 (6.89)
MSL11 (6)	**MS2+L17**	Distilled at 135°C and 0.01 mbar	83%	60.6 (60.7)	8.93 (8.92)	5.99 (5.90)
MSL12 (3)	**MS2+L2**	Distilled at 95°C and 0.04 mbar	87%	45.9 (45.9)	10.6 (10.4)	7.75 (7.64)

As steric effects seem to affect hydrosilylation, then it was anticipated that the 3-spacer chain products **MSL1, 3, 4, 5** may not prove as effective hydrolysis catalysts after metallation as their analogues containing a 6-carbon spacer chain. It is relevant to note that Menger *et al.*[20] reported that a catalyst, with a 6-carbon spacer chain between a polystyrene support and a diamine ligand supporting the active metal centre, accelerates hydrolysis of the GD simulant, NPDPP, by 8-fold compared to an analogue with just one carbon atom

between the support and ligand. It was hoped that kinetic studies could be carried out to resolve this issue, but as described in 3.3.2, these studies could not be completed.

An additional reaction was carried out using **L2**, in which the –OH functional group was reacted directly with the Si-H site on the model siloxane, **MS2**. This gave the product **MSL12**, in a yield of 87%.

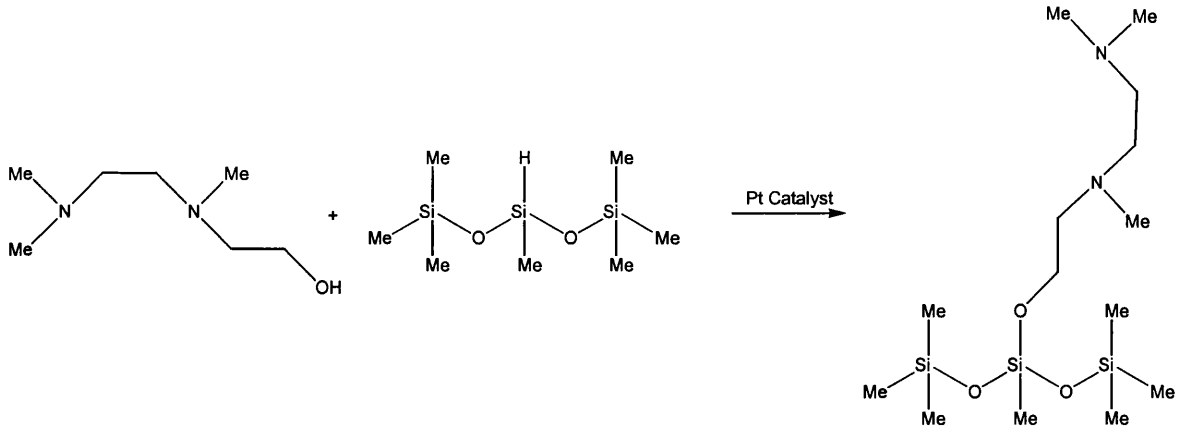

MSL12

This is a facile method for the addition of functional groups to siloxanes, and a good yield was obtained. The reaction does not involve alkene hydrosilylation, and so the reaction is not so readily inhibited by a bulky substituent. As alkenylation of ligands is not always viable, this route provides an alternative method for the modification of siloxanes. Its disadvantage is the formation of a Si-O-C, rather than a Si-C-C bond. The former is more susceptible to nucleophilic attack and hydrolysis than the latter, and so this may be a drawback under some conditions.

The successful reactions between the model trisiloxanes and alkenylated ligands indicated that the commercially available polymers, **CP1**, **CP2**, and **CP3** could also be loaded with these ligands, to produce functionalised polyorganosiloxanes. The range of concentration of active hydrosilylation sites allows the loading of a given ligand on the

polymer to be controlled. This in turn allows the concentration of copper(II) on the polymer to be adjusted to produce the optimum catalyst for a given reaction.

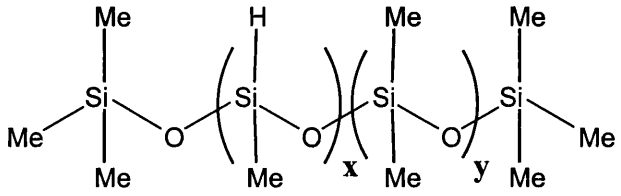

Before use, ^{1}H N.M.R and microanalysis were used to confirm the H-content of the three polysiloxane polymers **CP1**, **CP2** and **CP3** and showed:

CP1 – (3-4%) methylhydro-(96-97%)-dimethylsiloxane; y ~ 172, x ~ 6.7, M_w = 13,320

CP2 – (15-18%) methylhydro-(82-85%)-dimethylsiloxane; y ~ 27.5, x ~ 3.5, M_w = 2,412

CP3 – (30-35%) methylhydro-(65-70%)-dimethylsiloxane; y ~ 19, x ~ 9, M_w = 2,112

Initial loading of each polymer involved a single ligand present in small excess, to ensure complete reaction with all Si-H groups. The ligands **L9** and **L15** were attached using hydrosilylation reactions, and **L2** by reaction of its –OH terminus with the –Si-H groups in the polymer. Triethylene glycol monomethyl ether, **L18**, was also reacted with the polymers in order to determine how this side-chain modified the solubility of the functionalised polymer in polar solvents, including water. A combinational approach was used with sequential loading of **L15** and **L18** onto **CP2**, to afford **PL6**, in order to investigate a route to multi-functional group loading.

These reactions gave the polymer products **PL1** to **PL8** after purification by washing the products with cold methanol to remove any unreacted ligand, and pumping the products *in vacuo* to remove all volatiles. Infrared spectroscopy and ^{1}H N.M.R were used to confirm

the absence of any reactants. Microanalysis and ^{1}H N.M.R were used to characterise the functionalised polymer, and a summary of these data are given in Table 7.

Table 7: A Summary of the Results of Polymer Functionalisation

PRODUCT	REAGENTS	FUNCTIONALITY (% Available Sites Occupied)	MOLAR EQUIVALENT LOADING	C, H, N ANALYSIS ACTUAL % (EXPECTED %) C	H	N
PL1	**CP1+L9**	75%	2.8%	34.3 (34.6)	8.47 (8.46)	1.00 (1.00)
PL2	**CP1+L15**	94%	3.5%	36.8 (37.3)	8.15 (8.16)	1.83 (1.82)
PL3	**CP2+L9**	74%	7.9%	38.3 (38.5)	9.17 (9.06)	2.65 (2.66)
PL4	**CP2+L2**	86%	9.1%	36.5 (37.1)	8.98 (8.92)	3.15 (3.15)
PL5	**CP2+L18**	91%	9.7%	35.9 (36.7)	8.61 (8.54)	0.00 (0.00)
PL6	**CP2+L15+ L18**	86% (**L15** 57%, **L18** 29%)	9.1% (**L15** 6.1%, **L18** 3.0%)	41.0 (36.5)	8.16 (8.69)	3.10 (3.10)
PL7	**CP3+L2**	54%	16.3%	37.1 (39.1)	8.94 (9.23)	5.45 (5.43)
PL8	**CP3+L18**	86%	25.7%	38.6 (41.0)	8.36 (8.77)	0.00 (0.00)

The loading of each polymer was first calculated from the analytical data for nitrogen, using the basic polymer information listed above. Once a loading figure had been calculated this way, carbon and hydrogen microanalytical results, and ^{1}H N.M.R intensities were compared with the theoretical loading based on the nitrogen content. There was close agreement for these data (Table 7), and so these loading figures were used subsequently in copper(II) complexation reactions. Detailed examples can be found in Appendix B. For the polymers **PL5** and **PL8**, where no nitrogen analysis is available, a composition which best fitted the ^{1}H N.M.R intensities was determined, and then compared to the microanalysis results to confirm the composition of the product.

Yields of the organofunctional products were similar to those obtained using trisiloxanes and the same alkenylated ligand, with the exception of **PL7**. It appears that a high degree of

cross-linking occurred during this reaction. No Si-H moieties were present in **PL7** at the end of the reaction, as would be expected had only 54% of the polymer Si-H sites undergone reaction. This may be due to the presence of trace amounts of water in the reaction mixture, and highlights the need for absolutely anhydrous conditions in these reactions.

By using polymers with differing Si-H contents, it has been shown that functional group loadings from 2.8 mol% (or less) to 25.7 mol% can be achieved. Thus the properties of the polymer may be altered specifically to suit the needs of the application. Ligand loadings can be increased through the use of polymers with a greater Si-H content, such as commercially available $Me_3SiO(Si(H)(Me)O)_nSiMe_3$, where n = *ca* 35. The degree of loading can be controlled, within limits, by the amount of ligand added to the reaction mixture and further synthetic manipulation of the product is possible. This has been demonstrated by attaching both **L15** and **L18** to **CP2**, to produce the product **PL6** (below). Both N.M.R and microanalysis confirmed a w:x:y:z ratio of approximately 1:27.5:2:0.5 for this polymer. Detailed information of this calculation is given in Appendix B.

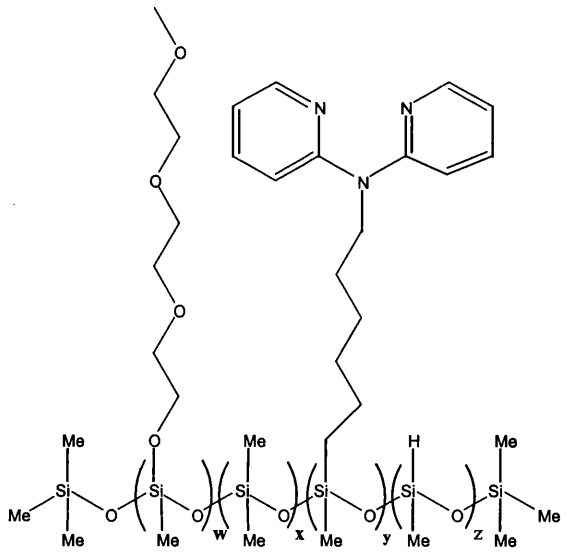

PL6

In excess of 95% of the **L15** added reacts with the polymer, however **L18** fails to cap the majority of remaining reactive sites, as occurs in the other polymers prepared involving this ligand. This may be due to steric hindrance caused by the ligand already present on the polymer.

All of the functionalised polymers are immiscible with water, but it was hoped that a high loading of triethylene glycol monomethyl ether (**L18**) would significantly increase hydrophilicity. However, even polymer **CP3**, containing 25.7 mol% of **L18**, was still essentially immiscible with water. Even so, the ether side-chain may promote the catalytic activity of metallated polymers as it creates a hydrophilic environment adjacent to the ligand/metal centres, whilst leaving the siloxane backbone unaffected and lipophilic. This would be an ideal scenario as increased hydrolytic activity is expected whilst the benefits of a water immiscible support, suitable for application in coatings, is retained. Surfaces so treated might then catalytically neutralise G-agents in the presence of water.

The ethylenediamine derivative **L2** was also chemically bonded, via its –OH terminus, to the polymers **CP2** and **CP3**. Obviously **L2** may be added as one of a number of functional side chains, and it may also be used to 'scavenge' any Si-H sites left after hydrosilylation reactions with the alkenylated ligands, in order to cap these remaining reactive sites with a ligand and so prevent cross-linking of the linear polymeric strands.

3.1.3 Metallation Reactions

Metallation of the ligands and functionalised siloxanes was undertaken using copper(II) salts, as this metal ion has been reported to be the most active species for the catalytic hydrolysis of G-agents[63]. Copper(II) chloride was used to metallate all ligands, and in

addition some copper(II) nitrate complexes were prepared, in order to investigate anion effects on the rate of agent hydrolysis (see section 3.3).

Products formed from the non-alkenylated ligands (**L1-L7**) and copper(II) salts, after reaction in a 1:1 mole ratio ligand:copper(II), are summarised below in Table 8. The products from these reactions are easily separated by filtration from the reaction mixtures with the exception of **L2**/$Cu(NO_3)_2$, which was isolated after removal of solvent, and recrytallisation of the residue from dichloromethane. No further purification of the other products was found necessary, as they were analytically pure after washing and drying. The complexes were generally formed in high yields, as air-stable, easily handled solids, which are soluble in water.

Table 8: Summary of the Metallation Reaction Products for Ligands L1 – L7

REACTANTS	RECOVERY	YIELD (%)	C, H, N ANALYSIS* ACTUAL % (EXPECTED %) C	H	N
L1 + $CuCl_2$	Filter from reaction solution	97	38.8 (39.3)	2.87 (2.97)	13.7 (13.7)
L1 + $Cu(NO_3)_2$	Filter from reaction solution	86	33.8 (33.5)	2.54 (2.53)	19.5 (19.5)
L2 + $CuCl_2$	Use MeCN as solvent and filter off product	81	29.8 (30.0)	6.47 (6.49)	10.0 (9.98)
L2 + $Cu(NO_3)_2$	Remove ethanol, add dichloromethane and filter	77	23.9 (23.9)	5.76 (5.73)	15.9 (15.9)
L3 + $CuCl_2$	Filter from reaction solution	89	25.3 (25.4)	6.07 (5.97)	11.8 (11.8)
L3 + $Cu(NO_3)_2$	Filter from reaction solution	56	20.7 (20.7)	4.91 (4.87)	19.4 (19.3)
L4 + $CuCl_2$	Filter from reaction solution	97	43.3 (43.4)	3.31 (3.63)	8.79 (9.19)
L4 + $Cu(NO_3)_2$	Filter from reaction solution	70	35.2 (35.6)	2.99 (3.22)	15.0 (14.9)
L5 + $CuCl_2$	Filter from reaction solution	91	42.6 (43.2)	3.98 (3.93)	12.5 (12.6)
L6 + $CuCl_2$	Filter from reaction solution	79	17.6 (17.8)	1.98 (1.99)	13.5 (13.8)
L7 + $CuCl_2$	Filter from reaction solution	92	40.9 (41.0)	3.37 (3.45)	9.56 (9.58)

* Calculated values refer to anhydrous 1:1 adducts, except for **L2**/$Cu(NO_3)_2$ and **L4**/$Cu(NO_3)_2$, which are 1:1 monohydrate adducts (-OH absorption evident in IR spectrum), and **L7**/$CuCl_2$, which is a 2:1 anhydrous complex.

Similar reactions were carried out between copper salts and the allyl- (vinyl in the case of **L7**) and hexenyl- chain modified ligands, **L8** – **L17**. Pure complexes were isolated by filtration as before and their analytical data are given below in Table 9. The IR spectra of all of the complexes with -CH=CH_2 containing ligands show absorptions in the region 1633-1653 cm^{-1} for the C=C stretching mode of the free alkenyl group, which is within the range typical for this group[131].

Table 9: Summary of the Metallation Reaction Products for Ligands L8 – L17

REACTANTS	RECOVERY	YIELD (%)	υ(C=C)	C, H, N ANALYSIS* ACTUAL % (EXPECTED %) C	H	N
L8 + $CuCl_2$	Filter from reaction solution	98	1653	44.9 (45.2)	3.73 (3.79)	12.0 (12.2)
L8 + $Cu(NO_3)_2$	Filter from reaction solution	53	1641	39.2 (39.2)	3.19 (3.29)	17.6 (17.6)
L9 + $CuCl_2$	Remove ethanol, redissolve in MeOH, precipitate diethyl ether	85	1635	37.4 (37.4)	6.99 (6.91)	8.51 (8.73)
L9 + $Cu(NO_3)_2$	Remove ethanol, redissolve in MeOH, precipitate diethyl ether	78	1643	32.4 (32.1)	6.24 (5.93)	15.0 (15.0)
L10 + $CuCl_2$	Filter from reaction solution	51	1641	34.6 (34.7)	6.61 (6.56)	10.0 (10.1)
L10 + $Cu(NO_3)_2$	Filter from reaction solution	80	1643	29.2 (29.1)	5.45 (5.50)	17.0 (17.0)
L11 + $CuCl_2$	Filter from reaction solution	74	1641	48.4 (48.8)	4.05 (4.09)	8.00 (8.13)
L11 + $Cu(NO_3)_2$	Filter from reaction solution	78	1633	40.4 (40.4)	3.90 (3.88)	13.4 (13.5)
L12 + $CuCl_2$	Filter from reaction solution	68	1643	48.3 (48.2)	4.61 (4.59)	11.3 (11.2)
L13 + $CuCl_2$	Filter from reaction solution	54	1645	30.9 (29.7)	3.39 (3.33)	11.9 (11.6)
L14 + $CuCl_2$	Filter from reaction solution	95	1633	48.5 (48.8)	4.09 (4.17)	8.05 (8.13)
L15 + $CuCl_2$	Filter from reaction solution	78	1641	49.4 (49.6)	4.88 (4.94)	10.8 (10.8)
L16 + $CuCl_2$	Filter from reaction solution	85	1643	40.3 (41.4)	7.79 (7.59)	8.87 (8.87)
L17 + $CuCl_2$	Filter from reaction solution	87	1639	52.7 (52.8)	5.24 (5.21)	7.10 (7.24)

* Calculated values refer to anhydrous 1:1 adducts, except for **L11**/$Cu(NO_3)_2$, which is a 1:1 monohydrate adducts, and **L14**/$CuCl_2$, which is a 2:1 anhydrous complex.

The final set of metallation reactions involved the functionalised model siloxanes and polymers. Again successful metallation occurred following reactions in a 1:1 ligand:copper(II) molar ratio, with little problem either in the preparation or isolation of the end products. All metallated functionalised model trisiloxanes were purified by dissolution in dichloromethane, and the solution filtered in order to remove excess copper(II) salts. Evaporation of the solvent afforded pure products. A summary of the microanalytical results on these products is provided in Table 10.

Table 10: Summary of Analysis for the Metallation Reaction Products of Functionalised Siloxanes

REACTANTS	ORIGINAL LIGAND	C, H, N ANALYSIS ACTUAL % (EXPECTED %)		
		C	H	N
MSL1 + $CuCl_2$	**L8**	42.2 (42.3)	6.24 (6.21)	7.35 (7.39)
MSL2 + $CuCl_2$	**L9**	37.4 (37.6)	8.28 (8.16)	4.69 (5.16)
MSL3 + $CuCl_2$	**L10**	35.9 (36.1)	8.18 (8.08)	5.64 (5.61)
MSL4 + $CuCl_2$	**L11**	44.4 (44.5)	6.47 (6.40)	4.84 (4.94)
MSL5 + $CuCl_2$	**L13**	32.0 (32.3)	6.91 (6.68)	5.83 (5.80)
MSL8 + $CuCl_2$	**L15**	44.9 (45.3)	6.66 (6.77)	6.88 (6.89)
MSL8 + $Cu(NO_3)_2$	**L15**	41.8 (41.6)	6.16 (6.23)	10.7 (10.6)
MSL9 + $CuCl_2$	**L9**	37.4 (37.6)	8.37 (8.16)	4.90 (5.16)
MSL10 + $CuCl_2$	**L16**	39.7 (39.9)	8.58 (8.57)	4.97 (5.18)
MSL10 + $Cu(NO_3)_2$	**L16**	34.0 (36.4)	7.44 (7.80)	9.54 (9.43)
MSL11 + $CuCl_2$	**L17**	47.3 (47.3)	7.09 (6.95)	4.61 (4.60)

The end products were all waxy solids, which are soluble in water and in many common organic solvents, including ethanol and dichloromethane. The product **MSL5**/$CuCl_2$ appeared to be a monohydrate from the analytical data, and its IR spectrum revealed –OH

absorptions. All products were formed in good yield, and the addition of the siloxane terminus did not have an adverse effect on the complexation of the ligands, although it did not prove possible to obtain crystalline samples of them for X-ray structural analysis.

The polymers **PL1** and **PL2** were both metallated with $CuCl_2$ by stirring the reactants together in ethanol for 24 hours. The resulting blue polymer was washed with water to remove excess copper(II) salts. It was noted that subsequent aqueous washings also contained traces of copper, indicating that metal ions may be leached slowly from the polymer by excess water, and specific studies confirmed that leaching of copper(II) did indeed occur. However, due to time limitations it was not possible to quantify the rate of leaching. Thereafter each metallated polymer was washed twice with a large excess of cold water (50 cm^3) before its activity was assessed in the studies reported in 3.3. The metallated polymers were also soluble in organic solvents, which would allow these materials to be cast as films or deposited as a coating on a solid surface, although this was not attempted in this study.

3.2 X-RAY CRYSTALLOGRAPHIC STUDIES

In order to define the coordination geometry around the copper(II) centre, X-ray studies were carried out on a number of model compounds. As attachment of the alkenyl spacer chain to a polymeric framework is unlikely to significantly affect the primary coordination sphere around the metal centre, the structure determinations reported below reveal important features about the solid-state metal coordination sphere of the copper complexes, which on dissolution yield catalytically active species. Crystals of the copper(II) chloride derivatives of **L2**, **L4**, **L9**, **L10**, **L12**, **L17** and a copper(II) nitrate adduct of **L10** were

prepared for single crystal X-ray diffraction studies, as described in section 2.2. The structures of these molecular complexes are shown in Figures 1-7 below.

As can be seen from the figures, all of the $CuCl_2$ adducts exhibit 5-coordination around the copper atom. In the $CuCl_2$ adducts of **L2**, **L9**, and **L12** the ligand acts as a tridentate, and the compounds contain two Cu-Cl terminal linkages. In the other complexes, in which the N-donor ligand cannot act as a tridentate, 5-coordination is achieved by the formation of one terminal Cu-Cl bond and two Cu-Cl bridges. A similar structural theme occurs in other copper(II) halide complexes[134,135]. In the single nitrate-complex investigated (**L10**/$Cu(NO_3)_2$) the metal centre attains 6-coordination with each nitrato-group behaving as a bidentate ligand.

Figure 1: Structure of L2/Copper(II) Chloride Dimer*

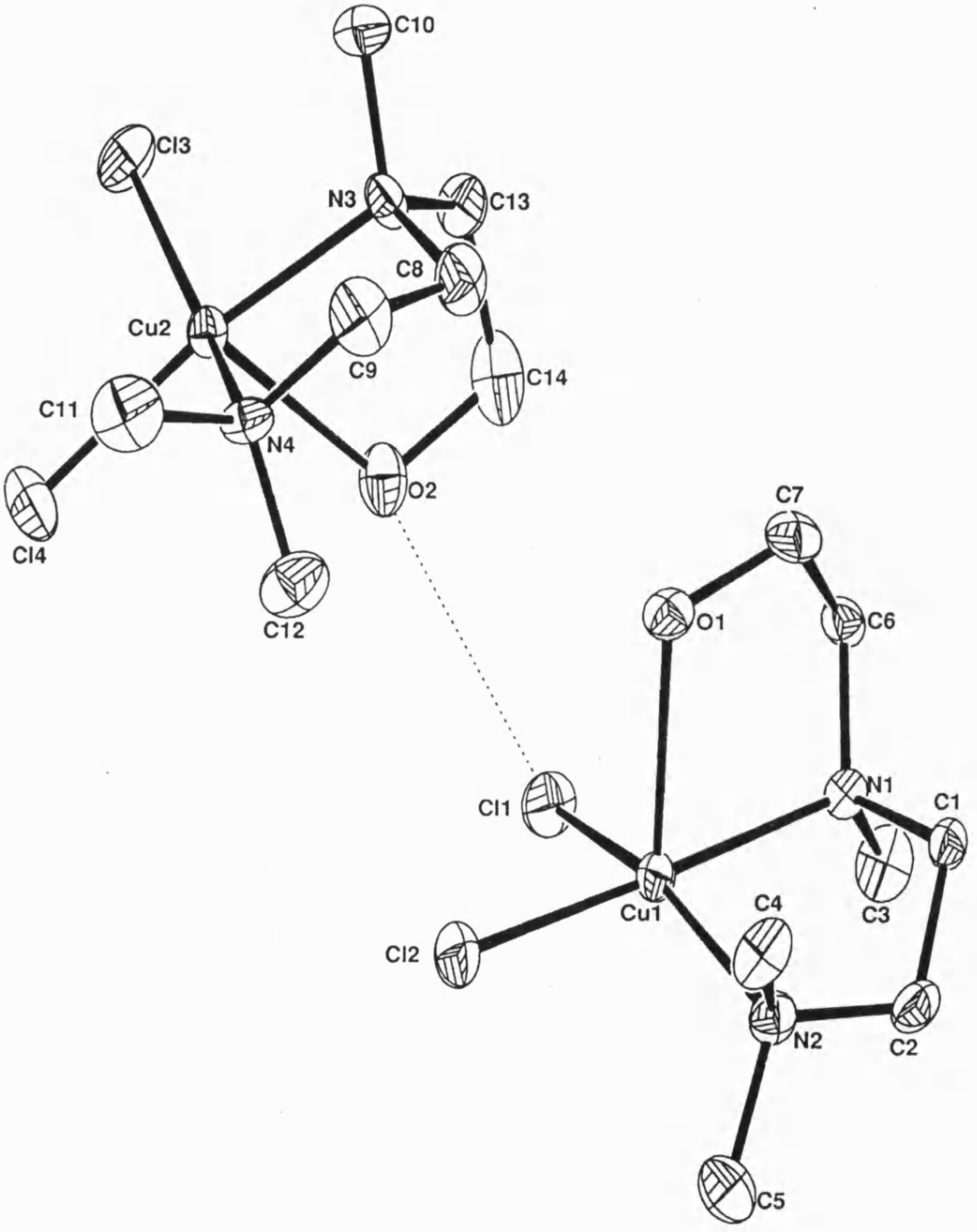

* Unfortunately, the hydroxyl protons could not be located satisfactorily.

Figure 2: Structure of L9/Copper(II) Chloride

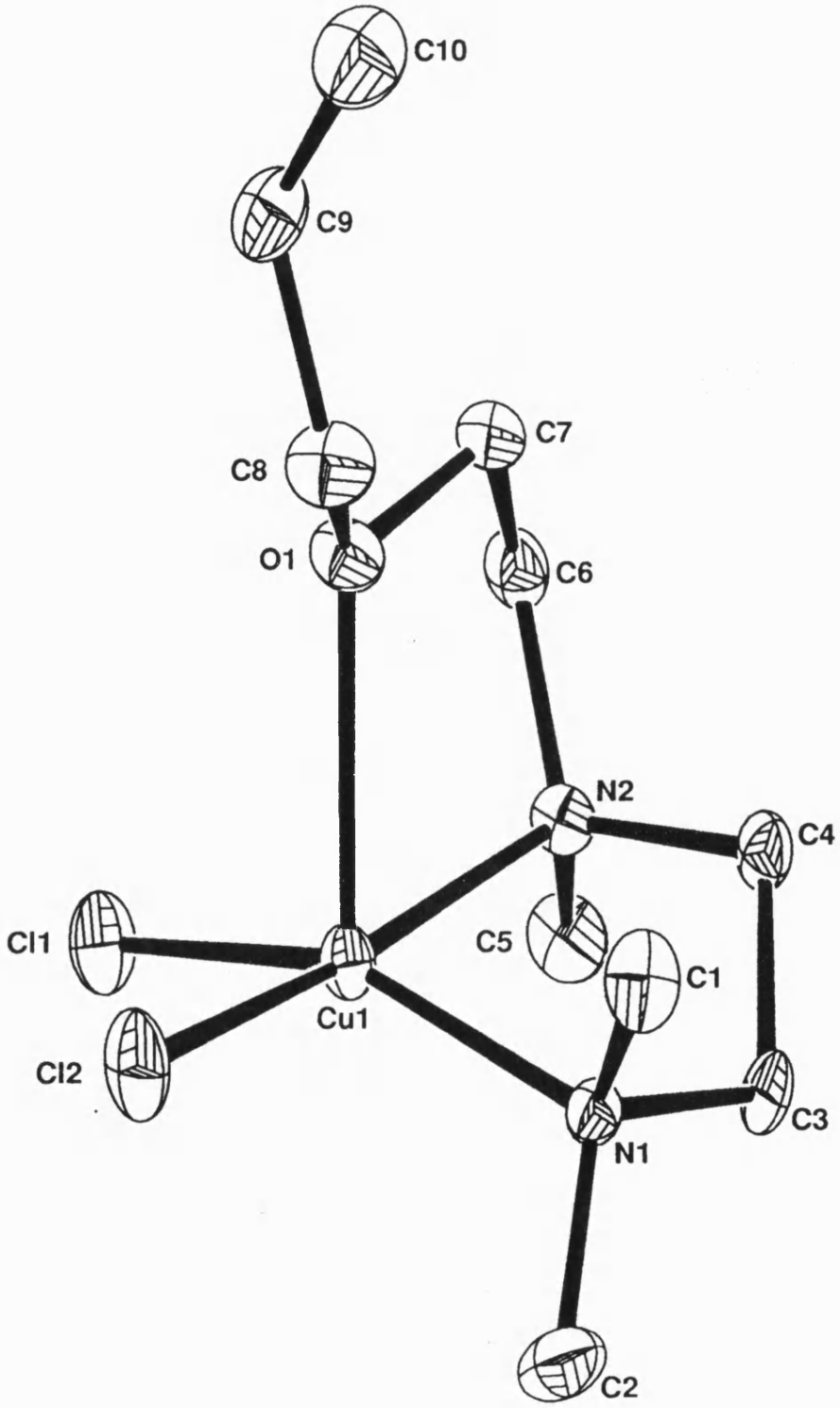

Figure 3: Structure of L4/Copper(II) Chloride Dimer

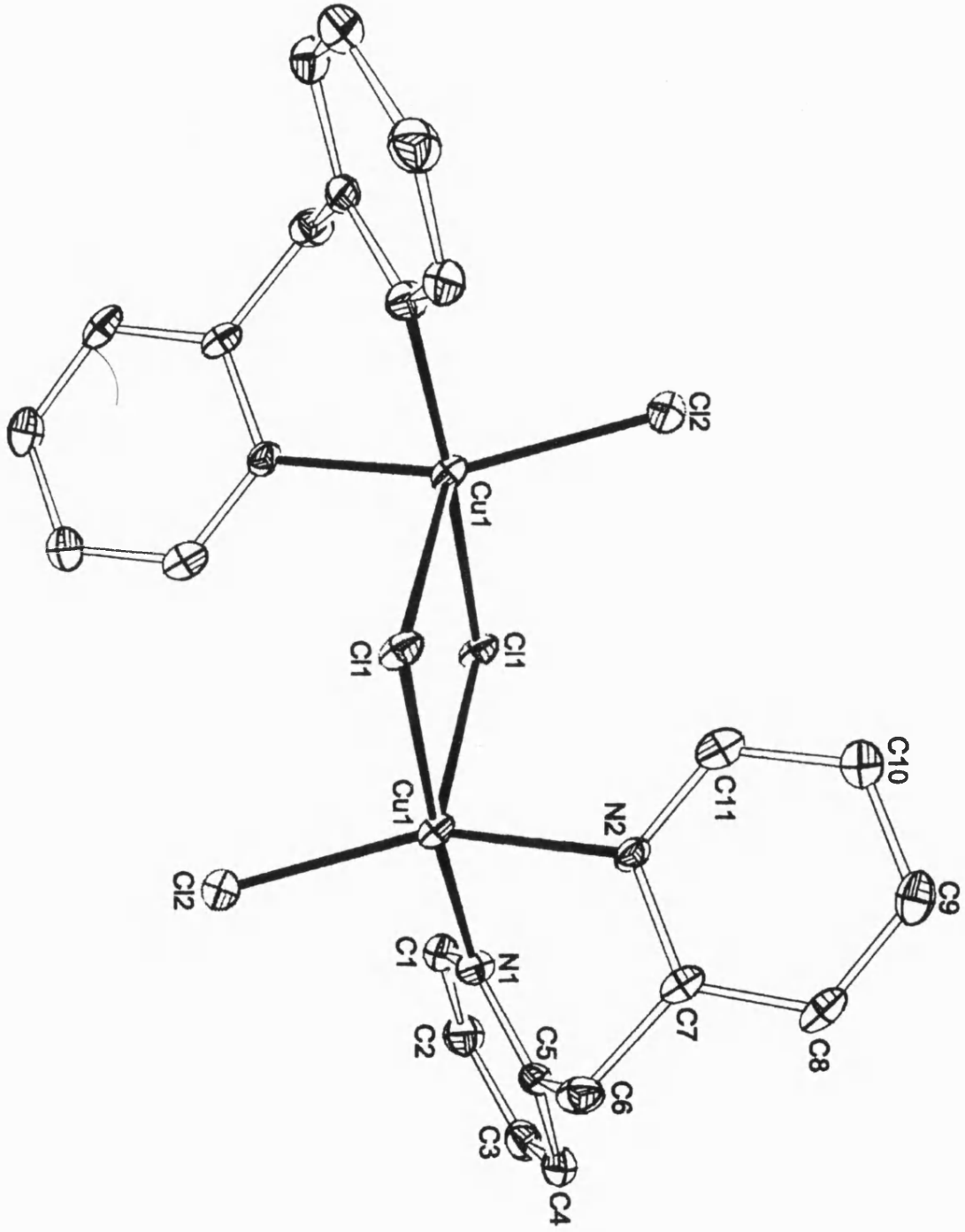

Figure 4: Structure of L17/Copper(II) Chloride Dimer

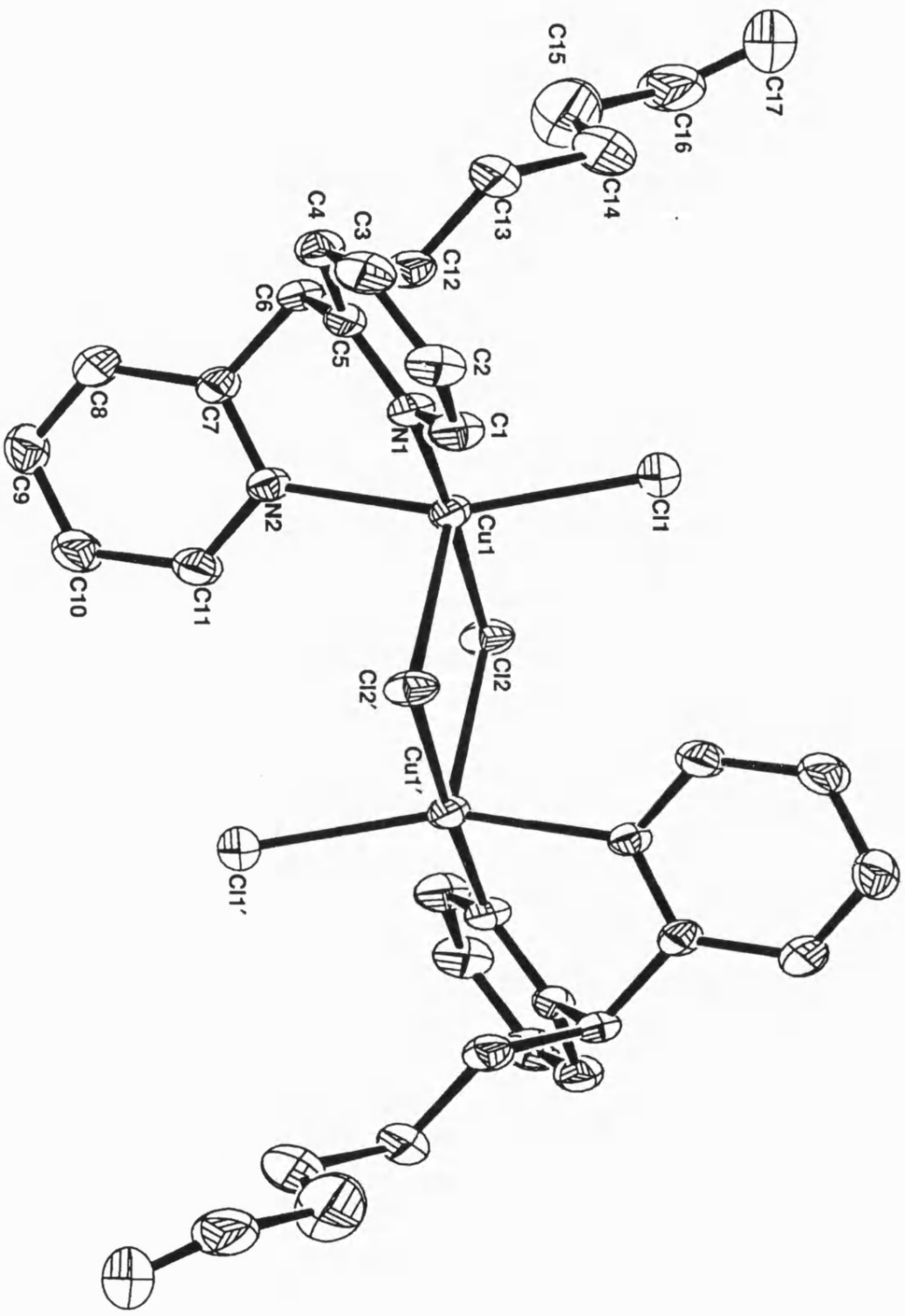

Figure 5: Structure of L12/Copper(II) Chloride

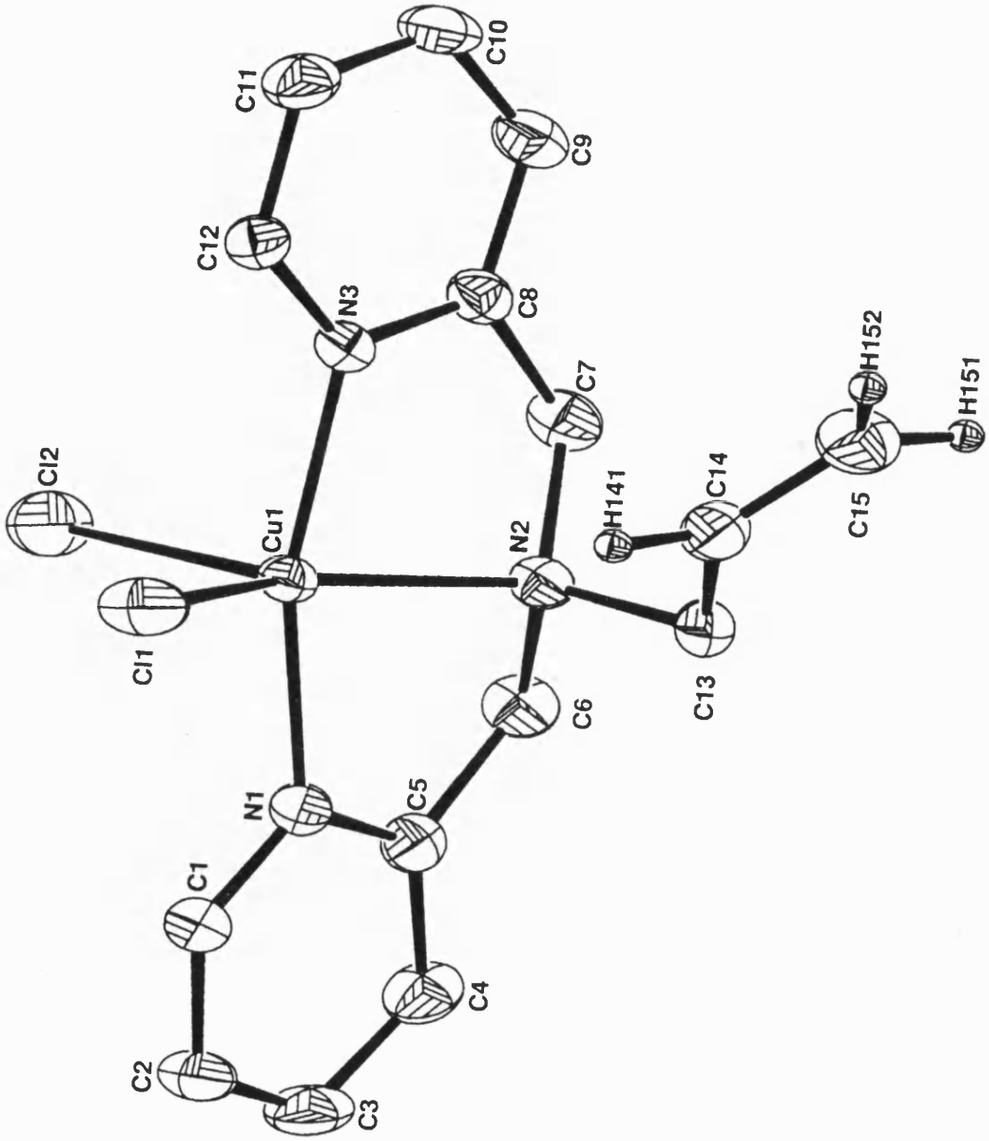

Figure 6: Structure of L10/Copper(II) Chloride Dimer

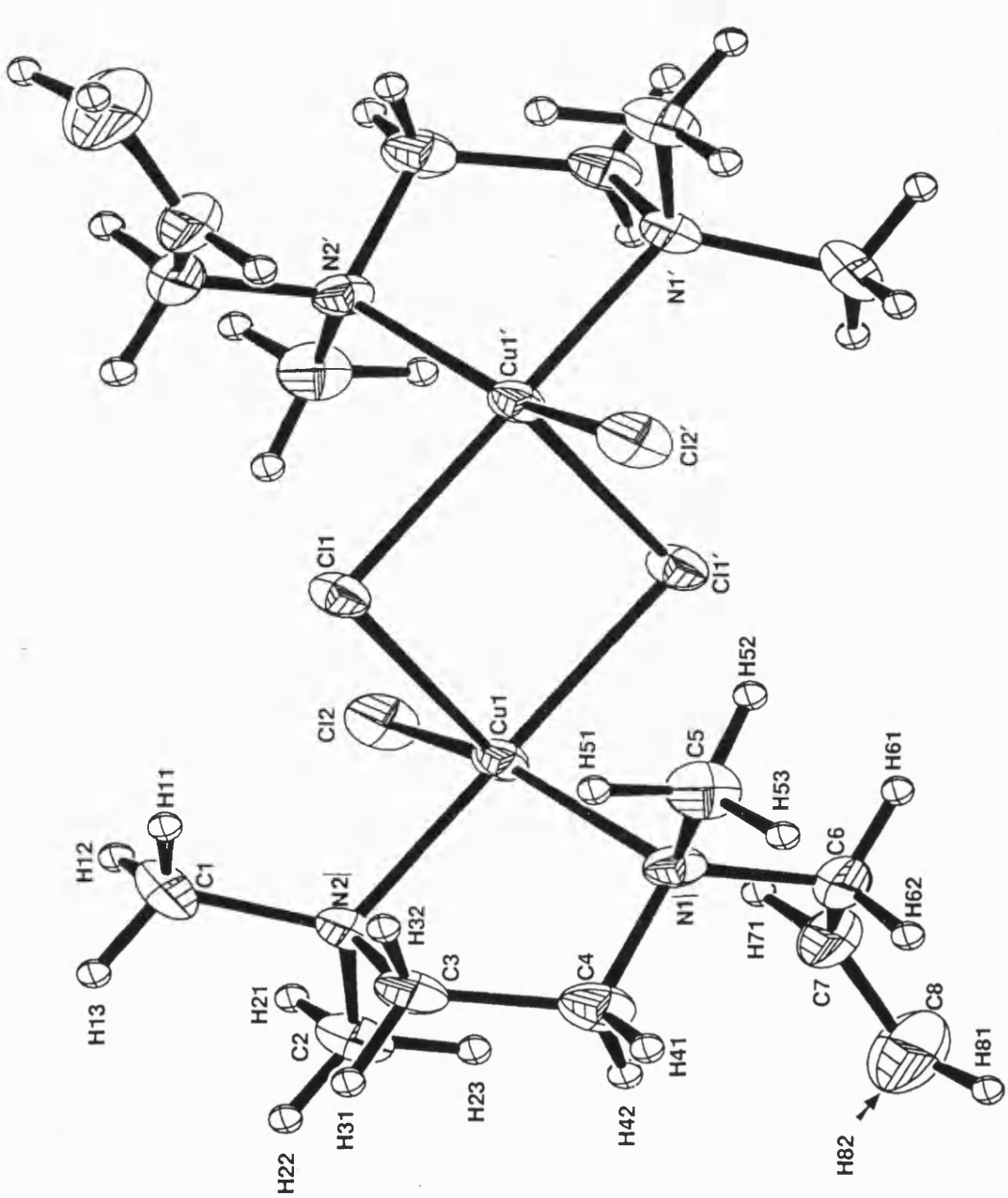

Figure 7: Structure of L10/Copper(II) Nitrate

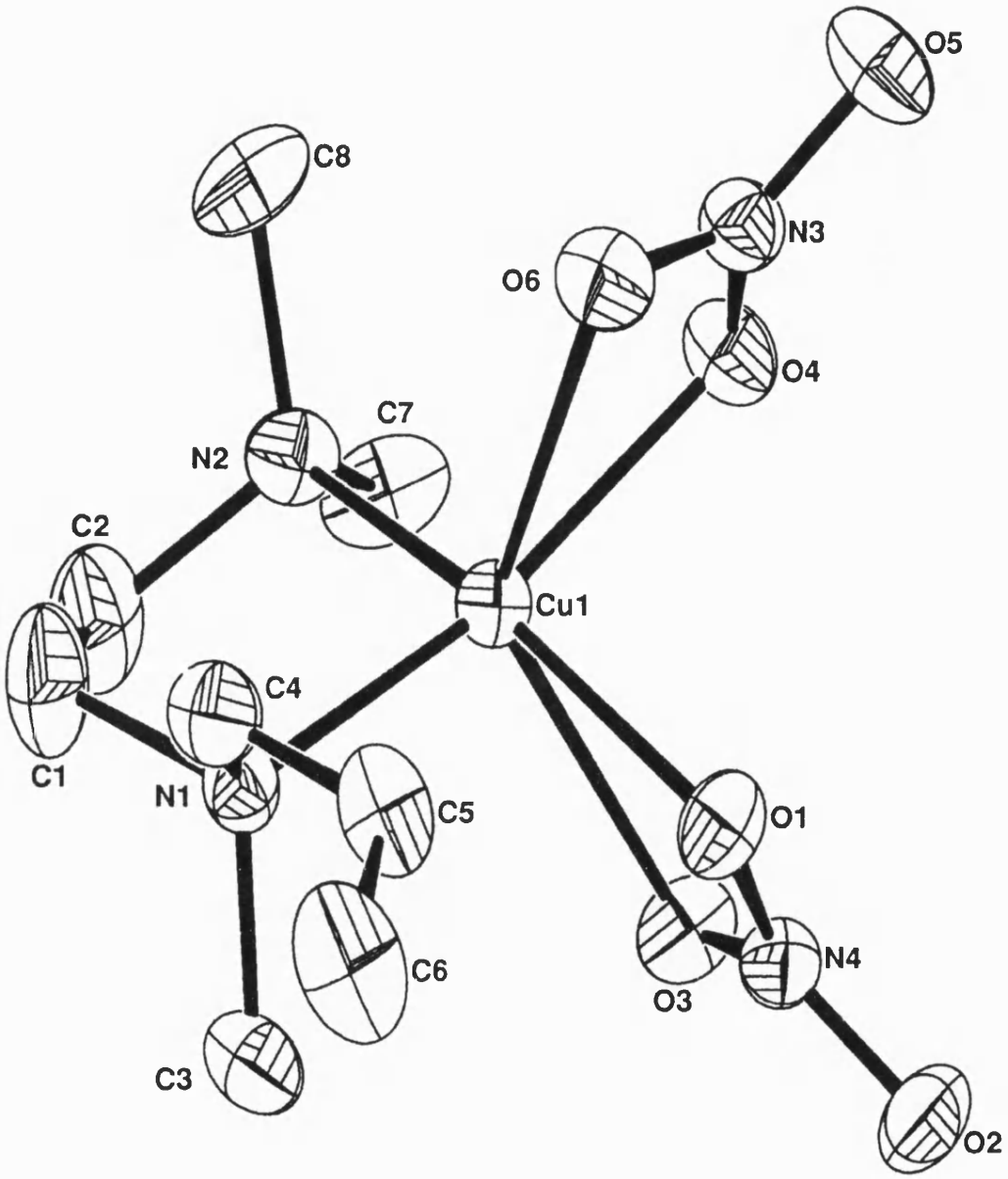

By far the largest group of five-coordinate copper(II) complexes exhibit structures based on regular square-based pyramidal or trigonal bipyramidal geometries[136]. There is a striking resemblance between the two geometries if the trigonal bipyramid is viewed down the C_2 axis and the square planar structure down the C_4 axis[137]. However, the idealised geometry of either of these two geometries is rarely found in practice, and structures are normally distorted from the idealised forms.

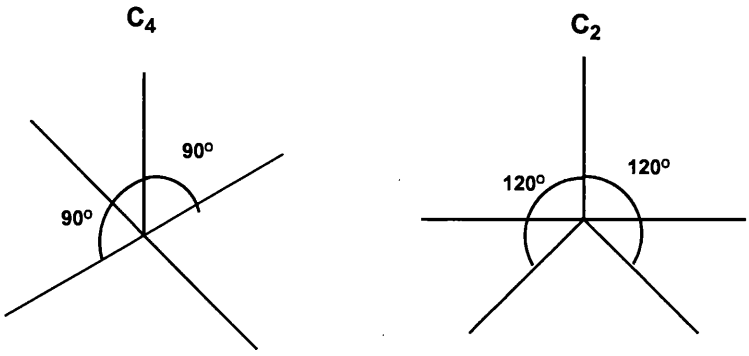

There have been many attempts to explain what factors govern the structure of a given penta-coordinate copper(II) complex. These include consideration of the relative stability of the two idealised forms[138], consideration of the interaction between bonding electron pairs and non-bonding d-electrons of the metal[139], and π-bonding factors[140]. The results of these studies gave rise to the definition of three forms of distortion from an idealised square pyramidal structure to describe the formation of intermediate, distorted species, and ultimately the idealised trigonal bipyramidal structure[141].

1. All four basal bonds depressed from apical atom to give a distorted square pyramid.
2. Two basal bonds depressed away from the apical atom towards a trigonal bipyramidal geometry.
3. One basal bond is distorted from the apical atom to give an intermediate structure.

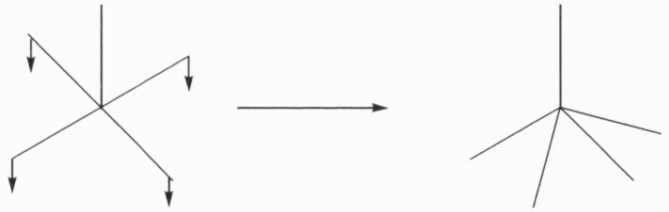

1.

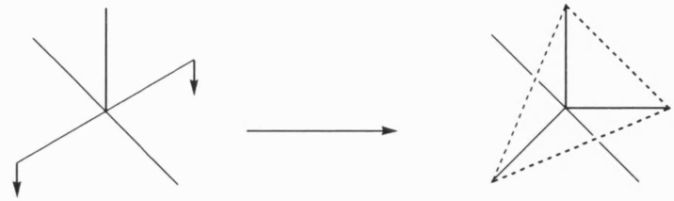

2.

3.

The degree of distortion of the structures determined in this study are assessed using a measure τ, which is a measure of the trigonal distortion away from an idealised square pyramidal stereochemistry. The value of τ is defined in the equation below, where 100% distortion means that the complex is exactly trigonal bipyramidal in shape[142].

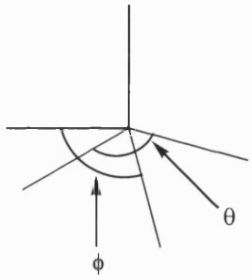

$$\tau = \frac{\theta - \phi}{60} \times 100$$

A summary of the key bond lengths and angles in the immediate coordination sphere around the copper(II) metal centres of the six copper(II) chloride complexes, whose structures were determined in the course of the project, are listed below in Table 11.

Table 11: Summary of the Bond Lengths and Angles in the Coordination Sphere Around the Copper(II) Centre of the $CuCl_2$ Complex Structures Defined*

COMPLEX	BOND LENGTHS (Å)					BOND ANGLES		
	Cu-N_1	Cu-N_2	Cu-Cl_1	Cu-Cl_2	Cu-X**	σ (°)	ϕ (°)	τ (%)
L2/$CuCl_2$ (2 molecules in asymmetric unit)	2.068 (9)	2.108 (14)	2.307 (7)	2.253 (5)	2.383 (9)	173.7 (3)	157.9 (3)	**26.3**
	2.056 (9)	2.072 (14)	2.266 (7)	2.260 (5)	2.474 (10)	171.3 (3)	157.4 (3)	**23.2**
L4/$CuCl_2$	2.027 (5)	2.029 (5)	2.311 (2)	2.259 (2)	2.630 (2)	176.1 (2)	153.0 (14)	**38.5**
L9/$CuCl_2$	2.079 (8)	2.088 (7)	2.254 (4)	2.264 (4)	2.393 (7)	169.0 (2)	155.2 (2)	**23.0**
L10/$CuCl_2$	2.098 (7)	2.050 (7)	2.303 (4)	2.260 (4)	2.764	174.0 (2)	150.3 (2)	**39.5**
L12/$CuCl_2$	2.004 (5)	2.084 (5)	2.270 (3)	2.467 (3)	2.003 (5)	163.3 (1)	145.7 (1)	**29.3**
L17/$CuCl_2$	2.016 (5)	2.048 (5)	2.264 (3)	2.284 (3)	2.789	175.9 (1)	155.3 (1)	**34.3**

*Complete details of all bond lengths and angles in these structures are listed in Appendix A.

X = N (L12**/$CuCl_2$), O (**L2**/$CuCl_2$, **L9**/$CuCl_2$), Cl (**L4**/$CuCl_2$, **L10**/$CuCl_2$, **L17**/$CuCl_2$)

3.2.1 The Structures of L2/$CuCl_2$ and L9/$CuCl_2$

The structure of **L2**/$CuCl_2$ (Figure 1) consists of two molecules within the unit cell. These are bound together by a hydrogen-bond between the proton attached to O(2) and atom Cl(1) (unfortunately, the hydroxyl protons could not be located satisfactorily). As a consequence the pair of molecules in the asymmetric unit are not identical. The Cu(1)-Cl(1) bond length of 2.307(7) Å, is slightly longer than the other Cu-Cl bonds in the structure (2.253(5)-2.266(7) Å). In addition, the Cu(2)-O(2) bond length of 2.474(10) Å is much longer than the comparative Cu(1)-O(1) separation of 2.383(9) Å. The lengthening of these bonds can be ascribed to the hydrogen-bonding between the two molecules in the unit cell.

L2/$CuCl_2$ is based on a square pyramid and the N(2)-Cu(1) bond is depressed out of the basal plane, away from the apical O(1) atom. The undistorted angle of 180° has been compressed to 157.9(3)° along N(2)-Cu(1)-Cl(1). The N(1)-Cu(1)-Cl(2) bond is relatively undistorted at 173.7(3)°. The average value of τ for the two molecules of **L2**/$CuCl_2$ is 24.8%, showing moderate distortion of the square pyramid structure towards a trigonal bipyramidal structure.

The molecular structure of **L9**/$CuCl_2$ (Figure 2) is essentially similar to that of **L2**/$CuCl_2$, with respect to the primary coordination sphere around the metal atom. However, no hydrogen-bonding occurs following the addition of the alkenyl chain to the apical oxygen atom of the ligand. The Cu-N and Cu-Cl bond lengths for **L9**/$CuCl_2$ and **L2**/$CuCl_2$ lie between 2.056(9)-2.108(14) Å and 2.253(5)-2.307(7) Å respectively (Table 11). These distances fall within the ranges observed for other typical ethylenediamine/copper(II) complexes[143-145]. The Cu(1)-O(1) bond length of 2.393(7) Å in

L9/$CuCl_2$ is very similar to that found in **L2**/$CuCl_2$ at 2.383(9) Å. Both bonds involving apical oxygen atoms are, as expected, longer than those found for basal Cu-O bonds[146-148].

Trigonal distortion of the **L9**/$CuCl_2$ complex takes place along the N(1)-Cu(1)-C1(1) bond, such that the undistorted angle of 180° is compressed to 155.2(2)°. The Cl(2)-Cu(1)-N(2) bond in **L9**/$CuCl_2$ at 169.0(2)° is slightly less than the equivalent N(1)-Cu(1)-Cl(2) angle of 173.7(3)° in **L2**/$CuCl_2$. This may indicate depression of all four basal bonds, and the distortion ratio, τ, of 23.0%, which is slightly less than that for **L2**/$CuCl_2$ would support this. However, the major distortion occurs by depression of one bond (Cu(1)-N(1) away from the apical atom), as in **L2**/$CuCl_2$.

Both **L2**/$CuCl_2$ and **L9**/$CuCl_2$ have two *cis*-orientated coordination sites, containing labile Cl atoms, which after Cl^- loss in aqueous solution, would be available to facilitate the copper(II) catalysed hydrolysis of G-agents by the mechanism described previously[65]. Therefore the tridentate behaviour of **L2** and **L9** should not impede the activity of either complex, as the Cu(1)-O(1) bond is formed in the axial position.

3.2.2 The Structures of L4/$CuCl_2$, L17/$CuCl_2$ and L10/$CuCl_2$

The chloride bridged structures adopted by **L4**/$CuCl_2$ (Figure 3), **L10**/$CuCl_2$ (Figure 6), and **L17**/$CuCl_2$ (Figure 4), exhibit very similar geometries and primary coordination spheres. The structures consist of discrete dimeric $[Cu(ligand)Cl_2]_2$ units, which are well separated from each other. The bridging Cu(1)-C1(1)-Cu(1')-C1(1') (**L4**/$CuCl_2$, **L10**/$CuCl_2$) and Cu(1)-C1(2)-Cu(1')-C1(2') (**L17**/$CuCl_2$) arrangements are strictly planar; there being a crystallographic inversion centre in the middle of each dimeric unit.

After a detailed literature search, it was found that the structure of **L4**/$CuCl_2$ had been reported previously[149]. A comparison of the parameters of the reported structure, and the structure determined for **L4**/$CuCl_2$ in this study, is given below in Table 12.

Table 12: Comparison of the Literature and Determined L4/$CuCl_2$ Structures

PROPERTY	LITERATURE L4/$CuCl_2$	DETERMINED L4/$CuCl_2$
Empirical Formula	$C_{11}H_{10}Cl_2N_2Cu$	$C_{11}H_{10}Cl_2N_2Cu.½CH_3OH$
Space Group	$P2_1/c$	P-1
Crystal System	Monoclinic	Triclinic
Unit Cell Dimensions		
a (Å)	8.7444(25)	8.3490(10)
b (Å)	12.1243(36)	10.005(2)
c (Å)	11.6478(22)	15.425(3)
β (deg)	104.425(19)	89.95(2)
Volume ($Å^3$)	1195.96(53)	1253.1(4)
Z	2	4
Density (calc, g cm^{-3})	1.69	1.70
Bond Lengths (Annotation as per derived structure)		
Cu(1)-N(1)	2.033(2)	2.027(5)
Cu(1)-N(2)	2.034(2)	2.029(5)
Cu(1)-Cl(1)	2.315(1)	2.311(2)
Cu(1)-Cl(2)	2.261(1)	2.259(2)
Cu(1)-Cl(1#)	2.629(1)	2.630(2)
Bond Angles (Annotation as per derived structure)		
N(1)-Cu(1)-Cl(1)	175.3(1)	176.1(2)
N(2)-Cu(1)-Cl(2)	150.7(1)	153.02(14)
N(2)-Cu(1)-Cl(1#)	102.7(1)	96.93(14)
Cl(2)-Cu(1)-Cl(1#)	106.6(1)	109.81(6)
Maximum deviation from 90.0° between equatorial and axial atoms	4.2°	4.75°

The product reported in the literature was prepared by addition of anhydrous $CuCl_2$ to a degassed solution of ligand in freshly distilled methanol in a 1:1 mole ratio. The reaction mixture was refluxed under a dinitrogen atmosphere and the structure determined on the dark green crystals formed on cooling the solution. Our product was prepared as described in 2.1.4, and it was recrystallised from a methanol/diethyl ether mix held at 5°C. The product formed in this study crystallises with methanol in the lattice, which accounts for

differences in the basic crystal data such as space group, crystal system and unit cell dimensions.

The structures from the two determinations have the same basic shape, described as a distorted trigonal bipyramidal in the literature report[149]. Atoms Cl(1) and N(1) occupy the axial positions with the equatorial positions occupied by Cl(2), N(2) and Cl(1#). Measurements made in the literature structure show that the equatorial atoms define a plane with a deviation of no more than 0.015 Å, and attempts to define a square planer geometry using N(1), N(2), Cl(1) and Cl(2) as a base, give a poorly defined plane with a deviation of more than 2 Å for most of the atoms.

Corresponding bond lengths in the two structures are very similar (Table 12), but bond angles differ noticeably in a number of cases, and by over 5° in the case of N(2)-Cu(1)-Cl(1#). These differences may reflect the presence of the methanol molecule, and indicate that deformations are influenced by minor changes in the bonding forces operative in the solid-state.

It would seem that two basal bonds distort towards a trigonal bipyramidal geometry to give a distortion ratio of 38.5%, which describes only a moderate distortion from a square planar arrangement. A ratio of over 50% would be expected if the structure were better described as distorted trigonal bipyramidal, and so the structure is better described as a distorted square pyramid using this method.

The geometry around the copper(II) atom in **L17**/$CuCl_2$ is similar to that found in **L4**/$CuCl_2$, and bond angles around the copper are also similar. The hexenyl derivative, **L17**/$CuCl_2$, shows slightly longer Cu(1)-Cl(1 and 2) bond lengths than those in **L4**/$CuCl_2$, and the **L17**/$CuCl_2$ Cu(1)-Cl(1#) bond length is significantly longer at 2.789 Å, compared

to 2.630 Å for **L4**/$CuCl_2$ (Table 11). The Cu(1)-N(1 and 2) bonds appear to be more tightly bound in **L17**/$CuCl_2$, as they show slightly shorter bond lengths of 2.016(5) Å and 2.048(5) Å compared with those in **L4**/$CuCl_2$, at 2.027(5) Å and 2.029(5) Å. This effect may result from the weak electron donating effect of the hexenyl chain, so increasing the electron donating capacity of the pyridinyl nitrogen atoms. The ^{13}C N.M.R data provide some support for this conjecture, as the chemical shift of the bridging carbon (**C1**) increases with the addition and lengthening of the alkenyl chain, as does the shift of **C2** (Table 13). This effect alone is expected to reduce the electropositivity of the copper(II) centre, and so moderate the reactivity of 2,2'-dipryidylmethane/copper(II) complexes.

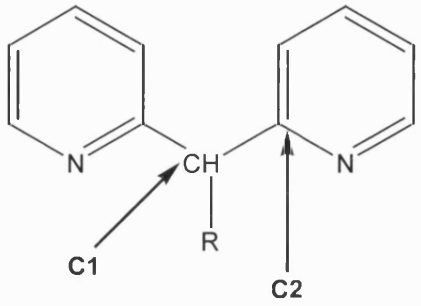

Table 13: ^{13}C Chemical Shifts of Selected Carbon Atoms in 2,2'-Dipyridylmethane and Analogues

	2,2'-Dipyridylmethane	2,2'-Dipyridylmethane, Allylic Derivative (L11)	2,2'-Dipyridylmethane, Hexenyl Derivative (L17)
C1 (as above)	46.9	55.6	56.0
C2 (as above)	159.1	162.0	162.8

The ability of both **L4**/$CuCl_2$ and **L17**/$CuCl_2$ to adopt chlorine-bridged structures in the solid-state indicates that, sterically at least, both have the ability to form inactive hydroxy-

bridged compounds in aqueous solution. This would reduce their overall activity as catalysts for the hydrolysis of phosphate esters.

The N-allyl derivative of the trimethylethlyenediamine copper(II) complex, **L10**/$CuCl_2$ (Figure 6), is also a chlorine-bridged dimer and has a similar geometry to those of the dipyridylmethane complexes, **L4**/$CuCl_2$ and **L17**/$CuCl_2$. Distortion occurs through the depression of the N(1) and Cl(2) atoms, and the distortion ratio of 39.5% again supports the argument that the geometry is best described as a distorted square pyramid, although it does show the greatest distortion of this group of complexes towards trigonal bypyramidal. The base of the square pyramid is formed by N(1), N(2), Cl(2) and Cl(1'), with Cl(1) in the apical position. The N(2)-Cu(1)-Cl(1') bond angle is relatively undistorted at 174.0(2)°, whereas the N(1)-Cu(1)-C1(2) angle at 150.3(2)°, compared with the regular angle of 180°, indicates significant distortion towards a trigonal bypyramid.

The Cu-Cu' separations of 3.797 Å (**L10**/$CuCl_2$) and 3.752 Å (**L17**/$CuCl_2$) and out-of-plane Cu-C1(1') (**L10**/$CuCl_2$), Cu-C1(2') (**L17**/$CuCl_2$) distances of 2.764 Å and 2.789 Å respectively fall within the range of values observed for other known dichloro-bridged complexes[144,150,151]. The in-plane Cu-Cl distances of 2.303(4), 2.260(4) Å, for **L10**/$CuCl_2$, and 2.264(3), 2.284(3) Å, for **L17**/$CuCl_2$, are normal, with the bridging Cu-Cl bond slightly longer, as expected (Table 11). The Cu-N(1 and 2) bond lengths in **L10**/$CuCl_2$ are similar to those in the previous structures.

Ligands such as 2.2'-bipyridine and 2,2'-bipyridylamine generally form shorter Cu-N bonds than ethylenediamine ligands, due to the additional electron density available for bonding to the copper from the delocalised π-system of the pyridine ring[152-155]. The Cu-N(1 and 2) bond lengths of 2.016(5)-2.048(3) Å in the dipyridylmethane/copper(II) complex,

L17/$CuCl_2$, are noticeably shorter than those in the trimethylethylenediamine complex, **L10**/$CuCl_2$, as expected. Thus the copper(II) ion will become less electropositive, and so it is expected that the complexes containing pyridine ring systems will be less active as hydrolysis catalysts than analogous ethylenediamine complexes[64].

3.2.3 The Structure of L12/$CuCl_2$

On first sight **L12**/$CuCl_2$ (Figure 5) also shows distortion from a trigonal bipyramidal geometry, with Cl(2), Cl(1) and N(2) in the equatorial plane and N(1) and N(3) in axial positions. The N(2)-Cu(1)-C1(1) bond, at 145.7°, shows the least angular distortion from the expected trigonal bipyramidal equatorial angle of 120°. However, the angle between the axial atoms, N(1)-Cu(1)-N(3) at 163.3(1)° (Table11), deviates more than those found in the other defined structures in this study. This indicates distortion through depression of all four basal atoms to produce a distorted square pyramidal geometry. The value of τ at 29.3% would support this, and it is notable that the apical Cu-C1(2) bond length of 2.467(3) Å is almost 0.2 Å longer than the basal Cu-C1(1) bond.

The Cu-C1(1), Cu-N(1) and Cu-N(3) bonds at 2.270(3), 2.004(5) and 2.003(5) Å (Table 11) are within the range expected[156], whilst the Cu-N(2) bond is a little longer at 2.084(5) Å than the Cu-N (1 and 3) bonds.

3.2.4 The Structure of L10/$Cu(NO_3)_2$

The structure of the only nitrate complex investigated crystallographically, **L10**/$Cu(NO_3)_2$ (Figure 7), reveals 6-coordination for copper, with two asymmetrically bound bidentate nitrate ligands. Vibrational spectroscopy may often be used to distinguish between unidentate and bidentate nitrate ligands[157], as for bidentate coordination the separation between the two high frequency stretching modes is greater than for unidentate

coordination. The I.R. spectrum of **L10**/$Cu(NO_3)_2$ shows three bands centred at 1460 ν(N=O), 1271 $\nu_a(NO_2)$, and 1016 cm^{-1} $\nu_s(NO_2)$, giving a difference of 189 cm^{-1} between the ν (N=O) and $\nu_a(NO_2)$ modes. This is in keeping with the bidentate nature of the ligand found in the solid-state structure, in which the bidentate nitrate groups are strongly asymmetric with the Cu-O(3) and Cu-O(6) bonds (2.441(5) and 2.402(4) Å) much longer than the equivalent Cu-O(1) and Cu-O(4) bonds (2.011(5) and 2.022(5) Å). Similar observations have been made in related structures, and all bond lengths in **L10**/$Cu(NO_3)_2$ fall within the published ranges for analogues[158-160]. The Cu-N(1) and Cu-N(2) bond lengths are slightly shorter than the analogous bonds in **L10**/$CuCl_2$.

Appendix A contains further details of bond lengths and angles for all structurally characterised complexes. Knowledge of the structures, coordination spheres and especially the structural and electronic effects of ligands and alkenyl chains on the electropositivity of the copper(II) centres, contribute to an understanding of the relative catalytic activity of the complexes towards agents, even though the active solution species will differ from the chloro- and nitrato- complexes characterised in the solid-state.

Attachment of ligands to a trisiloxane unit seems unlikely to prevent dimerisation of their copper(II) chloride analogues through anion bridges. The flexibility of linear siloxane supports may also be sufficient to allow dimerisation of polymer attached analogues, but that remains speculation.

3.3 STUDIES OF CATALYTIC HYDROLYSIS REACTIONS

Two sets of studies, including kinetic studies, have been undertaken in order to identify the relative catalytic activities of the copper complexes described herein for the hydrolysis of G-agents. The activities of the metallated ligands **L1-L7**, a number of their alkenylated derivatives, and an example of each of the metallated functionalised model and polymer siloxane species have been investigated as catalysts for the hydrolysis of the nerve agent, Sarin (GB). This investigation was carried out with Dr N. Blacker (DERA project supervisor), at the Ministry of Defence laboratories, Porton Down.

3.3.1 Catalytic Activity Studies

Initial studies were undertaken in order to obtain catalytic activity information for each ligand complex, and hence identify which are the best catalysts for hydrolysis of GB. These studies were also intended both to identify any trends on changing anion from Cl^- to $[NO_3]^-$, and elucidate the effect of adding an alkenyl chain to the ligand. Reactions were carried out using an agent:catalyst mole ratio of 200:1, except for experiments involving **PL1**, in which a small sample of metallated polymer (0.1 g) was added directly to the reaction solution, approximating to a 20:1 ratio of agent:metal centre.

Reactions were carried out under standard conditions of pH (6.5) and temperature (20°C). The temperature was maintained by the use of a water insulated reaction vessel, through which water was circulated. The pH was kept constant by addition of a standard solution of 2M sodium hydroxide from an auto-titrator, to neutralise the HF and phosphonic acid produced when GB is hydrolysed, as shown in the reaction below. All reactions were carried out for 30 minutes, except for the polymer catalyst reaction, where the reaction time

was 120 minutes. The amount of agent hydrolysed was calculated from the consumption of the standard NaOH solution.

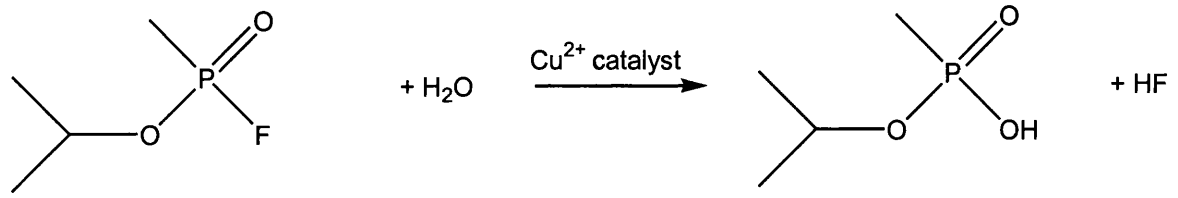

For pH ≥ 6.5, the half-life of GB in water at any temperature and constant pH can be calculated from the equation,

$$\log t_{½} = \frac{5039}{T} - 8.035 - pH$$

where $t_{½}$ is the half-life in hours and the temperature, T, is in K[161]. For a 10°C change in temperature, an approximate fourfold change in the rate of alkaline hydrolysis, at a given pH, is observed[37]. The hydrolysis of GB is at a minimum at pH 6.5 in water, when it has a half-life of approximately 460 hours at 20°C.

In order to calculate the amount of agent hydrolysed in 30 minutes, the theoretical amount of NaOH needed to neutralise the HF and the phosphonic acid produced from 100% decomposition of GB has to be calculated. GB has a molecular weight of 140.1 daltons, and a density of 1.088 g cm^{-3} [38]. During the reaction, exactly 0.1 ml of neat agent is added to the reaction solution. Given this,

Mass of GB (g) = Volume of GB (ml) x Density of GB (g cm^{-3}) = 0.1 x 1.088 = 0.1088 g

and so, the number of moles of GB can be calculated as 7.77 x 10^{-4}.

Before the catalyst was added, a pre-titration was carried out to neutralise traces of acidic impurities within the GB sample. This volume was measured and the equivalent number of moles of GB left for decomposition calculated using the equation below:

No. Moles GB Remaining After Pre-Titration (X) =

$$7.77 \times 10^{-4} - \left(\left\{ \frac{\text{Volume NaOH Used in Pre-Titration (ml)}}{1000} \right\} \times 1.999 \right)$$

Two equivalents of NaOH are needed to neutralise the HF and the phosphonic acid produced by the hydrolysis reaction, consequently $2X$ moles of NaOH are required for total neutralisation. Therefore, the amount of agent decomposed during the reaction can be calculated using the formula below.

$$\text{\% Agent Decomposed} = \frac{\text{Vol. NaOH Used During Hydrolysis (ml)}}{2X} \times 0.1999$$

In order to check that the results were repeatable, reactions involving **L5**/$CuCl_2$ and **L9**/$CuCl_2$ were duplicated, and the data were found to be very similar. For **L5**/$CuCl_2$, the amount of agent hydrolysed was 6.5% and 6.2% in 30 minutes and for **L9**/$CuCl_2$, 73.6% and 73.5%. Reaction time for **L5**/$CuCl_2$ was extended to 60 minutes in one reaction, as little activity compared to complexes containing the other ligands was observed. Reaction times for **MSL9**/$CuCl_2$ and **PL1**/$CuCl_2$ were also extended in order to increase the amount of data collected.

Summaries of the data for the reactions undertaken are given in Table 14 and graphical representations are given in Figures 8-24.

Table 14: The Decomposition of GB Using Copper(II) Catalysts at pH 6.5, 20°C in the Agent:Catalyst Ratio 200:1

CATALYST (Figure No.)	VOL. NaOH USED IN PRE-TITRATION (ml)	VOL. NaOH FOR TOTAL HYDROLYSIS (ml)	VOLUME NaOH USED IN REACTION (ml)	% AGENT DECOMPOSED IN 30 MINUTES
Unmodified Catalysts				
L1/$CuCl_2$ (8)	0.0237	0.7300	0.7078	97.0
L2/$CuCl_2$ (9)	0.0241	0.7292	0.3726	51.1
L3/$CuCl_2$ (10)	0.0247	0.7280	0.5881	80.8
L4/$CuCl_2$ (11)	0.0243	0.7288	0.5328	73.1
L5/$CuCl_2$ (12)	0.0293	0.7188	0.0470	6.5
L5/$CuCl_2$ After 60 minutes	0.0286	0.7202	0.0450 0.0806	6.2 11.2
L6/$CuCl_2$ (13)	0.0173	0.7428	0.2836	38.2
L7/$CuCl_2$ (14)	0.0190	0.7394	0.2875	38.9
Alkenylated Catalysts				
L8/$CuCl_2$ (15)	0.0237	0.7300	0.5940	81.4
L8/$Cu(NO_3)_2$ (16)	0.0194	0.7386	0.6086	82.4
L9/$CuCl_2$ (17)	0.0230	0.7314	0.5380	73.6
L9/$CuCl_2$	0.0248	0.7278	0.5351	73.5
L9/$Cu(NO_3)_2$ (18)	0.0240	0.7294	0.5644	77.4
L10/$CuCl_2$ (19)	0.0198	0.7378	0.6045	81.9
L10/$Cu(NO_3)_2$ (20)	0.0178	0.7418	0.6513	87.8
L11/$CuCl_2$ (21)	0.0171	0.7432	0.5839	78.6
L11/$Cu(NO_3)_2$ (22)	0.0195	0.7384	0.5882	79.7
L13/$CuCl_2$	0.0223	0.7328	0.2488	34.0
Functionalised Siloxane Catalysts				
MSL9/$CuCl_2$ (23) After 60 minutes	0.0262	0.7250	0.5168 0.6204	71.3 85.6
PL1/$CuCl_2$ (24) (120 minutes, 20:1)	0.0191	0.7392	0.4989	67.5

Figures 8 to 14 show the progress of the decomposition of GB for the unmodified ligand complexes.

Figure 8

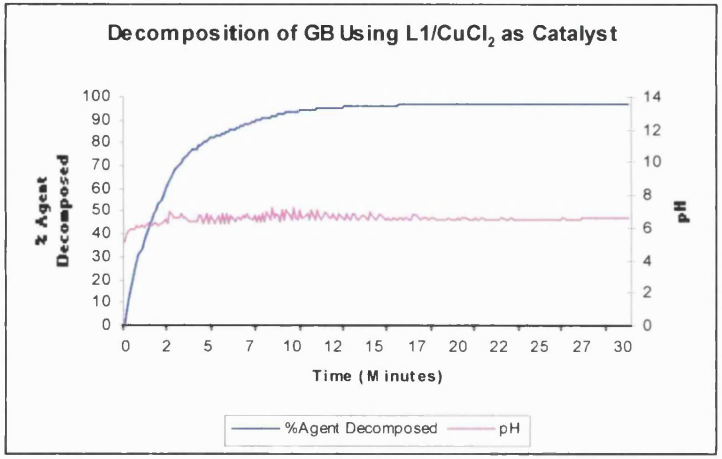

Figure 9

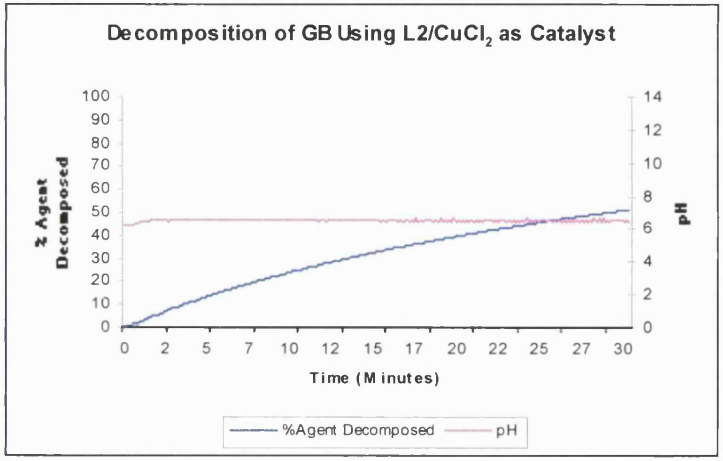

Figure 10

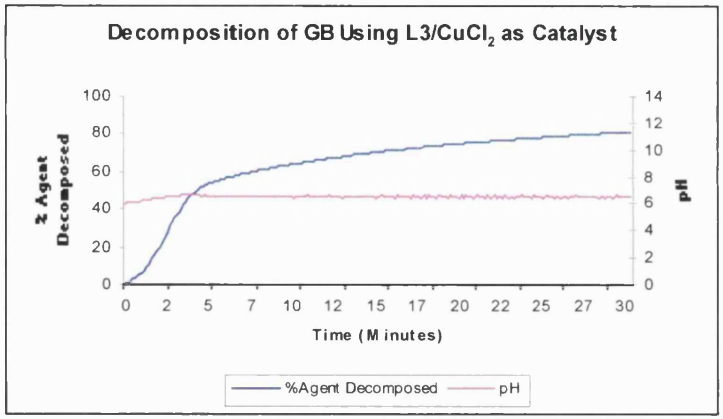

Figure 11

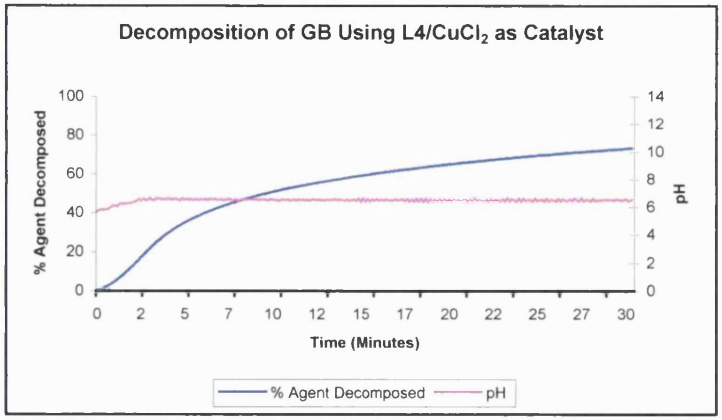

Figure 12

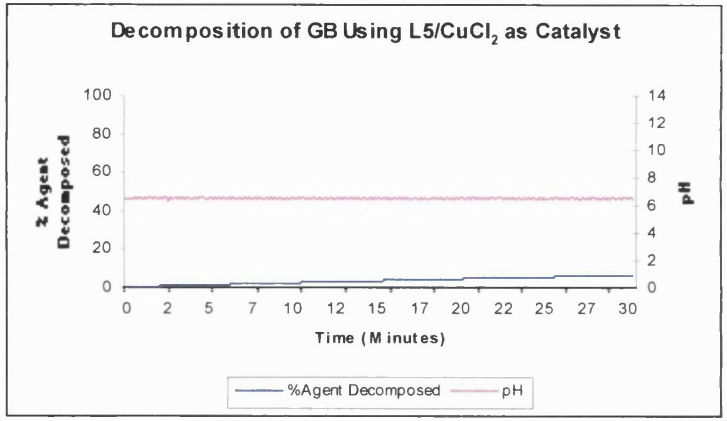

Figure 13

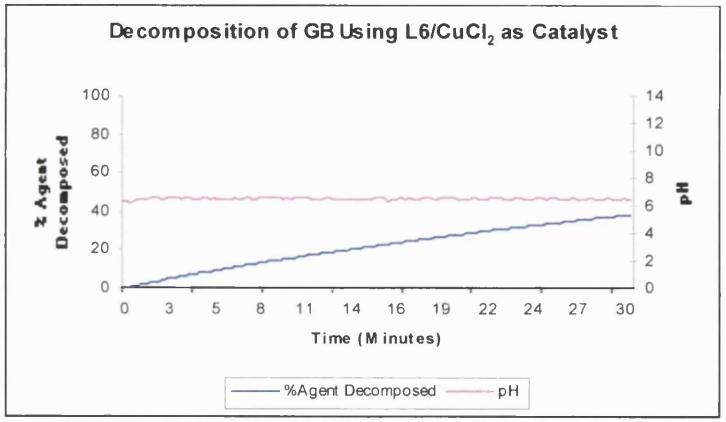

Figure 14

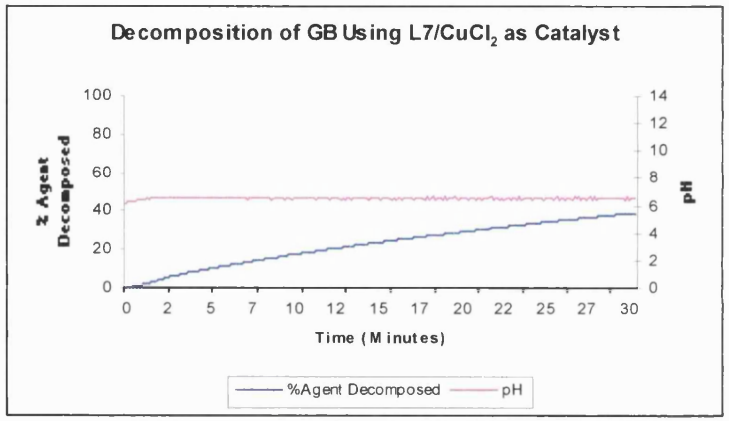

Figures 15 to 22 show the progress of reaction for the alkenylated ligand complexes.

Figure 15

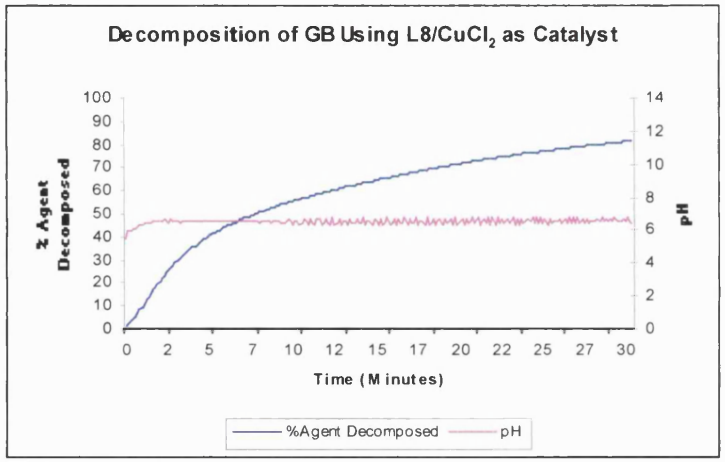

Figure 16

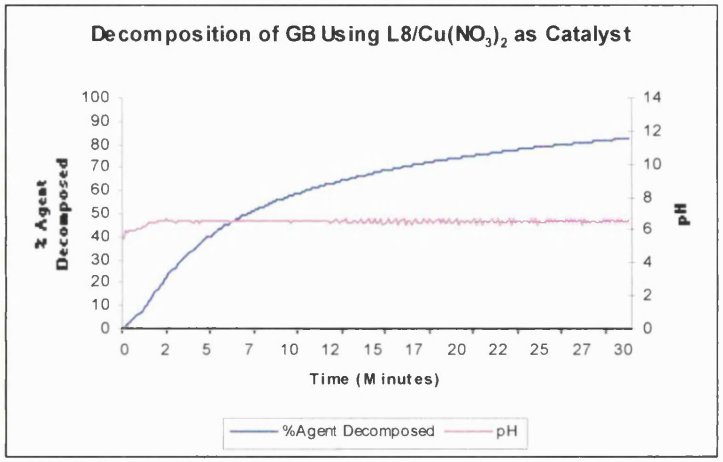

Figure 17

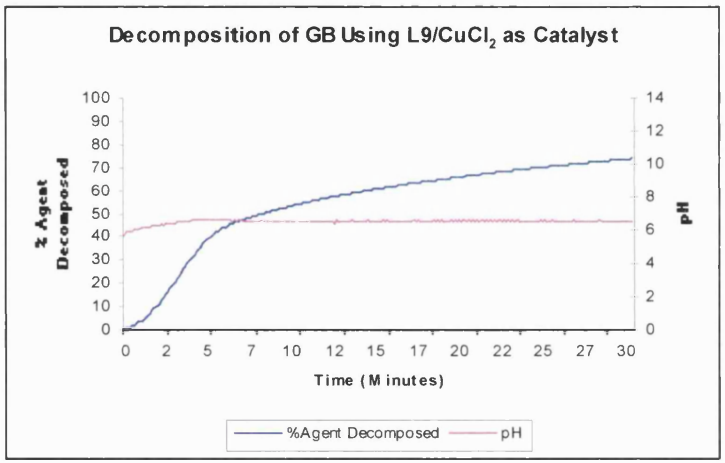

Figure 18

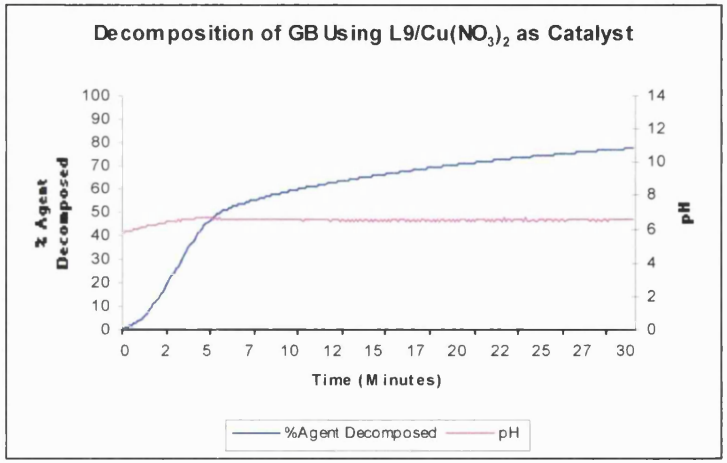

Figure 19

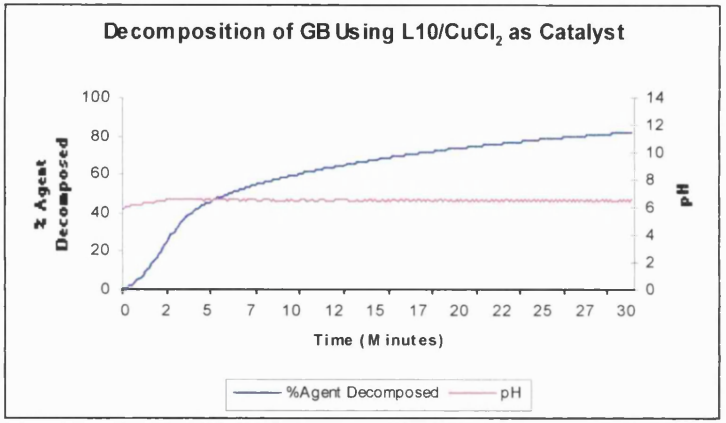

Figure 20

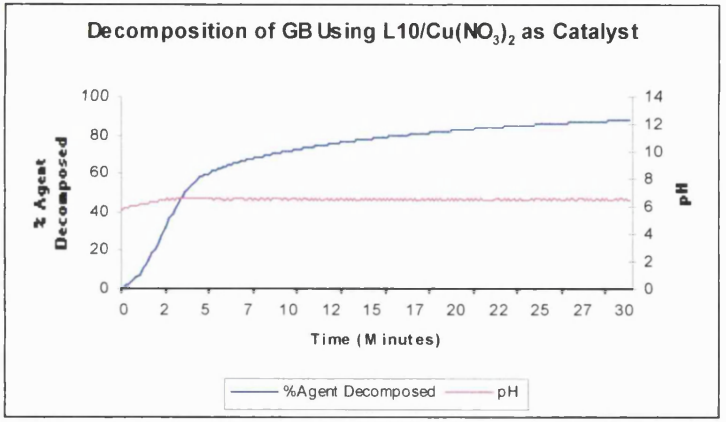

Figure 21

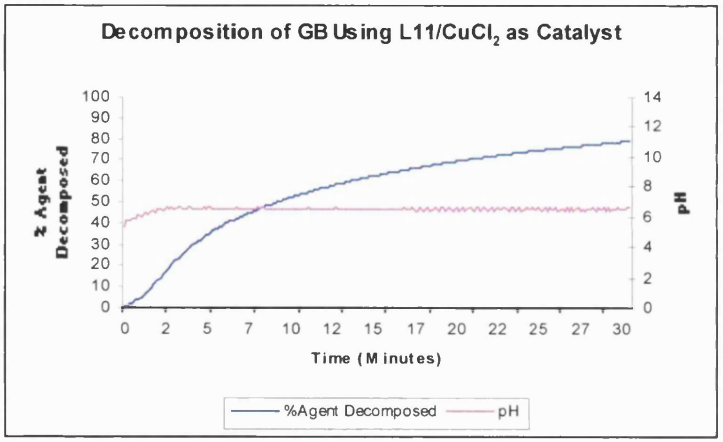

Figure 22

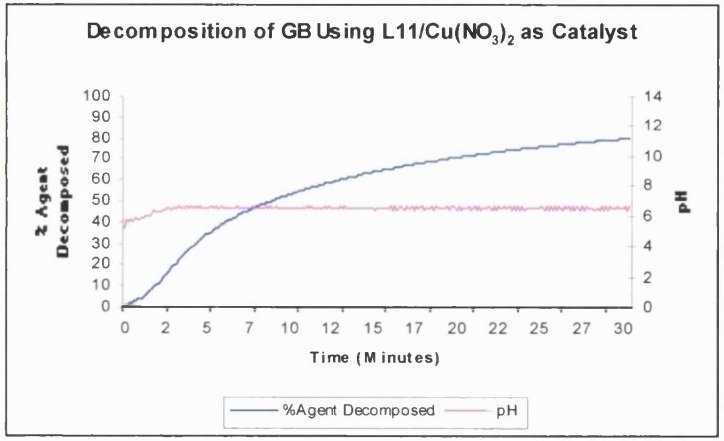

Figures 22 and 23 highlight the progress of reaction for the model siloxane and polymer catalysts tested.

Figure 23

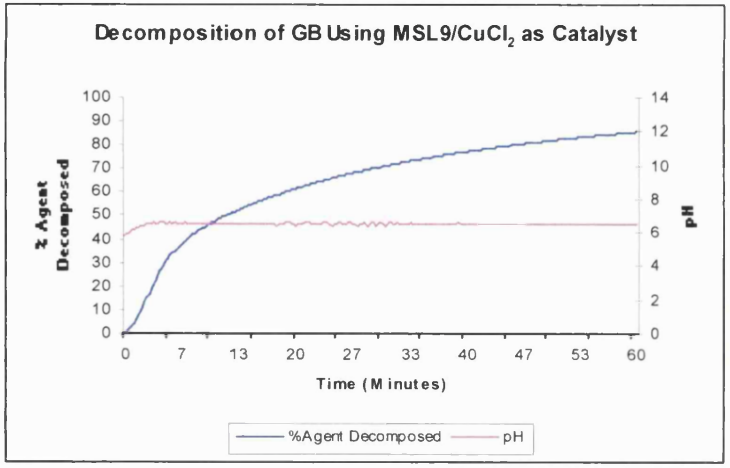

Figure 24

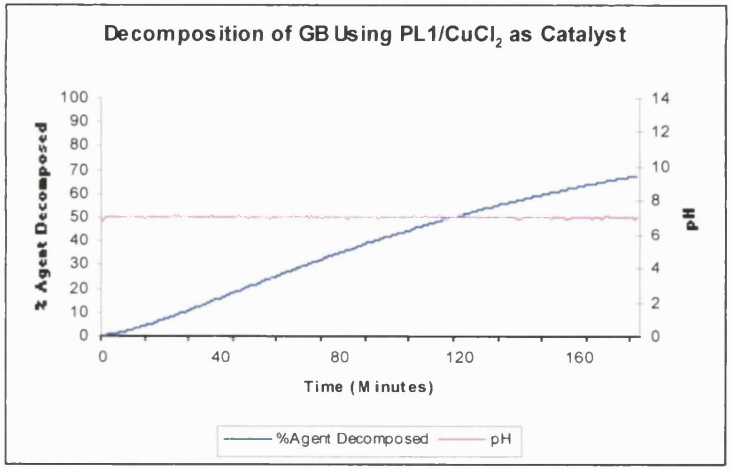

The decomposition of GB under these conditions shows that all complexes act as true catalysts, and a number of trends are apparent from the graphical results.

1. The rate of hydrolysis by the copper(II) reagents follows the general sequence:

Bidentate donors > monodentate donors > tridentate donors.

The monodentate and tridentate complexes, whilst not ineffective, were considerably slower at catalysing the hydrolysis of GB. The best only decomposed 39% of GB in 30 minutes, whereas all the bidentate complexes (with the exception of **L2**/$CuCl_2$) decomposed >70% GB in 30 minutes.

Courtney *et al.* reviewed the effects of ligands, charge, denticity of ligands and the influence of complex stability on the rates of decomposition of GB in copper(II) catalysed hydrolysis[64]. He noted that bidentate ligands were the most effective and increased denticity of the ligand reduced the effectiveness of the metal chelate as a catalyst i.e. bidentate > tridentate > tetradentate ligands, as partially confirmed in this study. Monodentate systems were not studied by Courtney, but other studies[45,61] have shown that for common monodentate ligand systems, a copper(II):imidazole molar ratio of 1:2 shows maximum activity for simulants. The imidazole complexes used in our study had a copper(II):imidazole mole ratio of 1:1. The low activity of the copper(II) complex with an imidazole ligand may be due to the formation in solution of a complex with a higher ligand:copper(II) mole ratio. It was noted that when the imidazole complexes (**L6**/$CuCl_2$ and **L13**/ $CuCl_2$) were dissolved in water at pH6.5 the solution became cloudy, possibly due to the precipitation of copper(II) hydroxide, so reducing the aqueous copper(II) concentration.

The copper(II) chloride/pyridine complex (**L7**/$CuCl_2$) contained a 1:2 metal:ligand molar ratio, and 38.9% of GB was decomposed in 30 minutes. Thus the activity of the pyridine complex was slightly better than that of the imidazole complexes. However, at pH 6.5 this complex also precipitated copper(II) hydroxide. The unstable nature of aqueous solutions of copper(II) complexes with monodentate donor ligands, under the conditions used, indicates that these systems are not suitable for use as polymer supported catalyst.

2. Of the bidentate species the rate of hydrolysis follows the general order:

Trimethylenediamine complexes > dipyridylamine complexes > Dipyridylmethane complexes > (dimethylaminoethyl)methylamino ethanol complexes.

The most active complex was the 2,2'-dipyridylamine/copper(II) chloride complex (**L1**/ $CuCl_2$), which decomposed 97% GB in 30 minutes. A similar trend has been observed in a previous study[61].

The activity of complexes relates to their stability and the charge on the aqueous copper(II) complex[42,64]. A positive metal ion centre facilitates hydrolysis to the active hydroxy-aqua complex, which interacts with GB forming the reaction intermediate, prior to intramolecular attack by the hydroxide ion. This mechanism is reproduced below.

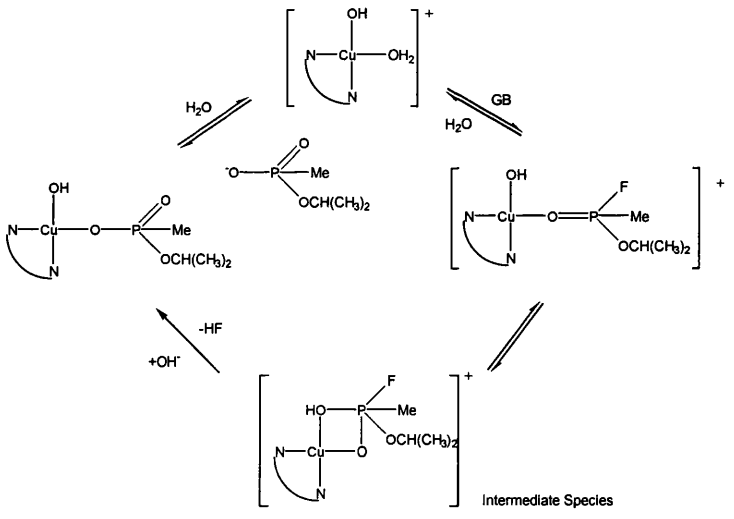

As described in 3.2.2, it would be expected that the activity of the complexes containing pyridine rings (**L1**, **L4** and analogues) would be less than that of analogues containing ethylenediamine ligands (**L2**, **L3** and analogues). Due to the extra electron density available for bonding to the copper from the delocalised π-system of the pyridine ring[152-154], the copper(II) centre is likely to be less electropositive, and so catalytic activity decreases.

However, whilst the trimethylethylenediame based complexes are indeed the most active, the (dimethylaminoethyl)methylamino)ethanol copper(II) chloride complex (**L2**/$CuCl_2$) and its allylic derivative (**L9**/$CuCl_2$) are less active than the pyridine ring based complexes. The decrease in activity is much more significant for **L2**/$CuCl_2$, where only 51.1% GB is decomposed in 30 minutes, compared to 73.6% for **L9**/$CuCl_2$. It is possible that hydrogen-bonding effects, as noted in the solid-state structure of **L2**/$CuCl_2$, have an impact on the catalytic activity of this complex. The catalytic process may be inhibited because another molecule of **L2**/$CuCl_2$ is hydrogen-bonded to the catalyst in solution. The hydrogen-bound molecules may remain in the vicinity of the metal ion, so inhibiting OH transfer to coordinated GB. No hydrogen-bonding occurs for the corresponding allyl derivative, and because the allylic group is fairly small, steric effects are minimal. As a result increased catalytic activity for **L9**/$CuCl_2$ is observed, to levels similar to those found for the other copper(II) complexes tested.

Whilst there have been no specific measurements of the charge on the metal centres of the chelates, the 2,2'-dipyridylamine complexes (**L1** and **L8**) have 3 electron withdrawing nitrogen atoms in the ligand compared to the 2,2'-dipyridylmethane complexes (**L4** and **L11**). Therefore, it might be expected that the copper centre would be more positively

charged in the former pair of complexes, and thus they should have greater activity, as observed experimentally.

3. The effect of the change of anion on copper(II) on the rate of hydrolysis follows the trend:

$Cu(NO_3)_2$ complexes > $CuCl_2$ complexes

The differences in activity are very small. Increases in the amount of GB decomposed in 30 minutes by the nitrate complexes, in comparison to the analogous chloride complexes, were of the order of 1% for **L8** and **L11**, 4% for **L9** and 6% for **L10**. These increases may possibly reflect differences in the aqueous stabilities of corresponding nitrate and chloride complexes.

4. The effect of the ligand substituent.

The effect of the addition of an alkenyl chain to the various metallated ligands gives conflicting results. Alkenylation of 2,2'-dipyridylamine and imidazole ligands reduces the activities of their copper(II) complexes, but increases the activity of copper(II) 2,2'-dipyridylmethane, N,N,N'-trimethylethylenediame and (dimethylaminoethyl)methylamino ethanol complexes. The effects of the alkenylated chain for analogues of **L1** are discussed in section 3.3.2, and the marked increase in activity of **L9**/$CuCl_2$ over **L2**/$CuCl_2$ is explained above.

The increase in activity from **L4**/$CuCl_2$ to **L11**/$CuCl_2$ is not expected as ^{13}C N.M.R data for the uncomplexed ligands indicate that addition of the alkenyl chain increases the electron density in the delocalised π-system, so reducing the positive charge on copper(II) in their complexes, and theoretically the catalytic activity. This was highlighted previously in Table 13.

The results of these reactions indicate that the siloxane-linked copper(II) catalysts, containing the bidentate ligands **L1** to **L4** and their analogues, should be very effective in decontaminating GB, provided they dissolve in water and that the support does not interfere with the formation of the catalytically active species. Experimentally **MSL9** shows a similar ability to catalyse the hydrolysis of GB to that of its precursor, **L9**/$CuCl_2$. After 30 minutes **L9**/$CuCl_2$ and **MSL9**/$CuCl_2$ had decomposed 73.6% and 71.3% of the agent respectively. This confirmed that little activity, for the same copper(II) concentration in solution, is lost by binding the alkenylated ligand to a trisiloxane support.

The metallated polymer, **PL1**, also showed catalytic activity when added to an aqueous solution of GB. Whilst the polymer is insoluble, and so is not expected to be as active as the soluble complexes described above, 67.5% of the GB was decomposed in 2 hours.

The activity shown by the polymer in this study is promising, and increased loadings of ligand and metal centre should increase activity, as found in the studies using polystyrene copper(II) supported catalysts performed by Menger *et al.*[20]. The polystyrene/copper(II) systems have $t_{1/2}$ = 2.7 minutes, but the equivalent of a 1:7.5 mole ratio of copper(II):simulant was used by Menger, which was three times the concentration of copper(II) used in our studies. However, there is a possibility that desorbed copper(II) (see equilibrium reaction below) could contribute to[47], or be the main source of, the activity observed for all the polymer reactions, and this needs to be further investigated.

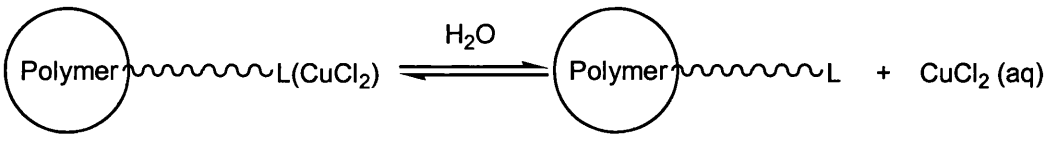

3.3.2 Reaction Kinetics Studies

The catalytic studies above identified complexes containing bidentate ligands as the best catalysts. Literature studies have shown that the longer the spacer chain between a solid polymer support and its active ligand/metal centres, then the more effective the catalyst is in hydrolysing agents and simulants[20]. Therefore, the ligands **L9**, **L15**, **L16** and **L17** were attached to the model siloxane, **MS2**, in order to produce a set of model siloxanes (**MSL8-11**) with long spacer chains, whose activities could be assessed.

These model siloxanes were also found to be water soluble, and so they could not accurately reflect the behaviour of an insoluble polymer supported system. However, the relative activities of the systems were to be measured through a second phase of evaluation, involving reaction kinetics studies, so that the most active model system could be identified and used to determine the constitution of an effective polysiloxane supported catalyst system.

A mole ratio of GB to copper(II) complex of 1:17 was maintained in these experiments, in order to negate any reliance on the concentration of copper(II) catalyst in the rate of the hydrolysis reaction. The hydrolysis reactions were carried out at 20°C and pH 6.5, in a 0.2M solution of HEPES, acting as a buffer. A fluoride electrode, calibrated using standard solutions of sodium fluoride, was used to follow the reaction by measuring the concentration of F^- produced on hydrolysis of GB. This method of following the reaction was dictated by the low molar mass of GB and the rate of reaction. It was evident that pH stat techniques would not give accurate results under these conditions. It can be seen from Figure 8 that the pH of the reaction solution in the catalytic activity studies showed wider variances than for all other reactions. The decomposition of GB was fastest in this reaction,

and the titration techniques being used were struggling to maintain a constant pH, even in a ratio of 200:1, agent:complex.

However, attempts to carry out kinetic studies on the model siloxane compounds **MSL8-11** had to be abandoned. After the addition of any of the siloxane-containing substrates to the reaction vessel, the fluoride electrode being used to collect data for the GB hydrolysis reaction began to give erroneous readings. Tests showed that the siloxane moiety interfered with the electrode, and so only data on copper(II) chloride complexes of ligands **L9** and **L15-17** were collected. The results are shown graphically in figures 25 - 38.

Previous studies on GB hydrolysis reactions have been described as being first order[57], and the observed rate coefficient for the base catalysed hydrolysis reaction, k_{obs}, is:

$$k_{obs} = k_2 [OH^-][M^{n+}] + k_{hyd}$$

where $[M^{n+}]$ = metal ion concentration, $[OH^-]$ = hydroxide ion concentration and k_{hyd} = spontaneous hydrolysis rate coefficient. Although not completely defined, the rate determining step is believed to involve the loss of F^- from the reaction intermediate species (as seen in the reaction scheme on page 111)[42,58,60]. The first-order rate constant for the decomposition of GB (k_{obs}) can be calculated from the plot of $\ln([GB]_t/[GB]_o)$, where $[GB]_t$ is the concentration of GB at time t, and $[GB]_o$ is the concentration of GB at the start of the reaction, versus time. The gradient of the line produced is the rate constant, k_{obs} (gradient = -k). A half-life for the reaction can then be calculated where $t_{½} = \ln 2/k$. The plots shown in figures 39 - 42 confirm that under the conditions employed these reactions are indeed first order within experimental limits. The associated half-lives have been calculated as described and are listed in Table 15.

Figure 25

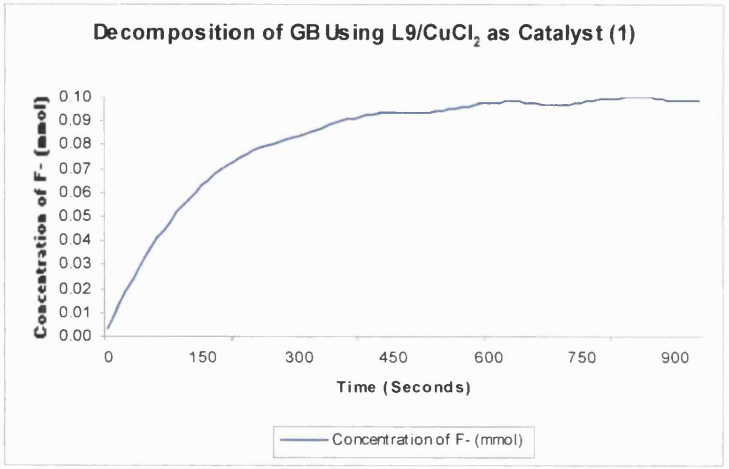

Figure 26

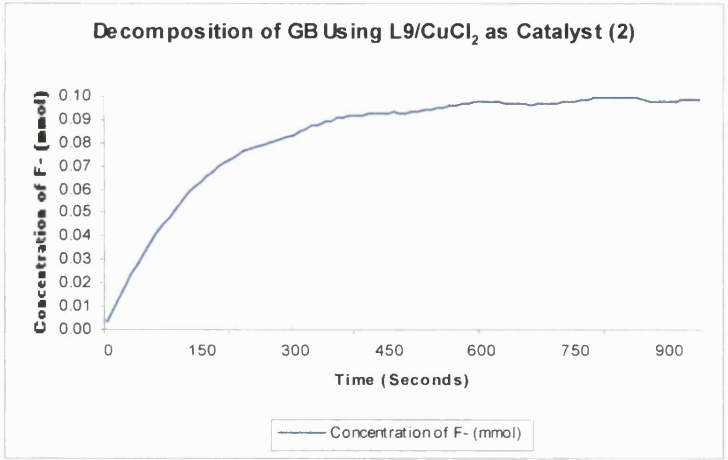

Figure 27

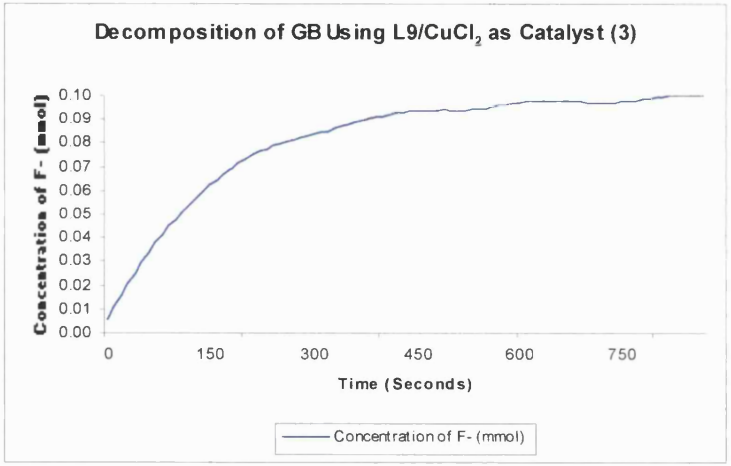

Figure 28

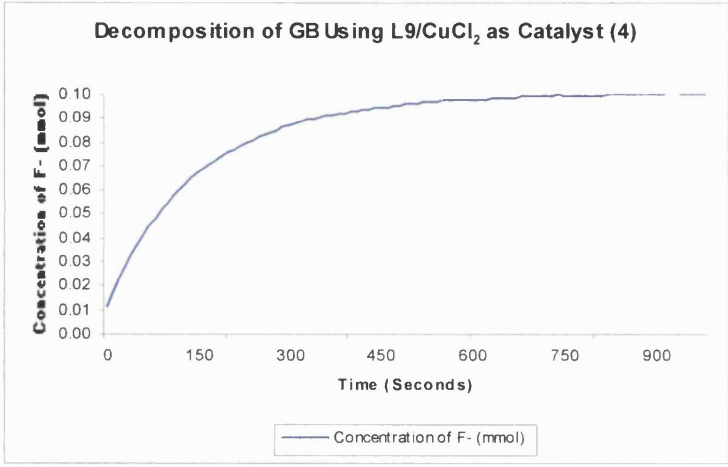

Figure 29

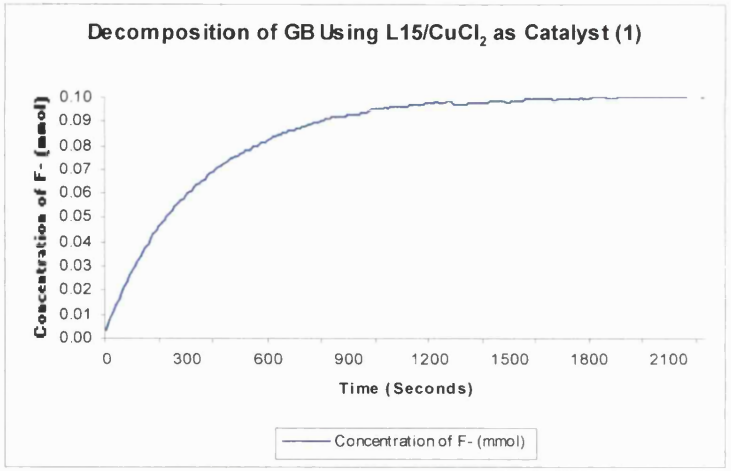

Figure 30

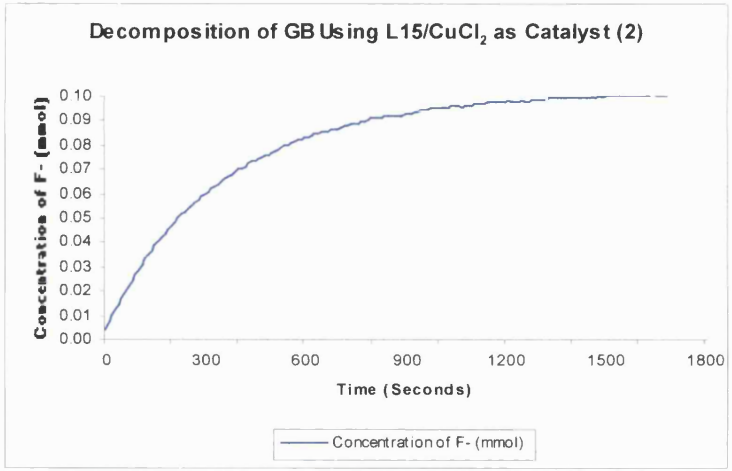

Figure 31

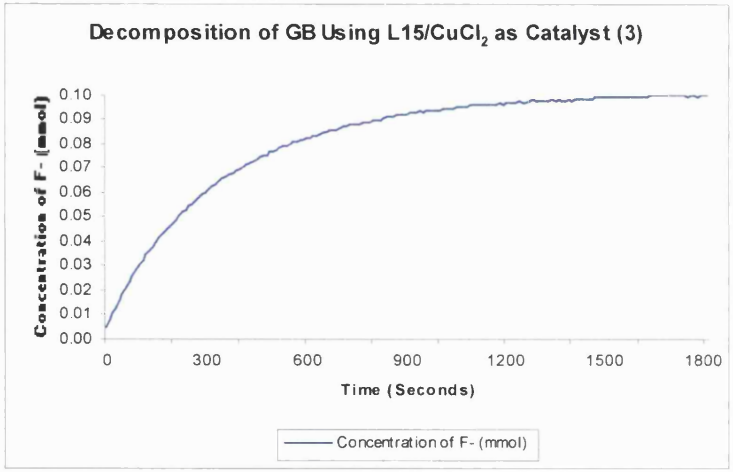

Figure 32

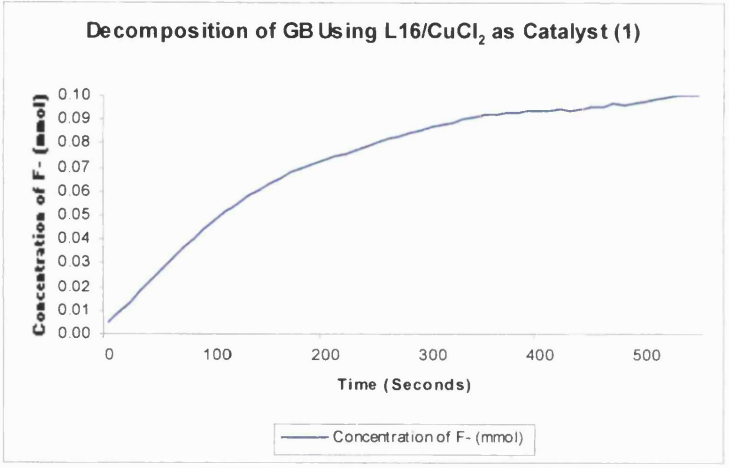

Figure 33

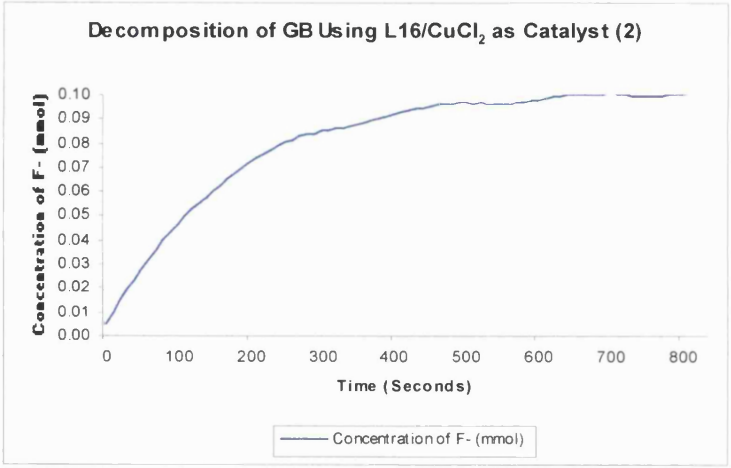

Figure 34

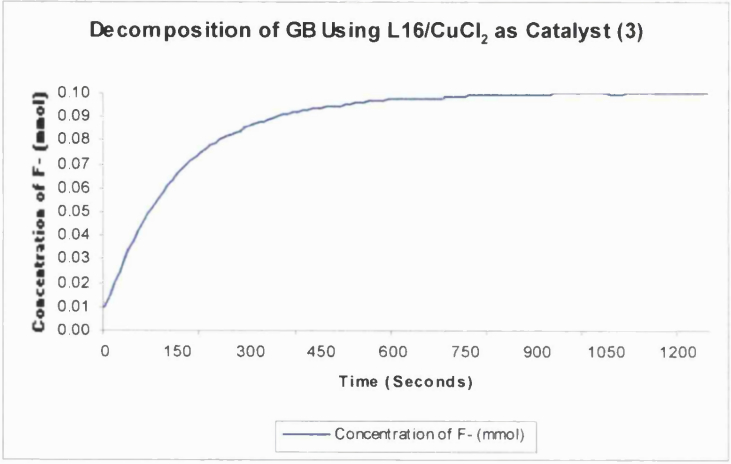

Figure 35

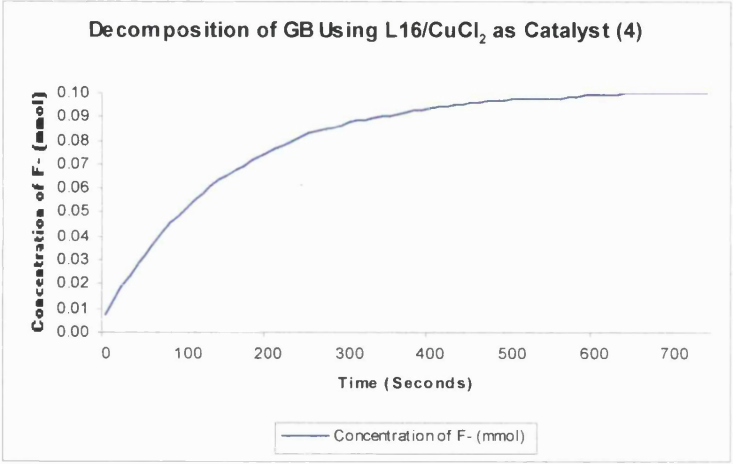

Figure 36

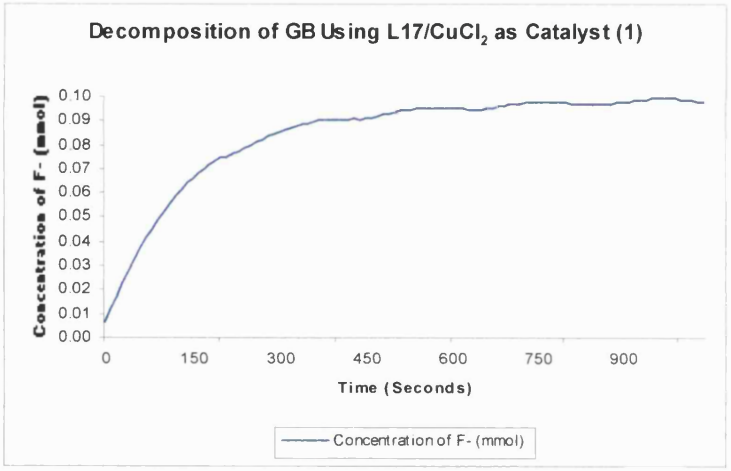

Figure 37

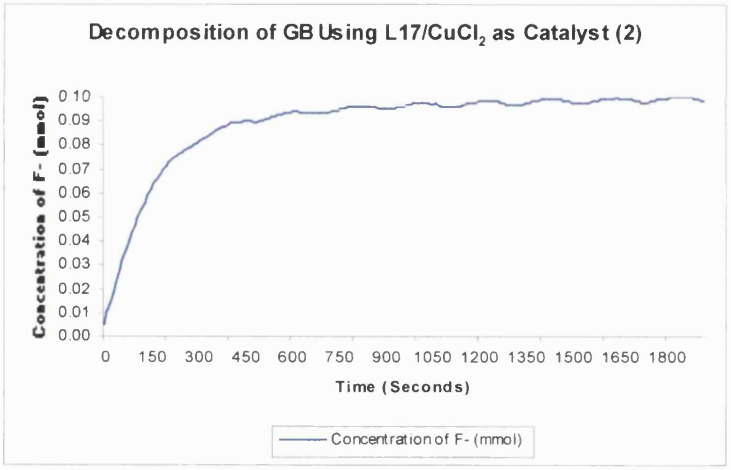

Figure 38

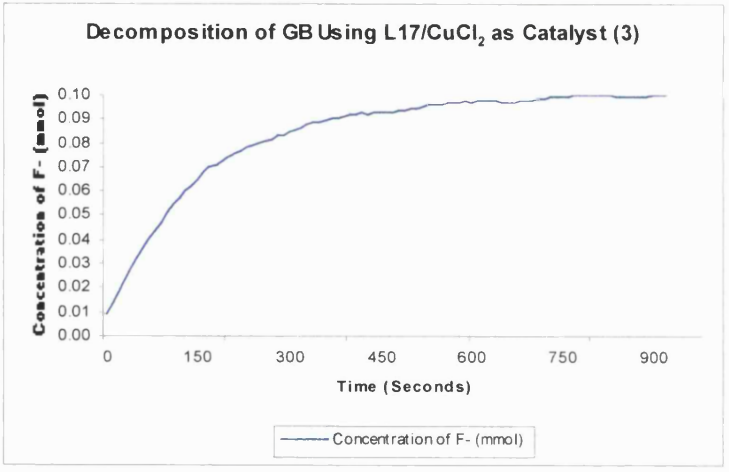

Table 15: Summary of Pseudo First Order rate Kinetics Studies For Hydrolysis of GB by Copper(II) Chloride Complexes of L9, L15, L16 and L17

Copper(II) Complex	Observed Rate Coefficient (k_{obs}, s^{-1})	Half Life ($t_{1/2}$, seconds)
L9/$CuCl_2$	6.07×10^{-3}	114
L9/$CuCl_2$	5.99×10^{-3}	116
L9/$CuCl_2$	5.90×10^{-3}	118
L9/$CuCl_2$	6.09×10^{-3}	114
		Average half life = 115.5 seconds ± 2.2%
L15/$CuCl_2$	2.82×10^{-3}	246
L15/$CuCl_2$	2.86×10^{-3}	242
L15/$CuCl_2$	2.75×10^{-3}	252
		Average half life = 246.67 seconds ± 2.2%
L16/$CuCl_2$	6.92×10^{-3}	100
L16/$CuCl_2$	7.10×10^{-3}	98
L16/$CuCl_2$	6.65×10^{-3}	104
		Average half life = 100.67 seconds ± 3.3%
L17/$CuCl_2$	5.33×10^{-3}	130
L17/$CuCl_2$	4.94×10^{-3}	140
L17/$CuCl_2$	5.63×10^{-3}	123
		Average half life = 131 seconds ± 6.9%

Figure 39

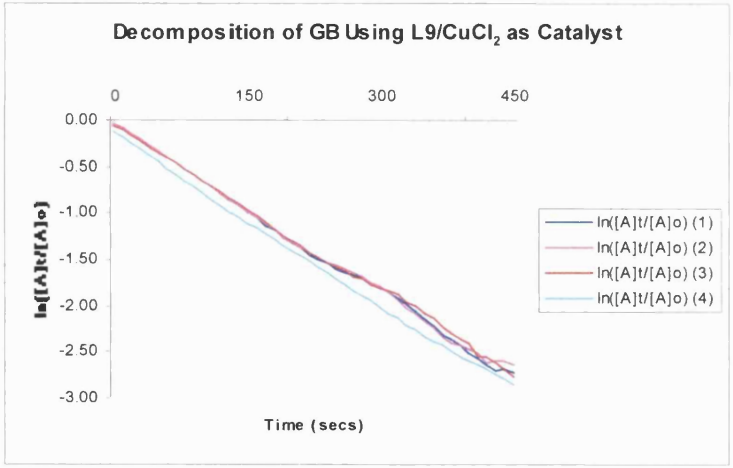

Figure 40

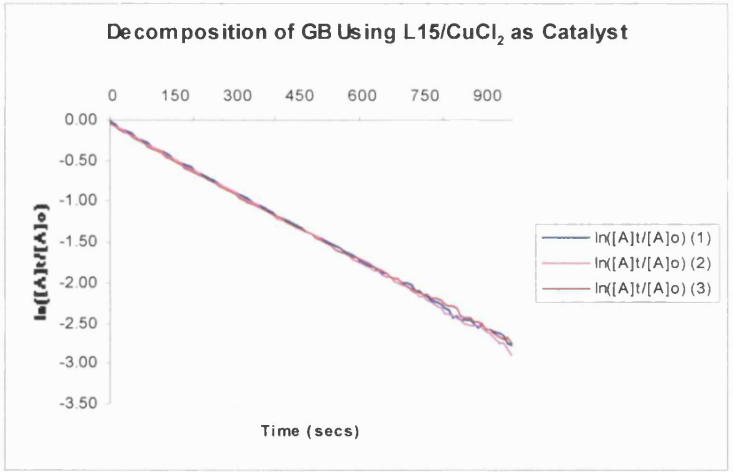

Figure 41

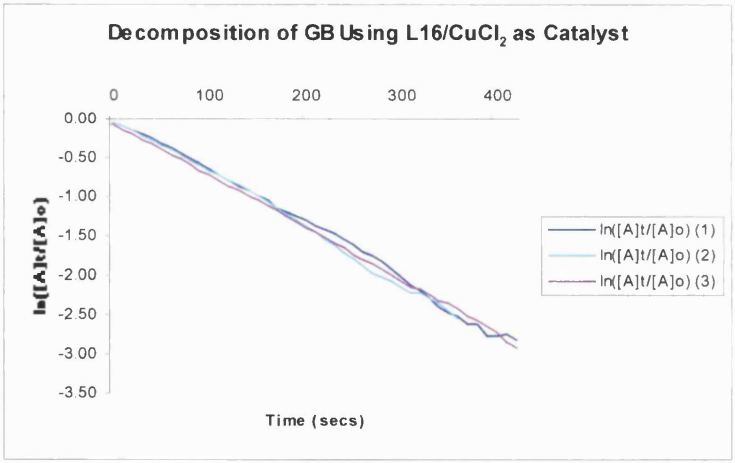

Figure 42

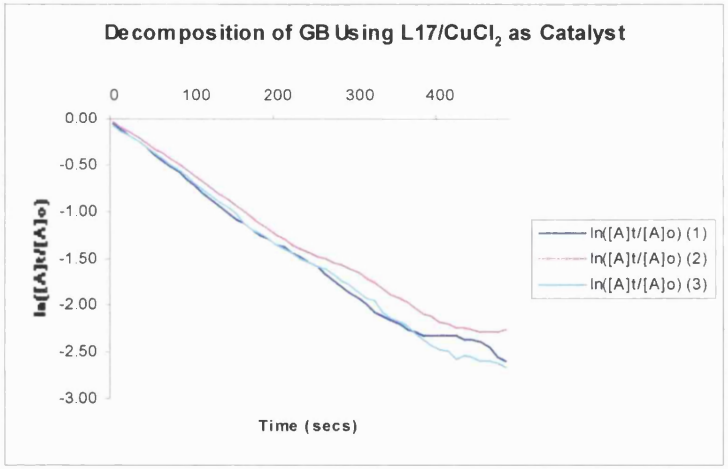

As is apparent from the figures, good reproducibility was obtained between duplicated runs, with the exception of the results for **L17**/$CuCl_2$, which were somewhat variable. The four catalysts studied hydrolysed GB at a rate of between $2.75x10^{-3}$ and $7.10x10^{-3}$ s^{-1}, where $t_{1/2}$ varied between 252 and 98 seconds. The $CuCl_2$ derivative of ligand **L16** is the most effective catalyst, followed by **L9**/ $CuCl_2$, **L17**/ $CuCl_2$, and then **L15**/ $CuCl_2$. This does not replicate the findings observed in the initial studies, however, some of the conditions, such as pH control and concentration of catalyst, are different. These results show the ethylenediamine series of copper(II) complexes to be the best catalysts for the hydrolysis of GB in these homogenous conditions. The activity of the 2,2'-dipyridylamine copper(II) chloride derivate (**L15**/$CuCl_2$) has fallen dramatically under the new conditions, whilst the other complexes appear to have retained their relative activities. Such a significant drop in activity of **L15**/$CuCl_2$ was unexpected, but as the kinetic runs were completed at the end of the programme, and in another establishment (Porton Down), it was not possible to extend these studies. Table 16 shows that the activity of the complexes tested compares well to the rates of reaction and half-life values for hydrolysis of GB by other copper(II) catalysts[63,64]. Both the copper(II) complexes of **L9** and **L16** are effective catalysts for the hydrolysis of GB, as defined by Mackay and highlighted in the paper by Menger[20].

Table 16: Comparison of the Activity of Some Copper(II) Complexes With GB

Complexing Agent	Molar Ratio Catalyst:GB	Rate Coefficient (min^{-1})	$t_{1/2}$ (minutes)
N,N,N',N'-tetramethylethylenediamine	5:1	1.4	0.5
Ethylenediamine	1:1.1	8.7×10^{-2}	8.0
2,2'-Dipyridyl	2.5:1	2.3×10^{-1}	3.0
N,N,N'-trimethyl-N'-tetradecylethylene diamine	132:1*	8.2×10^{-1}	0.85
L16	17:1	4.1×10^{-1}	1.7
L9	17:1	3.6×10^{-1}	1.9

* Agent used was GD for this reaction

4. CONCLUSIONS AND FUTURE WORK

As stated in the abstract, the overall aim of this project was **"to prepare and characterise polysiloxane bearing transition metal species that may catalyse the decomposition of chemical warfare agents"**.

We have accomplished the following specific targets in realising the overall aim of the project:

1. We have prepared and characterised eight alkenyl functionalised bi- and tri-dentate N-donor ligands in a form suitable for attachment to a linear siloxane framework.

2. We have prepared, analysed and characterised a series of fourteen copper(II) salts of these alkenyl functionalised bi- and tri-dentate N-donor ligands and two commercially available alkenylated monodentate ligands.

3. The crystal and molecular structures of five of these alkenylated/copper(II) complexes, and two non-alkenylated ligand/copper(II) complexes have been determined by single crystal X-ray crystallography, in order to reveal details about the primary coordination sphere around the metal centre.

4. A representative selection of alkenylated N-donor ligands have been attached to both short and long chain hydrosiloxanes, by means of Pt catalysed hydrosilylation reactions, to give a series of twelve organofunctional tri- and five poly-siloxanes, which have been spectroscopically characterised.

5. Tri- and poly-siloxanes containing N-donor functionalities have been metallated with copper(II) salts.

6. Increased hydrophilic character has been introduced into one siloxane polymer by incorporation of a short-chain polyether in addition to the ligating functional group.

7. Catalytic hydrolysis studies on GB have been carried out, in conjunction with Dr N. Blacker, using a range of model and siloxane linked copper(II) species. First-order kinetic data have been obtained for four complexes.

In reaching these targets, a general and facile methodology for preparing metallated organofunctional siloxanes has been developed. As a result, a range of copper(II) systems, all of which so far tested have been observed to be active in the catalytic hydrolysis of the nerve agent GB, have been prepared. Copper(II) complexes of trimethylethylenediamine and its alkenylated analogues were identified as the most active catalytic systems for the hydrolytic decomposition of GB in aqueous solution, with $t_{1/2}$ = 1.7 minutes. This is well within the criteria set by Mackay, as described in the paper by Menger[19], for an effective decontamination system.

Initial studies have also shown that a model trisiloxane attached to one of the copper(II)/ligand complexes is also effective in catalysing the decomposition of GB, with very little reduction in activity compared to the non-siloxane containing analogue. The water insoluble polymeric siloxane-supported complex was also active, decomposing 66% of GB in two hours, in experiments in which the agent was in a 20 fold molar excess over the copper(II) content of the polymer.

Whilst the catalyst systems studied herein have been shown to be active against GB, further work is required to assess the activity of copper(II)/ligand polymer attached species. A range of polymer supported copper(II) complexes of the hexenyl trimethylethylenediamine alkenylated analogue (**L16**/$CuCl_2$), where the loading of the ligand and concentration of copper(II) is varied, should be prepared using the methods outlined in these studies. Measurement of the kinetics of reaction, including half-life and confirmation of the order of reaction, can be completed using pH stat techniques where possible, as for the initial studies described in section 3.3.1. As the water

insoluble polymer systems have been shown to be less active than their water soluble counterparts, this procedure could provide a simple assessment of activity, as has been shown previously[93]. Should this method prove to be inappropriate, simulants such as PNPDPP may be used as an alternative to G-agents and due to the properties of their hydrolysis products, ultra-violet spectrometry is also be a useful technique for monitoring their reactions[76]. N.M.R spectroscopy[162,163] may also be used to monitor the decomposition of G-agents. Other methods such as vapour desorption, gas chromatography[162] and Fourier transform infrared spectroscopy techniques are also being developed[164].

Experiments designed to assess and quantify any leaching of copper(II) species from the copper(II) loaded polymeric catalyst should be carried out, using atomic absorption techniques, for example. This will also allow an assessment of the recyclability of the supported catalysts, and if leaching is significant then steps can be taken to reduce it, such as increasing the ligand:copper(II) ratio in the catalyst.

These studies have concentrated on the hydrolysis of a single G-agent, but the methodology is applicable to many other stoichiometric and catalytic reactions. The possibility of anchoring reactive organic decontaminants, such as modified *o*-iodosobenzoic acid[68-70,74-76] or quaternary heterocylic aldehyde[165] derivates, on siloxanes might be investigated. Both surface property modifiers and co-polymer formation could result in improved performances for active siloxane-based decontaminants, and in addition, the development of techniques for producing very thin coatings and cross-linked films of siloxane-containing reagents would extend their potential applications.

The development of new multifunctional siloxanes, to increase the activity of the catalyst, could be adapted to encompass oxidative decontamination routes. For

example a modified version of the ligand, $[CH_3C(O)CHC(O)CH_3]^-$ (acac), to the polymer, followed by metallation to afford the catalyst $V(O)(acac)_2$, which has been shown to catalyse the oxidation of HD by H_2O_2[15] is viable. If used in conjunction with a siloxane supported copper(II) catalyst the resulting material has the potential to both hydrolyse G-agents, and oxidise HD in the presence of an oxidant. An example of such a multifunctional catalyst is illustrated below. The polymer may be loaded with other combinations of metals for different applications.

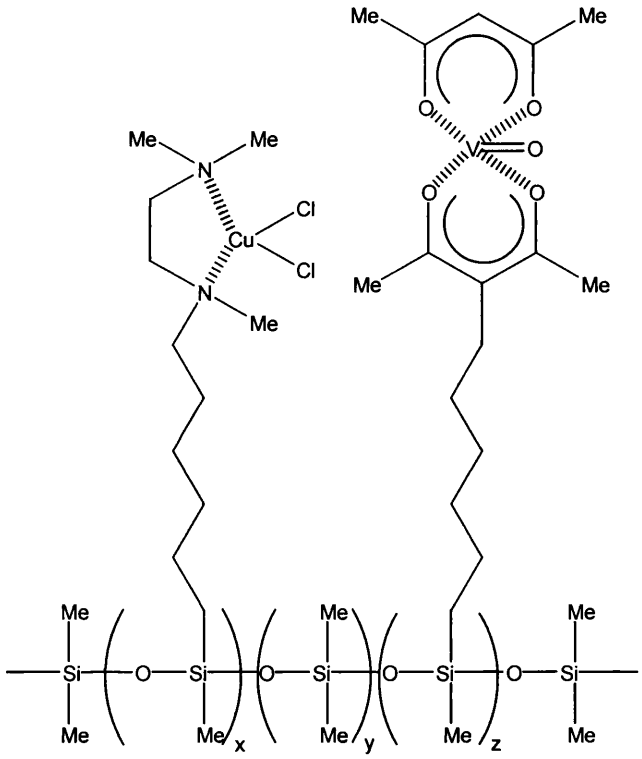

In conclusion this project has been very successful and production of siloxane supported copper(II) catalysts for the hydrolysis of GB has been achieved, and the products shown to be active in decontamination studies. The versatility of siloxane chemistry is such that the types of supported catalysts described above have great potential for the future.

REFERENCES

All references given below, with the exception of 164, are in the public domain.

1. W.J. Eckert, *J. Amer. For. Med. & Path.*, **12**, 119, 1991
2. J.L. McWilliams, R.J. Steel, *Gas! The Battle for Ypres, 1915*, Vanwell Publishing Ltd, Deydell Co., Canada, 1985
3. Organisation for the Prohibition of Chemical Weapons (OPCW), *Mustard Agents, An Overview of the Sulphur and Nitrogen Mustard Agents*, www.opcw.nl/chemhaz/mustard.htm, April 1997
4. B. Papirmeister, A.J. Feister, S.I. Robinson, R.D. Ford, *Medical Defence Against Mustard Gas: Toxic Mechanisms and Pharmacological Implications*, CRC Press Inc., Boca Raton, FL, 1991
5. G.S. Pearson, *Chemistry In Britain*, **10**, 782, 1995
6. J.A.F. Compton, *Military Chemical and Biological Agents, Chemical and Toxicological Properties*, The Telford Press, Caldwell, NJ, 1987
7. H.P. Benschop, L.P.A. de Jong, *Acc. Chem. Res.*, **21**, 368, 1988
8. R. Macy, G.N. Jarman, A. Morrison, E.E. Reid, *Science*, **106**, 355, 1947
9. Office of the Under Secretary of Defence for Acquisition and Technology, *The Military Critical Technologies List Part II: Weapons of Mass Destruction Technologies*, Washington D.C., February 1998
10. J.P. Clay, *J. Org. Chem.*, **16**, 892, 1951
11. US Army Office of the Program Manager for Chemical Demilitarisation, *'US Army Alternative Demilitarisation Report for Congress'*, Maryland: Aberdeen Proving Ground, 1994

12. The Harvard Sussex Program on CBW Armament and Arms Limitation, *CWC Signatures, Ratifications and Accessions*, www.fas.harvard.edu/~hsp/, March 2001

13. T.I.J. Toler, *War Gases in the Second World War, British Army Review no.95*, 67, 1990

14. Committee on Review and Evaluation of the Army Chemical Stockpile Disposal Program, National Research Council, *'Recommendations for Disposal of Chemical Agents and Munitions'*, Washington, DC: National Academy Press, 1994

15. Y-C. Yang, J.A. Baker, J.R. Ward, *Chem. Rev.*, **92**, 1729, 1992

16. J.M. Harris, M.S. Pailey, M.R. Sedaghat-Herati, S.P. McManus, *J. Org. Chem.*, **50**, 5230, 1985

17. J. Epstein, V.E. Bauer, M. Saxe, M.M. Demek, *J. Am. Chem. Soc.*, **78**, 4068, 1956

18. H.W. Yurow, *Decontamination and Disposal Methods for HD, GB and VX – A Literature Survey*, Chemical Systems Laboratory Report No. ARCSL-SP-80032, 1981

19. J.B. Jackson, *Development of Decontamination Solution DS2*, CWLR, 2368, 1960

20. F.M. Menger, T. Tsuno, *J. Am. Chem. Soc.*, **111**, 4903, 1989

21. O.B. Helfrich, E.E. Reid, *J. Am. Chem. Soc.*, **42**, 1208, 1920

22. M.M. Campbell, G. Johnson, *Chem. Rev.*, **78**, 65, 1978

23. F. Runf, A. Kucsmann, *J. Chem. Soc. Perkin Trans. 2*, 509, 1975

24. Y-C. Yang, *Chemistry and Industry*, **9**, 334, 1995

25. R.A. Rowe, M.M. Jones, *Inorganic Syntheses*, **5**, 114, 1957

26. B.E. Bryant, W.C. Femelins, *Inorganic Syntheses*, **5**, 115, 1957

27. N. Bodor, B. Radhakrishnan, *Novel Water-Soluble 'Soft' Brominating Agents – Potential Universal Decontaminants*, Taken from Abstract of the 1987 US Army CRDEC Scientific Conference on Chemical Defence Research, 17-20 November 1987

28. F-L Hsu, L.L. Szafraniec, W.T. Beaudry, Y-C Yang, *J. Org. Chem.*, **55**, 4153, 1990

29. F.M. Menger, A.R. Elrington, *J. Am. Chem. Soc.*, **113**, 9621, 1991

30. M.J. Coon, R.E. White, J.T. Groves, *Metal Ion Activation of Dioxygen*, John Wiley, New York, 73, 1980

31. Y-C. Yang, L.L. Szafraniec, W.T. Beaudry, D.K. Rohrbaugh, *J. Am. Chem. Soc.*, **112**, 6621, 1990

32. L.L. Szafraniec, W.T. Beaudry, D.K. Rohrbaugh, J.R. Ward, R*eactions Between Chemical Agents and the Chemicals in the M280 Decontamination Kit*, CRDEC-TR-134, CRDEC: Aberdeen Proving Test Ground, 1990

33. Y.C. Yang, L.L. Szafraniec, W.T. Beaudry, J.R. Ward, *The Reaction of VX with Chloramine-B, Proceedings of the 1991 U.S. Army CRDEC Scientific Conference on Chemical Defence Research*, U.S. Army CRDEC, Aberdeen Proving Ground, Maryland, 1993

34. Y-C, Yang, F.J. Berg, L.L. Szafraniec, W.T. Beaudry, C.A. Bunton, A. Kumar, *J. Chem. Soc., Perkin Trans.*, **2**, 607, 1997

35. G.T. Davis, M.M. Demeck, J.G. Gorrell, J. Bates, F. Block, H.Z. Sommer, J. Epstein, *Search for a Noncorrosive Decontaminant for VX and Application in Demilitarisation Operations*, Chemical Systems Laboratory Report No. ARCSL-TR-78028, July 1978

36. G.W. Wagner, P.W. Bartram, M.D. Brickhouse, T.R. Connell, W.R. Creasy, V.D. Henderson, J.W. Hovanec, K.M. Morrissey, J.R. Stuff, B.R. Williams, *J. Chem. Soc., Perkin Trans. 2*, 1267, 2000

37. *Chemical Agent Data Sheets, Volume 1*, Edgewood Arsenal Report No. EO-SR-74001, 1974

38. J. Epstein, *J. Am. Water Works Ass.*, **66**, 31, 1974

39. J. Epstein, *Science*, **170**, 1396, 1970

40. J.R. Ward, Y-C Yang, R.B. Wilson, W.D. Burrows, L. L. Ackerman, *Bioorganic Chemistry*, **16**, 12, 1988

41. T. C Bruice, S.J. Benkovic, *Bioorganic Mechanisms*, *Vol. 2*, Benjamin, New York, 110, 1966

42. R.L. Gustafson, A.E. Martell, *J. Am. Chem. Soc.*, **84**, 2309, 1962

43. T. Wagner-Jauregg, B.E. Hackley, *J. Am. Chem. Soc*, **75**, 2125, 1953

44. J. Epstein, P.L. Cannon, J.R. Sowa, *J. Am. Chem. Soc.*, **92**, 7390, 1970

45. T. Wagner-Jauregg, B.E. Hackley, T.A. Lies, O.O. Owens, R. Proper, *J. Am. Chem. Soc*, **77**, 922, 1955

46. F.M. Fowkes, G.S. Ronay, L.B. Ryland, *J. Phys. Chem.*, **62**, 867, 1958

47. J. Epstein, D.H. Rosenblatt, *J. Am. Chem. Soc.*, **80**, 3596, 1958

48. R.L. Gustafson, S. Chaberek, A.E. Martell, *J. Am. Chem. Soc.*, **85**, 598, 1963

49. R. Nakon, P.R. Rechani, R.J. Angelici, *J. Am. Chem. Soc.*, **96**, 2117, 1974

50. J.N. Burstyn, K.A. Deal, *Inorg. Chem.*, **32**, 3585, 1993

51. S.H. Gellman, R. Petter, R. Breslow, *J. Am. Chem. Soc.*, **108**, 2388, 1986

52. M.K. Stern, J.K. Bashkin, E.D. Sall, *J. Am. Chem. Soc.*, **112**, 5357, 1990

53. I.O. Kady, B. Tan, Z. Ho, T. Scarborough, *J. Chem. Soc. Chem. Commun.*, 1137, 1995

54. P.R. Norman, G. Williams, *Metal Catalysed Reactions for the Decontamination of CW Agents: The Interaction of Metal-Aquo Complexes with Phosphate and Phosphonate Esters*, CDE TN 469, 1987

55. R.S. Brown, M Zamkanei, *Inorg. Chim. Acta.*, **108**, 201, 1985

56. R.A. Kenley, R.H. Fleming, R.M. Laine, D.S. Tse, J.S. Winterle, *Inorg. Chem.*, **23**, 1870, 1984

57. J.R. Ward. L.L. Szafraniec, W.T. Beaudry, J.W. Hovanec, *Journal of Molecular Catalysis*, **58**, 373, 1990

58. J. Morrow, W.C. Trogler, *Inorg. Chem.*, **27**, 3387, 1989

59. R.W. Hay, C. You-Quan, *Polyhedron*, **14**, 869, 1995

60. K.A. Deal, A.C. Hengge, J.N. Burstyn, *J. Am. Chem. Soc.*, **118**, 1713, 1996

61. R.W. Hay, N. Govan, *Polyhedron*, **17**, No.4, 463, 1998

62. D. Wahnon, R.C. Hynes, J. Chin, *J. Chem. Soc., Chem. Commun.,* 1441, 1994

63. R.L. Gustafson, A.E. Martell, *J. Am. Chem. Soc.*, **81**, 525, 1959

64. R.C. Courtney, R.L. Gustafson, S.J. Westerback, H. Hyytiainen, S.C. Chaberek, A.E. Martell, *J. Am. Chem. Soc.*, **79**, 3030, 1957

65. E. Kovari, J. Heitker, R. Kramer, *J. Chem. Soc. Chem. Commun.*, 1205, 1995

66. F.M. Menger, L.H. Gan, E. Johnson, D.H. Durst, *J. Am. Chem. Soc.*, **109**, 2800, 1987

67. F.M. Menger, T. Tsuno, *J. Am. Chem. Soc.*, **112**, 6723, 1990

68. D.R. Leslie, S. Pantelidis, *Aust. J. Chem.*, **43**, 937, 1990

69. P.S. Hammond, J.S. Forster, C.N. Lieske, H. Dupont Durst, *J. Am. Chem. Soc.*, **111**, 7680, 1989

70. R.A. Moss, K.Y. Kim, S. Swarup, *J. Am. Chem. Soc.*, **108**, 788, 1986

71. R.A. Moss, S. Chatterjee, B. Wilk, *J. Org. Chem.*, **51**, 4303, 1986

72. R.A. Moss, K.W. Alwis, J-S Shin, *J. Am. Chem. Soc.*, **106**, 2651, 1984

73. R.A. Moss, K.W. Alwis, G.O. Bizzigotti, *J. Am. Chem. Soc.*, **105**, 681, 1983

74. R.A. Moss, D. Bolikal, H.D. Hurst, J.W. Hovanec, *Tetrahedron Lett.*, **29**, 2433, 1988

75. R.A. Moss, Y-C Chung, H.D. Hurst, J.W. Hovanec, *J. Chem. Soc. Perkin Trans.*, 1350, 1989

76. R.A. Moss, Y-C Chung, *J. Org. Chem.*, **55**, 2064, 1990

77. E.B. Dismikes, G.D. Sides, R.B. Spafford, *Evaluation of Decontamination Formulations*, Chemical Systems Laboratory Report No. ARCSL-CR-82045, 1982

78. P.D. Bartlett, C.G. Swain, *J. Am. Chem. Soc.*, **71**, 1406, 1949

79. Y-C Yang, L.L. Szafraniec, W.T. Beaudry, J.R. Ward, *J. Org Chem.*, **52**, No. 8, 1637, 1987

80. W.P. Analow, D.A. Karnofsky, B. Val Jager, H.W. Smith, *J. Pharmacol. Exp. Therap.*, **93**, 1, 1948

81. M.R. Sedaghat-Herati, S.P. McManus, J. Milton Harris, *J. Org. Chem.*, **53**, 2539, 1988

82. M. Brzostek, R. Malinowski, A. Bulhak, *Rocz. Chem.*, **46**, 741, 1972

83. Y-C Yang, J.R. Ward, T. Luteran, *J. Org. Chem.*, **51**, 2756, 1986

84. G.D. Sides, E.B. Dismukes, R.B. Spafford, *Evaluation of Decontamination Formulations*, Chemical Systems Laboratory Report No. ARCSL-CR-81080, 1981

85. J. Epstein, J.J Callahan, V.E. Bauer, *Phosphorus*, **4**, 157, 1974

86. Y-C. Yang, L.L. Szafraniec. W.T. Beaudry, *J. Org. Chem.*, **58**, 6964, 1993

87. J. Epstein, H.O. Michel, D.H. Rosenblatt, R.E. Plapinger, R.A. Stephani, E. Cook, *J. Am. Chem. Soc.*, **86**, 4959, 1964

88. J. Epstein, D.H. Rosenblatt, M.M. Demek, *J. Am. Chem. Soc.*, **78**, 341, 1956

89. A.L. Green, B. Saville, M. Stansfield, *J. Chem. Soc.*, 1583, 1958

90. G.F. Endres, J. Epstein, *J. Org. Chem.*, **24**, 1497, 1959

91. D.C. Sherrington, *Polymer Supported Reactions in Organic Synthesis*, Wiley, New York, 52, 1980

92. F.M. Menger, T. Tsuno, *J. Am. Chem. Soc.*, **112**, 1263, 1990

93. N.C. Blacker, P.H. Findlay, D.C. Sherrington, *Polym. Adv. Technol.*, **12**, 183, 2001

94. J. Emsley, *The Elements*, Clarendon Press, Oxford, 172, 1989

95. S. Shambayati, J.F. Blake, S.G. Wierschke, W.L. Jorgensen, S.L. Schreiber, *J. Am. Chem. Soc.*, **112**, 697, 1990

96. J.E. Mark, *Overview of Siloxane Polymers*, Silicones and Silicone Modified Materials, ACS Symposium Series 729, American Chemical Society, Washington DC, Eds. S.J. Clarson, J.J. Fitzgerald, M.J. Owen, S.D. Smith, 2000

97. R. Zhang, A.R. Pinhas, J.E. Mark, *Polymer Preprints*, **39**, 575, 1998

98. R. Zhang, A.R. Pinhas, J.E. Mark, *Macromolecules*, **30**, 2513, 1997

99. E.L. Lyszak, J.P. O'Brien, D.A. Kort, S.K. Hendges, R.N. Redding, T.L. Bush, M.S. Herman, K.B. Renkema, M.E. Silver, J.C. Huffman, *Organometallics*, **12**, 338, 1993

100. T.C Kendrick, B. Parbhoo, J.W. White, *The Chemistry of Organic Silicon Compounds*, John Wiley & Sons, Chapter 21, 1989

101. W. Noll, *Chemistry and Technology of Silicones*, Academic Press, London, 305, 1968

102. I. Yilgor, J.S. Riffle, J.E. McGrath, *ACS Symp. Ser.*, **282**, 161, 1983

103. W.G. Joslyn, T.J. Swihart, G. Chandra, *Misc. Symp. Conf. Meet. (US)*, 16, 1981

104. J.W. White, B.J. Griffiths, US Patent 4587136, May 1986

105. G.O. Yahaya, B.J. Brisdon, M. Maxwell, R. England, Preparation and Properties of Functionalised Polyorganosiloxanes, *J. Applied Polymer Science*, **82**, 808, 2001

106. V.G. Kumar Das, N.G. Seik Weng, M. Gielen, *Chemistry and Technology of Silicon and Tin*, Oxford University Press, 240, 1992

107. E.Y. Lukevits, M.G. Voronkov, *Organic Insertion Reactions of Group IV Elements*, Plenum, New York, 1966

108. C.S. Cundy, B.M. Kingston, M.F. Lappert, *Adv. Organomet. Chem.*, **11**, 330, 1973

109. J.L. Speier, *Adv. Organomet. Chem.*, **17**, 407, 1979

110. A.J. Chalk, J.F. Harrod, *J. Am. Chem. Soc.*, **87**, 16, 1965

111. L.N. Lewis, R.J. Uriarte, N. Lewis, *J. Catal.*, **127**, 67, 1991

112. J.A.S. Smith, B.J. Brisdon, S.A. Brewer, C.R. Willis, *J. Mater. Chem.*, **10**, 1765, 2000

113. A.J. Ashworth, B.J. Brisdon, B.S.R. Reddy, I. Zafar, R. England, *British Polymer Journal*, **21**, 491, 1989

114. B.J. Brisdon, A. M. Watts, *J. Chem. Soc. Dalton Trans.*, 2191, 1985

115. G. Sonnek, C. Rabe, G. Schmaucks, *J. Organomet. Chem.*, **405**, 179,1991

116. B.J. Brisdon, R.G. Phillips, A.M. Watts, *Transition Met. Chem.*, **13**, 303, 1988

117. B. Marciniec, J. Gulinski, *J. Organomet. Chem.*, **15**, 446, 1993

118. J-K Liu, G.E. Wnek, *Macromolecules*, **27**, 4080, 1994

119. Z. Zhu, A.G. Einset, C-Y Yang, W-X Chen, G.E. Wnek, *Macromolecules*, **27**, 4076, 1994

120. S.S. Abed-Ali, B.J. Brisdon, R. England, *Macromolecules*, **22**, 3969, 1989

121. M. Bennett, B.J. Brisdon, R. England, R.W. Field, *Journal of Membrane Science*, **137**, 63, 1997, and references therein

122. A.J. Ashworth, B.J. Brisdon, R. England, B.S.R. Reddy, I. Zafar, *Journal of Membrane Science*, **56**, 217, 1991

123. S. Westall, British Patent 2110258, June 1983

124. R.P Eckberg, US Patent 4348454, September 1982

125. S.S. Abed-Ali, B.J. Brisdon, R. England, *J. Chem. Soc. Chem. Commun.*, 1565, 1987

126. J.R. Cook, *J. Text. Inst.*, **75**, 191, 1984

127. A.J. Canty, N.J. Minchin, *Aust. J. Chem.*, **39**, 1063, 1986

128. J.K. Romary, J.D. Barger, J.E. Burns, *Inorganic Chemistry*, **7**, 1142, 1968

129. G.M. Sheldrick, *SHELX76, a computer program for crystal structure determination*, University of Cambridge, 1976

130. G.M. Sheldrick, *SHELX86, a computer program for crystal structure determination*, University of Göttingen, 1986 and *Acta Cryst.*, **A46**, 467, 1990

131. G.M. Sheldrick, *Int. Union Crystallogr.*, Crystallogr. Symp., **6** (Crystallographic Computing 6), 111, 1993

132. K.P.C. Vollhardt, N.E. Schore, *Organic Chemistry Structure and Function*, 3rd Edition, W.H. Freeman & Co., New York, 1998

133. A. Streitweiser, C.H. Heathcock, *Introduction to Organic Chemistry*, 3rd Edition, Macmillan Publishing, New York, 341, 1985

134. M.T. Garland, D. Grandjean, E. Spodine, J. Manzur, *Acta. Crystallogr., Section C*, **43**, 643, 1987

135. I.I. Matthews, H. Manohar, *Acta. Crystallogr., Section C*, **47**, 1621, 1991

136. G.E. Kimball, *J. Chem. Phys.*, **8**, 188, 1940

137. E.L. Maeiterties, R.A. Schunn, *Quart. Rev. Chem. Soc.*, **20**, 245, 1966

138. J. Zemann, *Z. Anorg, Allg. Chem.*, **B24**, 241, 1963

139. R.J. Gillespie, *J. Chem. Soc.*, 4672, 1963

140. C. Furlani, *Coord. Chem. Rev.*, **3**, 141, 1968

141. B.F. Hoskins, F.D. Williams, *Coord. Chem. Rev.*, **9**, 365, 1972

142. A.W. Addison, T.N. Rao, J. Deedjik, J. van Rijn, and G.C. Verschoor, *J. Chem. Soc., Dalton Trans.*, 1349, 1984

143. D.S. Brown, J.D. Lee, B.G.A. Melsom, *Acta Crystallogr., Sect. A*, **24**, 730, 1968

144. D.W. Phelps, W.H. Goodman, D.J. Hodgson, *Inorg. Chem.*, **15**, 2266, 1976

145. A. Walsh, B.J. Hathaway, *J. Chem. Soc., Dalton Trans.*, 15, 1984

146. R.D. Ball, D. Hall, C.E.F. Richards and T.N. Walters, *J. Chem. Soc. (A)*, 1435, 1967, J. Robertson, R. Truter, *J. Chem. Soc (A)*, 309, 1967

147. A. Pabst, *Acta. Crytallogr.*, **12**, 733, 1959

148. V.A. Roesler, D. Reinen, *Z. Anorg. Allg, Chem.*, **479**, 119, 1981

149. E. Spodine, J. Manzur, M.T. Arland, J.P. Fackler, A J. Staples, B. Trzcinska-Bancroft, *Inorg. Chim. Acta.*, **203**, 73, 1993

150. J.A. Carrabine, M. Sundaralingam, *J. Am. Chem. Soc.*, **92**, 369, 1970

151. S. Menon, C. Balagopalakrishna, C. Rajasekharan, L. Ramakrishna, *Inorg. Chem.*, **33**, 950, 1994

152. D.J. Hodgson and J.A. Ibers, *Inorg. Chem.*, **8**, 1282, 1969

153. H. Nakai, *Bull. Chem. Soc. Japan*, **56**, 1637, 1983

154. A. Walsh, B. Walsh, B. Murphy and B.J. Hathaway, *Acta Crystallogr., Sect. B*, **37**, 1512, 1981

155. S. Menon, M.V. Rajesekharan and J.P. Tuchagies, *Inorg. Chem.*, **36**, 4341, 1997 and references therein

156. F.S. Stephens, *J. Chem. Soc. (A)*, 2232, 1969

157. K. Nakamoto, *Infrared and Raman Spectra of Inorganic Compounds*, 3rd Edition, 244, 1978

158. T.J. King, A. Morris, *Inorg. Nucl. Chem. Lett.*, **10**, 237, 1974

159. S.F. Parkovic, D. Miller, *Acta Crystallogr., Section B*, **33**, 2894, 1977

160. D.L. Lewis, D.J. Hodgson, *Inorg. Chem.*, **12**, 2935, 1973

161. L. Larsson, *Acta Chem. Scand.*, **11**, 1131, 1957

162. J.R. Ward, J.W. Hovanec, J.M. Albizo, L.L. Szafraniec, W.T. Beaudry, *J. Fluorine Chemistry*, **51**, 277, 1991

163. G.W. Wagner, O.B. Koper, E. Lucas, S. Decker, K.J. Klabunde, *J. Phys. Chem. B*, **104**, 5118, 2000

164. Personal copy of D.W. Anderson, N. Blacker, N. Govan, K. Parchment, A Ridding and M. Houghton, *Proceedings of the Third Annual Decontamination Seminar, CBDE Porton Down*, 1995

165. G.M. Steinberg, E.J. Poziomek, B.E. Hackley Jr., *J. Org. Chem.*, **26**, 368, 1961

APPENDIX A

SUMMARY OF CRYSTALLOGRAPHIC DATA

1. The Structure of L2/$CuCl_2$ Dimer

A crystal of approximate dimensions 0.3 x 0.3 x 0.5 mm was used for data collection.

Crystal data: $C_7H_{18}N_2Cl_2OCu$, M = 280.71 monoclinic, a = 8.030(3), b = 39.480(8), c = 8.357(2) Å, β = 118.82(3)°, U = 2321.3 $Å^3$, space group $P2_1/a$, Z = 4, D_c = 1.60 g cm^{-3}, μ(Mo-K_α) = 23.2 cm^{-1}, F(000) = 1160. Data were measured at room temperature on a CAD4 automatic four-circle diffractometer in the range $2 \leq \theta \leq 22°$. 3150 reflections were collected of which 2117 were unique with $I > 2\sigma(I)$. Data were corrected for Lorentz and polarization but not for absorption. The structure was solved by Patterson methods and refined using the SHELX[90, 91] suite of programs.

The asymmetric unit consists of 2 molecules that are involved in a single hydrogen bond via Cl(l) and O2. (Cl(1)-O(2), 3.17 Å) As a consequence of this solo hydrogen bond, the pair of molecules in the asymmetric unit are not altogether identical. Typically, the Cl(1)-Cu(l) bond length of 2.307(7) Å is slightly longer than the other Cl-Cu bonds. (Cl(2)-Cu(l), 2.253(5); Cl(3)-Cu(2), 2.266(7); Cl(4)-Cu(2), 2.260(5) Å). In addition, the O(2)-Cu(2) bond length of 2.474(10) Å is longer than the comparative O(l)-Cu(1) length of 2.383(9) Å.

In the final least squares cycles all atoms were allowed to vibrate anisotropically. Hydrogen atoms were included at calculated positions on the carbon atoms. Unfortunately, the hydroxyl protons could not be located satisfactorily.

Final residuals after 12 cycles of least squares were R = 0.0680, R_w = 0.0700, for a weighting scheme of $w = 5.7279/[\sigma^2(F) + 0.000331\ (F)^2]$. Max. final shift/esd was 0.005. The max. and min. residual densities were 0.43 and -0.26 e $Å^{-3}$ respectively.

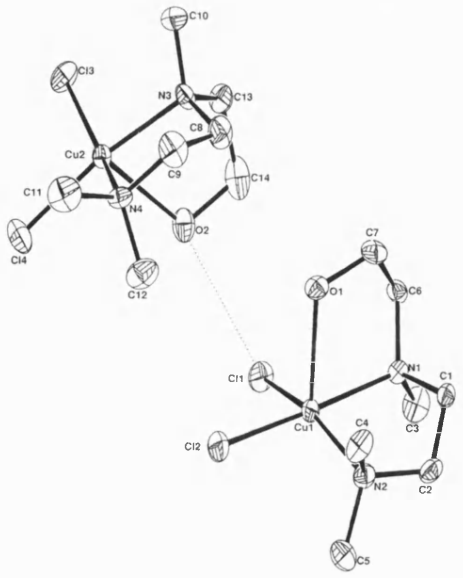

Bond Lengths (Å)

Cl(l)-Cu(l)	2.307 (7)	C(13)-N(3)	1.472 (16)	H(62)-C(6)	0.960 (21)
Cl(2)-Cu(1)	2.253 (5)	C(9)-N(4)	1.501 (18)	H(71)-C(7)	0.960 (19)
N(1)-Cu(1)	2 .068 (9)	C(11)-N(4)	1.443 (15)	H(72)-C(7)	0.960 (22)
N(2)-Cu(1)	2 .108 (14)	C(12)-N(4)	1.448 (18)	H(81)-C(8)	0.960 (18)
O(l)-Cu(l)	2.383 (9)	C(14)-O(2)	1.415 (14)	H(82)-C(8)	0.960 (21)
C(l)-N(l)	1.539 (19)	C(9)-C(8)	1.480 (18)	H(91)-C(9)	0.960 (26)
C(3)-N(1)	1.456 (18)	C(14)-C(13}	1.519 (21)	H(92)-C(9)	0.960 (22)
C(6)-N(l)	1.460 (15)	H(11)-C(l)	0.960 (17)	H(101)-C(10)	0.960 (20)
C(2)-N(2)	1.477 (13)	H(12)-C(1)	0.960 (13)	H(102)-C(10)	0.960 (25)
C(4)-N(2)	1.459 (19)	H(21)-C(2)	0.960 (18)	H(103)-C(10)	0.960 (16)
C(5)-N(2)	1.491 (15)	H(22)-C(2)	0.960 (21)	H(111)-C(11)	0.960 (22)
C(7)-O(1)	1.440 (12)	H(31)-C(3)	0.960 (20)	H(112)-C(11)	0.960 (27)
C(2)-C(1)	1.455 (17)	H(32)-C(3)	0.960 (15)	H(113)-C(11)	0.960 (21)
C(7)-C(6)	1.529 (19)	H(33)-C(3)	0.960 (24)	H(121)-C(12)	0.960 (18)
C(3)-Cu(2)	2.266 (7)	H(41)-C(4)	0.960 (17)	H(122)-C(12)	0.960 (21)
C(4)-Cu(2)	2.260 (5)	H(42)-C(4)	0.960 (24)	H(123)-C(12)	0.960 (29)
N(3)-Cu(2)	2.056 (9)	H(43)-C(4)	0.960 (15)	H(131)-C(13)	0.960 (24)
N(4)-Cu(2)	2.072 (14)	H(51)-C(5)	0.960 (21)	H(132)-C(13)	0.960 (16)
O(2)-Cu(2)	2.474 (10)	H(52)-C(5)	0.960 (15)	H(141)-C(14)	0.960 (25)
C(8)-N(3)	1.499 (21)	H(53)-C(5)	0.960 (23)	H(142)-C(14)	0.960 (23)
C(10)-N(3)	1.475 (16)	H(61)-C(6)	0.960 (13)		

Bond Angles (°)

Cl(2)-Cu(1)-Cl(1)	93.5(2)	C(7)-C(6) -N(l)	111.9(11)	C(9)-C(8) -N(3)	108.4 (11)
N(l)-Cu(l)-Cl(l)	91.4 (4)	C(6)-C(7)-0(1)	109.7(9)	C(8) -C(9) -N(4)	110.3(13)
N(l)-Cu(l)-Cl (2)	173.7(3)	Cl(4)-Cu(2)-Cl (3)	91.6(2)	C(14)-C(13) -N(3)	111.0(11)
N(2)-Cu(1)-Cl (1)	157.9(3)	N(3)-Cu(2)-Cl(3)	92.2 (4)	C(13)-C(14)-O(2)	111.0(11)
N(2)-Cu(1) -Cl(2)	91.3(3)	N(3)-Cu(2) -Cl (4)	171.3(3)	H(11)-C(l)-N(l)	109.7(13)
N(2)-Cu(1)-N(1)	85.7 (5)	N(4)-Cu(2)-Cl(3)	157.4 (3)	H(12)-C(1)-N(1)	109.6(15)
O(l)-Cu(l)-Cl(l)	96.1(4)	N(4)-Cu(2)-Cl (4)	93.5(4)	H(12)-C(1)-H(11)	109.5(14)
O(1)-Cu(1)-Cl(2)	98.5(3)	N(4)-Cu(2)-N(3)	85.9(5)	C(2)-C(1)-H(11)	109.7(14)
O(l)-Cu(l)-N(l)	77.0(4)	O(2)-Cu(2)-Cl(3)	101.5(4)	C(2)-C(1)-H(12)	109.6(13)
O(1)-Cu(1)-N(2)	104.6(5)	O(2)-Cu(2)-Cl(4)	96.8(3)	H(21)-C(2)-N(2)	109.1(12)
C(l)-N(l)-Cu(l)	104.4 (7)	O(2)-Cu(2)-N(3)	74.8 (4)	H(21)-C(2)-C(1)	109.1(15)
C(3)-N(1)-Cu(1)	113.0(7)	O(2)-Cu(2)-N(4)	99.7(4)	H(22)-C(2)-N(2)	109.0(14)
C(3)-N(1)-C(1)	110.4 (10)	C(8)-N(3)-Cu(2)	105.6(7)	H(22)-C(2)-C(1)	109.0(12)
C(6)-N(1) -Cu(l)	110.5(7)	C(10)-N(3)-Cu(2)	113.2(7)	H(22)-C(2)-H(21)	109.5(17)
C(6)-N(1)-C(1)	111.0(9)	C(10)-N(3) -C(8)	109.4 (12)	H(31)-C(3)-N(1)	109.5(17)
C(6) -N(l) -C(3)	107.5(10)	C(13)-N(3)-Cu(2)	108.5(8)	H(32)-C(3)-N(1)	109.4(15)
C(2)-N(2)-Cu(1)	104.5(9)	C(13)-N(3) -C(8)	113.4 (10)	H(32)-C(3)-H(31)	109.5(17)
C(4)-N(2)-Cu(1)	110.0(9)	C(13)-N(3)-C(10)	106.9(10)	H(33)-C(3)-N(1)	109.5(14)
C(4) -N(2)-C(2)	110.9(10)	C(9)-N(4)-Cu(2)	104.9(9)	H(33)-C(3)-H(31)	109.5(18)
C(5)-N(2)-Cu(1)	112.4 (9)	C(11)-N(4)-Cu(2)	112.7(11)	H(33)-C(3)-H(32)	109.5(20)
C(5)-N(2)-C(2)	109.5(10)	C(11)-N(4)-C(9)	110.5(11)	H(41)-C(4)-N(2)	109.5(16)
C(5)-N(2)-C(4)	109.4 (11)	C(12)-N(4)-Cu(2)	110.7(10)	H(42) -C(4)-N(2)	109.5(14)
C(7)-0(1)-Cu(1)	109.0(7)	C(12)-N(4)-C(9)	109.0(12)	H(42)-C(4)-H(41)	109.5(18)
C(2)-C(1)-N(1)	108.7(9)	C(12)-N(4)-C(11)	109.0(10)	H(43)-C(4)-N(2)	109.5(16)
C(1)-C(2)-N(2)	111.2(10)	C(14)-0(2)-Cu(2)	107.2 (8)	H(43)-C(4)-H(41)	109.5(16)

H(43)-C(4)-H(42)	109.5(19)	H(82)-C(8)-H(81)	109.5(17)	H(113)-C(11)-H(112)	109.5(19)
H(51)-C(5)-N(2)	109.5(14)	C(9)-C(8) -H(81)	109.8 (17)	H(121)-C(12)-N(4)	109.5(16)
H(52)-C(5)-N(2)	109.4 (14)	C(9)-C(8)-H(82)	109.7(15)	H(122)-C(12)-N(4)	109.5(18)
H(52)-C(5)-H(51)	109.5(18)	H(91)-C(9)-N(4)	109.3(14)	H(122)-C(12)-H(121)	109.5(20)
H(53)-C(5)-N(2)	109.4(14)	H(91)-C(9)-C(8)	109.3(14)	H(123)-C(12)-N(4)	109.5(16)
H(53)-C(5)-H(51)	109.5(18)	H(92)-C(9)-N(4)	109.2(14)	H(123)-C(12)-H(121)	109.5(22)
H(53)-C(5)-H(52)	109.5(18)	H(92)-C(9)-C(8)	109.2(15)	H(123)-C(12)-H(122)	109.5(20)
H(61)-C(6)-N(1)	108.8(13)	H(92)-C(9)-H(91)	109.5(22)	H(131)-C(13)-N(3)	109.1(13)
H(62)-C(6)-N(1)	108.9(12)	H(101)-C(10)-N(3)	109.5(15)	H(132)-C(13)-N(3)	109.1(15)
H(62)-C(6)-H(61)	109.5(16)	H(102)-C(10)-N(3)	109.5(15)	H(132)-C(13)-H(131)	109.5(17)
C(7)-C(6) -H(61)	108.9(13)	H(102)-C(10)-H(101)	109.5(18)	C(14)-C(13)-H(131)	109.1 (15)
C(7)-C(6)-H(62)	108.9(13)	H(103)-C(10)-N(3)	109.5(14)	C(14)-C(13)-H(132)	109.1(14)
H(71)-C(7)-0(1)	109.4(12)	H(103)-C(10)-H(101)	109.5(19)	H(141)-C(14)-0(2)	109.1(16)
H(71)-C(7)-C(6)	109.4 (16)	H(103)-C(10)-H(102)	109.5(19)	H(141)-C(14)-C(13)	109.1(17)
H(72)-C(7)-0(1)	109.4 (15)	H(111)-C(11)-N(4)	109.5(14)	H(142)-C(14)-0(2)	109.1(16)
H(72)-C(7)-C(6)	109.4(13)	H(112)-C(11)-N(4)	109.5(16)	H(142)-C(14)-C(13)	109.1(17)
H(72)-C(7)-H(71)	109.5(16)	H(112)-C(11)-H(111)	109.5(22)	H(142)-C(14)-H(141)	109.5(18)
H(81)-C(8)-N(3)	109.8(16)	H(113)-C(11)-N(4)	109.5(17)		
H(82)-C(8)-N(3)	109.7 (18)	H(113)-C(11)-H(111)	109.5(22)		

2. The Structure of L9/$CuCl_2$

A crystal of approximate dimensions 0.4 x 0.3 x 0.1 mm was carefully cut from a large block and used for data collection.

Crystal data: $C_{10}H_{22}N_2OCl_2Cu$, M = 320.7 orthorhombic, a = 8.284(1), b = 11.609(2), c = 15.042(1) Å, U = 1446.6 $Å^3$, space group $P2_12_12_1$, Z = 4, D_c = 1.47 g cm^{-3}, μ(Mo-K_α) = 18.7 cm^{-1}, F(000) = 668. Data were measured at room temperature on a CAD4 automatic four-circle diffractometer in the range $2 \leq \theta \leq 24°$.1837 reflections were collected of which 1257 were unique with $I > 2\sigma(I)$. Data were corrected for Lorentz and polarization effects but not for absorption. The structure was solved by Direct methods and refined using the SHELX[90, 91] suite of programs. In the final least squares cycles all atoms were allowed to vibrate anisotropically. Hydrogen atoms were included at calculated positions in all cases except for the allylic protons (H9, H101, H102), which were located in the penultimate Difference Fourier and refined at a fixed distance of 1.07 Å from the parent atoms (C9, C10). Also, the chiral integrity of the molecule as presented is considerably greater than 99% based on the Hamilton significance test. Final residuals after 8 cycles of least squares were R = 0.0386, R_w = 0.0365, for a weighting scheme of $w = 1.3262/[\sigma^2(F) + 0.000698\ (F)^2]$. Max. final shift/esd was 0.009. The max. and min. residual densities were 0.21 and -0.44 e $Å^{-3}$ respectively.

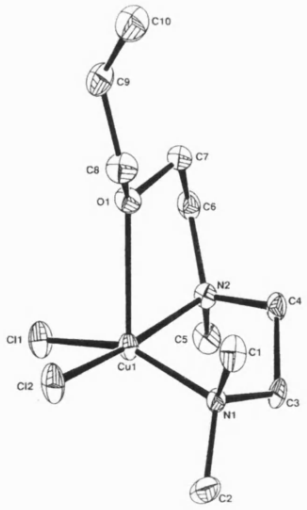

Bond Lengths (Å)

Cl(l)-Cu(l)	2.254(4)	C(8)-O(1)	1.455(9)	C(6)-N(2)	1.488(10)
Cl(2)-Cu(1)	2.264(4)	C(l)-N(l)	1.487(10)	C(4)-C(3)	1.508(12)
O(1)-Cu(1)	2 .3 93(7)	C(2)-N(1)	1.481(10)	C(7)-C(6)	1.507(12)
N(1)-Cu(1)	2. 079(8)	C(3)-N(1)	1.481(10)	C(9)-C(8)	1.479(13)
N(2)-Cu(1)	2.088(7)	C(4)-N(2)	1.488(10)	C(10)-C(9)	1.291(13)
C(7)-O(1)	1.413(9)	C(5)-N(2)	1.500(11)		

Bond Angles (°)

Cl(2)-Cu(1)-Cl(1)	94.2(2)	C(8)-O(1)-Cu(1)	124.6(6)	C(6)-N(2)-Cu(1)	108.6(5)
O(l)-Cu(l)-Cl(l)	96.7(2)	C(8)-O(1)-C(7)	113.6(7)	C(6)-N(2) -C(4)	111.6(7)
O(1)-Cu(1)-Cl(2)	93.9(2)	C(l)-N(l)-Cu(l)	110.6(6)	C(6)-N(2)-C(5)	108.0(7)
N(l)-Cu(l)-Cl(l)	155.2(2)	C(2)-N(1)-Cu(1)	112.8(6)	C(4)-C(3)-N(1)	109.3(7)
N(1)-Cu(1)-Cl(2)	92.3 (3)	C(2)-N(1)-C(1)	108.5(8)	C(3)-C(4)-N(2)	108.2(7)
N(1)-Cu(1)-O(1)	106.8(3)	C(3)-N(1)-Cu(1)	106.2(5)	C(7)-C(6)-N(2)	112.6(7)
N(2)-Cu(1)-Cl(1)	93.1(3)	C(3)-N(1)-C(1)	109.6(7)	C(6)-C(7)-0(1)	108.2(7)
N(2)-Cu(1)-Cl(2)	169.0(2)	C(3)-N(1)-C(2)	109.0(7)	C(9)-C(8)-0(1)	113.4(8)
N(2)-Cu(1)-O(1)	77.0(3)	C(4)-N(2)-Cu(1)	106.7(5)	C(10)-C(9)-C(8)	124.1(11)
N(2)-Cu(1)-N(l)	84.5(3)	C(5)-N(2)-Cu(1)	113.0(5)		
C(7)-O(1)-Cu(1)	109.3(5)	C(5)-N(2) -C(4)	109.0(7)		

3. The Structure of L4/$CuCl_2$ Dimer

A crystal of approximate dimensions 0.2 x 0.2 x 0.15 mm was used for data collection.

Crystal data: $C_{11}H_{10}Cl_2N_2Cu.½CH_3OH$, M = 320.67, Triclinic, a = 8.3490(10), b = 10.005(2), c = 15.425(3) Å, α = 99.35(2), β = 89.95(2), γ = 99.59(2)°, U = 1253.1(4) $Å^3$, space group P-1 (No.2), Z =4, D_o = 1.700 g cm^{-3}, μ(Mo-$K_α$) = 2.149 mm^{-1}, F(000) = 648. Crystallographic measurements were made at 170(2)°K on a CAD4 automatic four-circle diffractometer in the range $2.09<\theta<23.93°$. Data (4238 reflections) were corrected for Lorentz and polarization but not for absorption.

The asymmetric unit consists of 2 separate halves of dimer molecules, both straddling nearby inversion centres, and one molecule of methanol. The dimer containing Cu1 is completed from the symmetry transformation -x, -y, - z, while the Cu2 containing dimer is generated via the operator 1-x, - y, 1-z. In addition, the oxygen atom in the solvent molecule is disordered between sites O1A and O1B in the ratio 1:1.

In the final least squares cycles all atoms were allowed to vibrate anisotropically. Hydrogen atoms were included at calculated positions where relevant except on the solvent molecule.

The solution of the structure (SHELX86)[91] and refinement (SHELX93)[92] converged to a conventional [i.e. based on 2875 with Fo>4θ(Fo)] R1 = 0.0418 and wR2 = 0.0970. Goodness of fit = 0.958. The max. and min. residual densities were 0.847 and -0.645 e $Å^{-3}$ respectively.

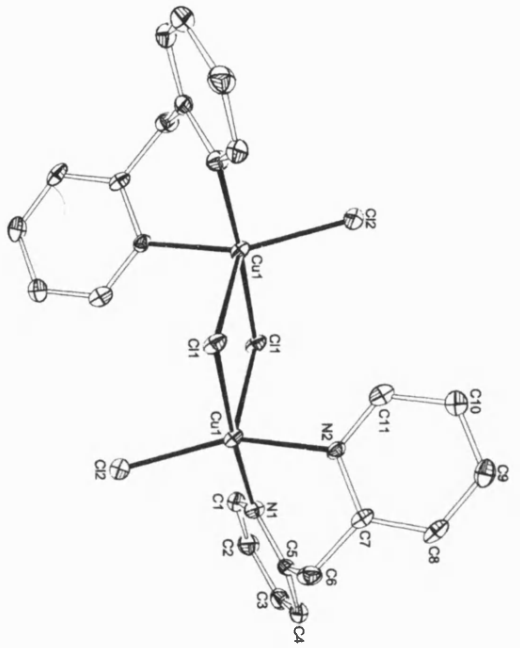

Bond Lengths (Å)

Cu(1)-N(1)	2.027(5)	N(2)-C(7)	1.366(7)	C(8)-C(9)	1.382(9)
Cu(1)-N(2)	2.029(5)	N(3)-C(12)	1.332(7)	C(9)-C(10)	1.385(8)
Cu(1)-Cl(2)	2.259(2)	N(3)-C(16)	1.355(7)	C(10)-C(11)	1.379(8)
Cu(1)-Cl(1)	2.311(2)	N(4)-C(22)	1.343(7)	C(12)-C(13)	1.381(9)
Cu(1)-Cl(1)#1	2.630(2)	N(4)-C(18)	1.361(7)	C(13)-C(14)	1.397(9)
Cu(2)-N(3)	2.024(5)	O(1A)-O(1B)	1.31(2)	C(14)-C(15)	1.373(9)
Cu(2)-N(4)	2.028(5)	O(1A)-C(23)	1.373(11)	C(15)-C(16)	1.386(8)
Cu(2)-Cl(3)	2.273(2)	O(1B)-C(23)	1.335(13)	C(16)-C(17)	1.495(8)
Cu(2)-Cl(4)	2.303(2)	C(1)-C(2)	1.387(9)	C(17)-C(18)	1.502(8)
Cu(2)-Cl(4)#2	2.627(2)	C(2)-C(3)	1.401 (9)	C(18)-C(19)	1.380(8)
Cl(1)-Cu(1)#1	2.630(2)	C(3)-C(4)	1.362(9)	C(19)-C(20)	1.386(9)
Cl(4)-Cu(2)#2	2.627(2)	C(4)-C(5)	1.383(8)	C(20)-C(21)	1.389(8)
N(1)-C(1)	1.331(8)	C(5)-C(6)	1.501(8)	C(21)-C(22)	1.370(8)
N(1)-C(5)	1.365(7)	C(6)-C(7)	1.495(8)		
N(2)-C(11)	1.343(8)	C(7)-C(8)	1.379(8)		

Bond Angles (°)

N(1)-Cu(1)-N(2)	86.0(2)	C(1)-N(1)-Cu(1)	122.4(4)	C(8)-C(7)-C(6)	123.6(5)
N(1)-Cu(1)-Cl(2)	89.1(2)	C(5)-N(1)-Cu(1)	118.3(4)	C(7)-C(8)-C(9)	119.8(5)
N(2)-Cu(1)-Cl(2)	153.02(14)	C(11)-N(2)-C(7)	118.7(5)	C(10)-C(9)-C(8)	118.9(6)
N(1)-Cu(1)-Cl(1)	176.1(2)	C(11)-N(2)-Cu(1)	122.6(4)	C(11)-C(10)-C(9)	119.1(6)
N(2)-Cu(1)-Cl(1)	90.93(14)	C(7)-N(2)-Cu(1)	118.6(4)	N(2)-C(11)-C(10)	122.3(5)
Cl(2)-Cu(1)-Cl(1)	94.72(6)	C(12)-N(3)-C(16)	118.9(5)	N(3)-C(12)-C(13)	123.4(6)
N(1)-Cu(1)-Cl(1)#1	92.81(14)	C(12)-N(3)-Cu(2)	121.6(4)	C(12)-C(13)-C(14)	117.6(6)
N(2)-Cu(1)-Cl(1)#1	96.93(14)	C(16)-N(3)-Cu(2)	119.5(4)	C(15)-C(14)-C(13)	119.4(6)
Cl(2)-Cu(1)-Cl(1)#1	109.81(6)	C(22)-N(4)-C(18)	118.2(5)	C(14)-C(15)-C(16)	119.7(5)
Cl(1)-Cu(1)-Cl(1)#1	85.25(6)	C(22)-N(4)-Cu(2)	122.8(4)	N(3)-C(16)-C(15)	121.0(5)
N(3)-Cu(2)-N(4)	87.0(2)	C(18)-N(4)-Cu(2)	119.0(4)	N(3)-C(16)-C(17)	115.4(5)
N(3)-Cu(2)-Cl(3)	89.82(14)	O(1B)-O(1A)-C(23)	59.7(7)	C(15)-C(16)-C(17)	123.6(5)
N(4)-Cu(2)-Cl(3)	150.36(14)	O(1A)-O(1B)-C(23)	62.6(7)	C(16)-C(17)-C(18)	110.7(5)
N(3)-Cu(2)-Cl(4)	176.29(14)	N(1)-C(1)-C(2)	123.3(6)	N(4)-C(18)-C(19)	121.6(5)
N(4)-Cu(2)-Cl(4)	90.78(14)	C(1)-C(2)-C(3)	116.7(6)	N(4)-C(18)-C(17)	115.5(5)
Cl(3)-Cu(2)-Cl(4)	93.60(6)	C(4)-C(3)-C(2)	120.4(6)	C(19)-C(18)-C(17)	122.8(5)
N(3)-Cu(2)-Cl(4)#2	92.84(14)	C(3)-C(4)-C(5)	119.9(6)	C(18)-C(19)-C(20)	119.6(5)
N(4)-Cu(2)-Cl(4)#2	105.63(14)	N(1)-C(5)-C(4)	120.4(5)	C(19)-C(20)-C(21)	118.4(5)
Cl(3)-Cu(2)-Cl(4)#2	103.95(6)	N(1)-C(5)-C(6)	115.6(5)	C(22)-C(21)-C(20)	119.3(5)
Cl(4)-Cu(2)-Cl(4)#2	84.94(6)	C(4)-C(5)-C(6)	124.0(5)	N(4)-C(22)-C(21)	122.9(5)
Cu(1)-Cl(1)-Cu(1)#1	94.75(6)	C(7)-C(6)-C(5)	111.1(5)	O(1B)-C(23)-O(1A)	57.7(7)
Cu(2)-Cl(4)-Cu(2)#2	95.06(6)	N(2)-C(7)-C(8)	121.1(5)		
C(1)-N(1)-C(5)	119.2(5)	N(2)-C(7)-C(6)	115.2(5)		

4. The Structure of L17/$CuCl_2$ Dimer

A crystal of approximate dimensions 0.2 x 0.2 x 0.4 mm was used for data collection.

Crystal data: $C_{17}H_{20}N_2C1_2Cu$, M = 386.8 monoclinic, a = 9.753(2), b = 12.414(2), c = 14.520(2) Å, β = 97.79(2)°, U = 1741.8 $Å^3$, space group $P2_1/n$, Z = 4, D_c = 1.47 g cm^{-3}, μ(Mo-K_α) = 15.6 cm^{-1}, F(000) = 796. Data were measured at room temperature on a CAD4 automatic four-circle diffractometer in the range $2 \leq \theta \leq 24°$. 3062 reflections were collected of which 2035 were unique with $I > 2\sigma(I)$. Data were corrected for Lorentz and polarization but not for absorption. The structure was solved by Direct methods and refined using the SHELX[90, 91] suite of programs. In the final least 3quares cycles all atoms were allowed to vibrate anisotropically. Hydrogen atoms were included at calculated positions in all cases except for C15, C16 and C17. The difference electron density map exhibited some smudging in the C16/C17 region. This was largely due to disorder in the positions of these 2 atoms with C16a and C17a in the ratio 62:38.

The molecule as presented forms one half of a dimer. The remaining portion of the dimer, as illustrated in the ORTEP plot, is generated by inversion through the origin. Final residuals after 10 cycles of least squares were R = 0.0322, R_w = 0.0348, for a weighting scheme of $w = 1.6341/[\sigma^2(F) + 0.000698(F)^2]$. Max. final shift/esd was 0.025. The max. and min. residual densities were 0.19 and -0.15 e $Å^{-3}$ respectively.

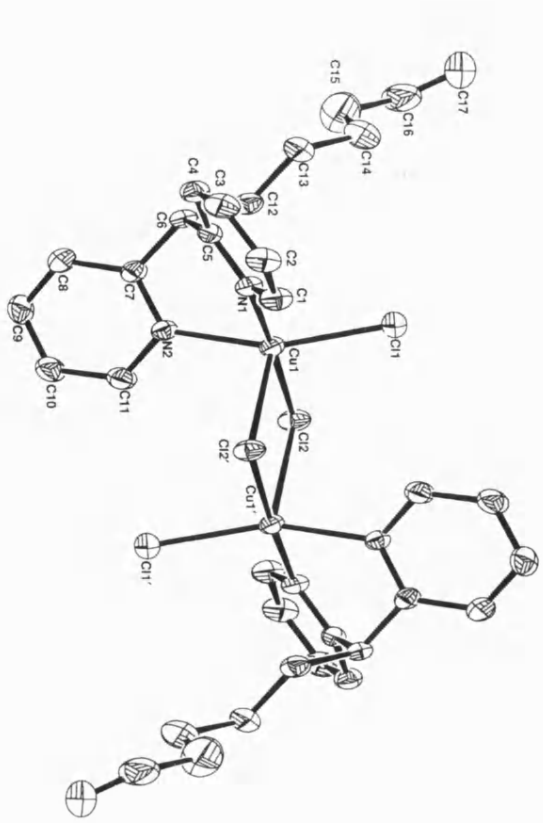

Bond Lengths (Å)

Cl(l)-Cu(l)	2.264(3)	C(9)-C(8)	1.373(7)	H(31)-C(3)	0.960
Cl(2)-Cu(1)	2.284(3)	C(10)-C(9)	1.370(7)	H(41)-C(4)	0.960
N(1)-Cu(1)	2 .016(5)	C(11)-C(10)	1.376(7)	H(61)-C(6)	0.960
N(2)-Cu(1)	2 .048(5)	C(13)-C(12)	1.523(8)	H(81)-C(8)	0.960
C(l)-N(l)	1.339(6)	C(14)-C(13)	1.546(10)	H(91)-C(9)	0.960
C(5)-N(1)	1.337(5)	C(15)-C(14)	1.407(10)	H(10)-C(10)	0.960
C(7)-N(2)	1.349(5)	C(16a)-C(15)	1.687(37)	H(11)-C(11)	0.960
C(11)-N(2)	1.337(6)	C(16)-C(15)	1.651(27)	H(121)-C(12)	0.960
C(2)-C(1)	1.367(7)	C(17a)-C(16a)	1.254 (64)	H(122)-C(12)	0.960
C(3)-C(2)	1.377(7)	C(16)-C(16a)	0.931(24)	H(131)-C(13)	0.960
C(4)-C(3)	1 .386(7)	C(17)-C(16a)	0.914(29)	H(132)-C(13)	0.960
C(5)-C(4)	1.401(6)	C(16)-C(17a)	0.752(16)	H(141)-C(14)	0.960
C(6)-C(5)	1.507(7)	C(17)-C(17a)	0.925(37)	H(142)-C(14)	0.960
C(7)-C(6)	1.514(7)	C(17)-C(16)	1.199(59)		
C(12)-C(6)	1.534 (7)	H(11)-C(l)	0.960		
C(8)-C(7)	1.385(6)	H(21)-C(2)	0.960		

Bond Angles (°)

Cl(2)-Cu(1)-Cl(1)	92.9	C(5)-N(1)-Cu(1)	121.6(3)	C(4)-C(3)-C(2)	118.7(5)
N(l)-Cu(l)-Cl(l)	89.3(2)	C(5)-N(1)-C(1)	119.3(4)	C(5)-C(4)-C(3)	119.2(5)
N(1)-Cu(1)-Cl(2)	175.9(1)	C(7)-N(2)-Cu(1)	120.5(3)	C(4)-C(5)-N(1)	120.9(4)
N(2)-Cu(1)-Cl(1)	155.3(1)	C(11)-N(2)-Cu(1)	120.7(4)	C(6)-C(5)-N(1)	118.0(4)
N(2)-Cu(1)-C1(2)	92.3(2)	C(11) -N(2)-C(7)	118.7 (4)	C(6)-C(5)-C(4)	121.1 (4)
N(2)-Cu(1)-N(1)	87.1(2)	C(2)-C(1)-N(1)	122.7(5)	C(7)-C(6)-C(5)	111.0(4)
C(l)-N(l)-Cu(l)	119.1(4)	C(3)-C(2)-C(1)	119.2(5)	C(12)-C(6)-C(5)	112.7 (4)

C(12)-C(6)-C(7)	111.3(4)	C(17)-C(17a)-C(16)	90.7(67)	C(9)-C(8)-H(81)	120.2(4)
C(6)-C(7)-N(2)	117.8 (4)	C(16a)-C(16)-C(15)	75.9(33)	H(9.1)-C(9)-C(8)	120.6(4)
C(8) -C(7)-N(2)	121.1(4)	C(17a)-C(16)-C(15)	168.7(48)	C(10)-C(9)-H(91)	120.6(4)
C(8)-C(7)-C(6)	121.1 (4)	C(17a)-C(16)-C(16a)	95.7(68)	H(10)-C(10)-C(9)	120.3(4)
C(9)-C(8)-C(7)	119.7 (5)	C(17)-C(16)-C(15)	123.6(42)	C(11)-C(10)-H(10)	120.3(4)
C(10)-C(9)-C(8)	118.8 (5)	C(17)-C(16)-C(16a)	48.9(29)	H(11)-C(11)-N(2)	118.9(3)
C(11)-C(10)-C(9)	119.5(5)	C(17)-C(16)-C(17a)	50.5(46)	H(11)-C(11)-C(10)	118.9(4)
C(10)-C(11)-N(2)	122.2(5)	C(17a)-C(17)-C(16a)	86.0(52)	H(121)-C(12)-C(6)	108.4 (3)
C(13)-C(12)-C(6)	113.8(4)	C(16)-C(17)-C(16a)	50.1(28)	H(122)-C(12)-C(6)	108.4(3)
C(14)-C(13)-C(12)	112.9(6)	C(16)-C(17)-C(17a)	38.9(24)	H(122)-C(12)-H(121)	109.5
C(15)-C(14)-C(13)	115.8(7)	H(11)-C(l)-N(l)	118.6(3)	C(13)-C(12)-H(121)	108.4(3)
C(16a)-C(15)-C(14)	100.7(13)	C(2)-C(1)-H(11)	118.6(4)	C(13)-C(12)-H(122)	108.4(3)
C(16)-C(15)-C(14)	121.7(11)	H(21)-C(2)-C(1)	120.4(4)	H(131)-C(13)-C(12)	108.6(3)
C(16)-C(15)-C(16a)	32.4(8)	C(3)-C(2)-H(21)	120.4(3)	H(132)-C(13)-C(12)	108.6(3)
C(17a)-C(16a)-C(15)	108.0(38)	H(31)-C(3)-C(2)	120.7(3)	H(132)-C(13)-H(131)	109.5
C(16)-C(16a)-C(15)	71.7(34)	C(4)-C(3)-H(31)	120.7(3)	C(14)-C(13)-H(131)	108.6(4)
C(16)-C(16a)-C(17a)	36.7(28)	H(41)-C(4) -C(3)	120.4 (3)	C(14)-C(13)-H(132)	108.6(5)
C(17)-C(16a)-C(15)	150.0(50)	C(5)-C(4)-H(41)	120.4 (3)	H(141)-C(14)-C(13)	107.9(4)
C(17)-C(16a)-C(17a)	47.4(30)	H(61)-C(6)-C(5)	106.8(3)	H(142)-C(14)-C(13)	107.9(4)
C(17)-C(16a)-C(16)	81.0(51)	C(7)-C(6)-H(61)	108.3(3)	H(142)-C(14)-H(141)	109.5
C(16)-C(17a)-C(16a)	47.6(42)	C(12)-C(6)-H(61)	106.5(3)	C(15)-C(14)-H(141)	107.9(6)
C(17)-C(17a)-C(16a)	46.7(31)	H(81)-C(8)-C(7)	120.2(3)	C(15)-C(14)-H(142)	107.9(5)

5. The Structure of L12/$CuCl_2$

A crystal of approximate dimensions 0.3 x 0.3 x 0.5 mm was used for data collection.

Crystal data: $C_{15}H_{17}N_3Cl_2Cu$, M = 373.8 monoclinic, a = 9.031(1), b = 13.518(2), c = 13.891(1) Å, β = 109.307(9)°, U = 1650.3 $Å^3$, space group $P2_1/n$, Z = 4, D_c = 1.50 g cm^{-3}, μ(Mo-K_α) = 16.5 cm^{-1}, F(000) = 764. Data were measured at room temperature on a CAD4 automatic four-circle diffractometer in the range $2 \leq \theta \leq 24°$. 2894 reflections were collected of which 2023 were unique with $I > 2\sigma(I)$. Data were corrected for Lorentz and polarization but not for absorption. The structure was solved by Patterson methods and refined using the SHELX[90, 91] suite of programs. In the final least squares cycles all atoms were allowed to vibrate anisotropically. Hydrogen atoms were included at calculated positions except in the instance of the H141, H151 and H152 (attached to olefinic carbons C14 and CI5). These protons were located in an advanced Difference Fourier and refined at a distance of 0.96 Å from the relevant parent atoms.

The lattice was also seen to contain some residual solvent straddling the centre of symmetry at 0,0.5,0.5. Unfortunately, due to disorder, this fragment did not approximate to anything recognisable, and the best results were obtained by 'mopping-up' this electron density as partial isotropic carbon atoms. (Cl', C2' with occupancies 0.48 and, 0.31 respectively)

Final residuals after 12 cycles of least squares were R = 0.0343, R_w = 0.0369, for a weighting scheme of $w = 2.3376/[\sigma^2(F) + 0.000550(F)^2]$. Max. final shift/esd was 0.000. The max. and min. residual densities were 0.28 and -0.13 $eÅ^{-3}$ respectively.

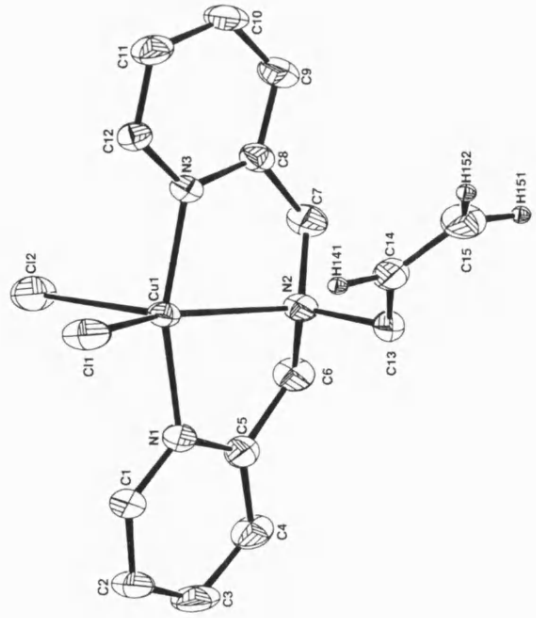

Bond Lengths (Å)

Cl(1)-Cu(1)	2.270(3)	C(4)-C(3)	1.392 (8)	H(41)-C(4)	0.960
Cl(2)-Cu(1)	2.467(3)	C(5)-C(4)	1.381 (6)	H(61)-C(6)	0.960
N(l)-Cu(l)	2.004(5)	C(6)-C(5)	1.498 (6)	H(62)-C(6)	0.960
N(2)-Cu(1)	2.084(5)	C(8)-C(7)	1.505(7)	H(71)-C(7)	0.960
N(3)-Cu(1)	2.003(5)	C(9)-C(8)	1.378(6)	H(72)-C(7)	0.960
C(5)-Cu(1)	2.832(7)	C(10)-C(9)	1.374(7)	H(91)-C(9)	0.960
C(8)-Cu(1)	2.835(7)	C(11)-C(10)	1.388(7)	H(101)-C(10)	0.960
C(l)-N(l)	1.341 (6)	C(12)-C(11)	1.385(6)	H(111)-C(11)	0.960
C(5)-N(1)	1.350(6)	C(14)-C(13)	1.502(7)	H(121)-C(12)	0.960
C(6) -N(2)	1.497 (5)	C(15)-C(14)	1.303(7)	H(131)-C(13)	0.960
C(7)-N(2)	1.480(6)	C(2')-C(1')	0.891	H(132)-C(13)	0.960
C(13)-N(2)	1.498(5)	C(l')-C(l'a)	1.326	H(141)-C(14)	0.960(2)
C(8)-N(3)	1.346(5)	C(2')-C(2'a)	1.452	H(152)-C(15)	0.960(2)
C(12)-N(3)	1.336(5)	H(11)-C(1)	0.960	H(151)-C(15)	0.960(2)
C(2) -C(l)	1.376(6)	H(21)-C(2)	0.960		
C(3)-C(2)	1.364 (8)	H(31)-C(3)	0.960		

Bond Angles (°)

Cl(2)-Cu(1)-Cl(1)	109.7	C(5)-Cu(1)-N(2)	57.5(2)	C(7)-N(2)-C(6)	113.5(4)
N(l)-Cu(l)-Cl(l)	96.7(2)	C(5)-Cu(1)-N(3)	138.2(1)	C(13)-N(2)-Cu(1)	112.4(3)
N(1)-Cu(1)-Cl(2)	92.0(2)	C(8)-Cu(1)-Cl(1)	121.3(2)	C(13)-N(2)-C(6)	108.9(4)
N(2)-Cu(1)-Cl(1)	145.7(1)	C(8)-Cu(1)-Cl(2)	91.3(2)	C(13)-N(2)-C(7)	111.1 (4)
N(2)-Cu(1) -Cl (2)	104.6(2)	C(8)-Cu(1)-N(1)	138.0(1)	C(8) -N(3) -Cu(l)	114.3 (3)
N(2) -Cu(l)-N(l)	81.2 (2)	C(8)-Cu(1)-N(2)	57.6(2)	C(12) -N(3) -Cu(l)	126.2 (3)
N(3)-Cu(1) -Cl (1)	97.2 (2)	C(8)-Cu(1)-N(3)	25.6(1)	C(12)-N(3)-C(8)	119.4 (4)
N(3) -Cu(l) -Cl (2)	91.8 (2)	C(8) -Cu(l) -C(5)	112.5 (2)	C(2)-C(1) -N(l)	122.6(5)
N(3)-Cu(1)-N(1)	163.3(1)	C(l) -N(l) -Cu(l)	127.1 (4)	C(3)-C(2)-C(1)	118.8(5)
N(3)-Cu(1)-N(2)	82.1(2)	C(5)-N(1)-Cu(1)	113.8(3)	C(4)-C(3)-C(2)	119.5(5)
C(5)-Cu(1)-Cl(1)	121.9(2)	C(5)-N(1)-C(1)	118.7(4)	C(5)-C(4)-C(3)	118.9(5)
C(5)-Cu(1)-Cl(2)	88.4(2)	C(6)-N(2)-Cu(1)	104.6(3)	N(1)-C(5)-Cu(1)	40.4 (2)
C(5)-Cu(1)-N(1)	25.9(1)	C(7)-N(2)-Cu(1)	106.2(3)	C(4)-C(5)-Cu(1)	160.9(3)

C(4) -C(5)-N(1)	121.3(5)	H(11)-C(1)-N(l)	118.7(3)	H(91)-C(9)-C(8)	120.1(3)
C(6)-C(5)-Cu(1)	75.6(3)	C(2)-C(1)-H(11)	118.7 (4)	C(10)-C(9)-H(91)	120.1 (3)
C(6)-C(5)-N(1)	115.9(4)	H(21)-C(2)-C(1)	120.6(4)	H(101)-C(10) -C(9)	120.6(3)
C(6)-C(5)-C(4)	122.8 (5)	C(3)-C(2)-H(21)	120.6(3)	C(11)-C(10)-H(101)	120.6(3)
C(5)-C(6)-N(2)	110.0(4)	H(31)-C(3)-C(2)	120.3(3)	H(111)-C(11)-C(10)	120.6(3)
C(8)-C(7) -N(2)	110.9 (4)	C(4)-C(3)-H(31)	120.3(4)	C(12)-C(11)-H(111)	120.6(3)
N(3) -C(8) -Cu(l)	40.1 (2)	H(41)-C(4)-C(3)	120.6(4)	H(121)-C(12)-N(3)	119.1(3)
C(7)-C(8)-Cu(1)	76.1 (3)	C(5)-C(4)-H(41)	120.5(4)	H(121)-C(12)-C(11)	119.1 (3)
C(7)-C(8)-N(3)	116.2 (4)	H(61)-C(6)-N(2)	109.3(3)	H(131)-C(13)-N(2)	108.4 (3)
C(9)-C(8)-Cu(1)	161.3(3)	H(61)-C(6)-C(5)	109.3(3)	H(132)-C(13)-N(2)	108.4(3)
C(9)-C(8)-N(3)	121.3(5)	H(62)-C(6)-N(2)	109.3(3)	H(132)-C(13)-H(131)	109.5
C(9)-C(8)-C(7)	122.5(4)	H(62)-C(6)-C(5)	109.3(3)	C(14)-C(13)-H(131)	108.4 (3)
C(10)-C(9)-C(8)	119.8(5)	H(62)-C(6)-H(61)	109.5	C(14)-C(13) -H(132)	108.4 (3)
C(11)-C(10)-C(9)	118.8(5)	H(71)-C(7)-N(2)	109.1 (3)	H(141)-C(14)-C(13)	115.2(26)
C(12)-C(11)-C(10)	118.9(5)	H(72)-C(7)-N(2)	109.1(3)	C(15)-C(14)-H(141)	121.6(26)
C(11)-C(12)-N(3)	121.8(5)	H(72)-C(7)-H(71)	109.5	H(152)-C(15)-C(14)	121.3(25)
C(14)-C(13)-N(2)	113.7(4)	C(8)-C(7)-H(71)	109.1(3)	H(151)-C(15)-C(14)	122.4(26)
C(15)-C(14)-C(13)	123.0(5)	C(8)-C(7)-H(72)	109.1(3)	H(151)-C(15)-H(152)	115.8(36)

6. The Structure of L10/$CuCl_2$ Dimer

A crystal of approximate dimensions 0.3 x 0.3 x 0.07 mm was used for data collection.

Crystal data: $C_8H_{18}N_2Cl_2Cu$, M = 276.7 monoclinic, a = 8.546(1), b = 11.992(2), c = 12.542(2) Å, β = 101.61(1)°, U = 1259.1 $Å^3$, space group $P2_1/n$, Z = 4, D_c = 1.46 g cm^{-3}, μ(Mo-K_α) = 21.3 cm^{-1}, F(000) = 572. Data were measured at room temperature on a CAD4 automatic four-circle diffractometer in the range $2 \leq \theta \leq 23°$. 1988 reflections were collected of which 1143 were unique with $I > 2\sigma(I)$. Data were corrected for Lorentz and polarization but not for absorption. The structure was solved by Patterson methods and refined using the SHELX[90, 91] suite of programs. In the final least squares cycles all atoms were allowed to vibrate anisotropically. Hydrogen atoms were located in an advanced Difference Fourier map and refined at a fixed distance (0.98 Å) from the relevant parent atoms. Final residuals after 8 cycles of least squares were R = 0.0388, R_w = 0.0381, for a weighting scheme of $w = 1.7671/[\sigma^2(F) + 0.001126(F)^2]$. Max. final shift/esd was 0.000. The max. and min. residual densities were 0.24 and -0.19 e $Å^{-3}$ respectively.

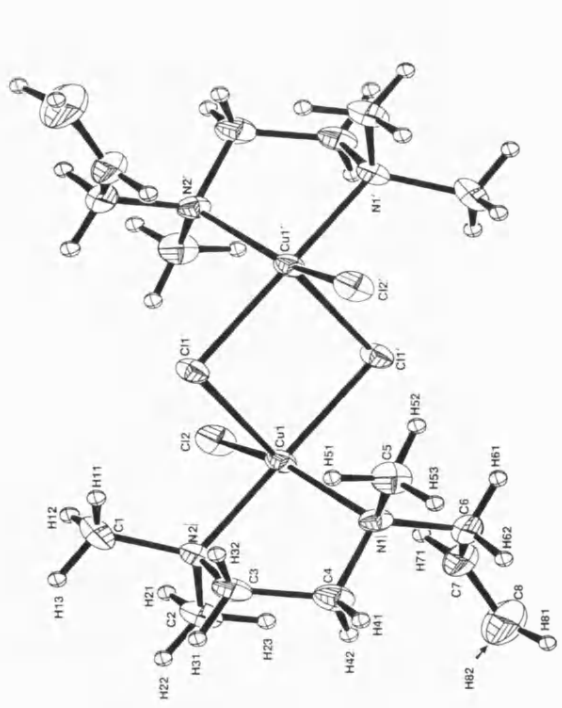

Bond Lengths (Å)

Cl(1)-Cu(1)	2.303(4)	C(4)-C(3)	1.490(11)	H(41)-C(4)	0.981(20)
Cl(2)-Cu(1)	2.260(4)	C(7)-C(6)	1.467(11)	H(42)-C(4)	0.976(20)
N(l)-Cu(l)	2.098(7)	C(8)-C(7)	1.313(13)	H(Sl)-C(5)	0.987(20)
N(2)-Cu(1)	2.050(7)	H(11)-C(1)	0.979(20)	H(52)-C(5)	0.984(15)
C(3)-Cu(1)	2.818(9)	H(12)-C(1)	0.971 (20)	H(53)-C(5)	0.925(72)
C(4)-N(1)	1.499(9)	H(13)-C(1)	0.970(20)	H(61)-C(6)	0.982(20)
C(5)-N(1)	1.479(10)	H(21)-C(2)	0.976(20)	H(62)-C(6)	0.986(20)
C(6)-N(1)	1.493(10)	H(22)-C(2)	0.970(20)	H(71)-C(7)	0.981(20)
C(1)-N(2)	1.475(10)	H(23)-C(2)	0.978(20)	H(81)-C(8)	0.973(20)
C(2)-N(2)	1.497(10)	H(31)-C(3)	0.983(20)	H(82)-C(8)	0.982(20)
C(3)-N(2)	1.487 (9)	H(32)-C(3)	0.975(20)		

Bond Angles (°)

Cl (2) -Cu(l) -Cl (1)	93.7 (2)	C(1)-N(2) -Cu(1)	113.6(5)	H(13)-C(1)-H(11)	120.6(61)
N(.1)-Cu(l) -Cl (1)	91.0 (2)	C(2)-N(2)-Cu(1)	112.4 (5)	H(13)-C(1)-H(12)	91.3(57)
N(1)-Cu(1)-Cl(2)	150.3(2)	C(2)-N(2)-C(1)	107.8(7)	H(21)-C(2)-N(2)	105.4(45)
N(2)-Cu(1)-Cl(1)	174.0(2)	C(3)-N(2)-Cu(1)	104.5(5)	H(22)-C(2)-N(2)	108.2(44)
N(2) -Cu(l) -Cl (2)	91.7 (3)	C(3)-N(2)-C(1)	110.0 (7)	H(22)-C(2)-H(21)	102.3(57)
N(2) -Cu(l) -N(l)	85.4 (3)	C(3)-N(2)-C(2)	108.5(6)	H(23)-C(2)-N(2)	105.8(42)
C(3)-Cu(1)-Cl(1)	144.1 (2)	N(2)-C(3)-Cu(1)	44.8(2)	H(23)-C(2)-H(21)	112.5(62)
C(3)-Cu(1)-Cl(2)	122.2(3)	C(4)-C(3)-Cu(1)	77.6(4)	H(23)-C(2)-H(22)	121.6(62)
C(3)-Cu(1)-N(1)	57.3(3)	C(4)-C(3)-N(2)	109.1(6)	H(31)-C(3)-Cu(1)	148.5(38)
C(3)-Cu(1)-N(2)	30.7(2)	C(3)-C(4)-N(1)	109.5(7)	H(31)-C(3) -N(2)	104.5(39)
C(4)-N(1)-Cu(1)	105.8(5)	C(7)-C(6)-N(1)	113.8(6)	H(3.1)-C(3)-C(4)	115.4 (41)
C(5)-N(1)-Cu(1)	111.3(5)	C(8)-C(7)-C(6)	123.3(9)	H(32)-C(3)-Cu(1)	90.1 (41)
C(5)-N(1)-C(4)	109.1(6)	H(11)-C(1)-N(2)	105.0(43)	H(32)-C(3)-N(2)	107.7(42)
C(6)-N(1)-Cu(1)	111.5(5)	H(12)-C(1)-N(2)	111.3(44)	H(32) -C{3)-C(4)	109.7(43)
C(6)-N(1)-C(4)	111.1 (6)	H(12)-C(1)-H(11)	118.2 (61)	H(32)-C(3)-H(31)	110.0(57)
C(6)-N(1)-C(5)	108.1 (6)	H(13)-C(1)-N(2)	110.2(42)	H(41)-C(4)-N(1)	108.9(44)

H{41-)-C(4)-C(3)	109.9(45)	H(53)-C(5)-H(51)	108.1(59)	H(71)-C(7)-C(8)	115.2(44)
H(~2)-C(4)-N(1)	110.2(43)	H(53)-C(5)-H(52)	106.2(60)	H(81)-C(8)-C(7)	114.5(48)
H(42)-C(4)-C(3)	112.5(43)	H(61)-C(6)-N(1)	105.3(42)	H(82)-C(8)-C(7)	116.6(42)
H(42)-C(4)-H(41)	105.7(61)	H(61)-C(6) -C(7)	115.8(41)	H(82)-C(8)-H(81)	122.9(63)
H(51)-C(5)-N(1)	107.0(41)	H(62)-C(6)-N(1)	102.4 (42)	H(13)-H(12)-C(1)	44.3(29)
H(52)-C(5)-N(1)	109.4 (40) I	H(62)-C(6)-C(7)	118.6(42)	H(12)-H(13)-C(1)	44.4(29)
H(52)-C(5)-H(51)	114.7(60)	H(62)-C(6)-H(61)	98.8 (54)		
H(53)-C(5)-N(1)	111.6(48)	H(71)-C(7)-C(6)	121.4 (44)		

7. The Structure of L10/$Cu(NO_3)_2$

A crystal of approximate dimensions 0.2 x 0.2 x 0.7 mm was used for data collection.

Crystal data: $C_8H_{18}N_4O_6CU$, M = 329.8 monoclinic, a = 8.594(2), b = 13.675(3), c = 12.510(3) Å, β = 105.92(9)°, U = 1413.8 $Å^3$, space group $P2_1/n$, Z = 4, D_c = 1.55 g cm^{-3}, μ(Mo-K_α) = 15.7 cm^{-1}, F(000) = 684. Data were measured at room temperature on a CAD4 automatic four-circle diffractometer in the range $2 \leq \theta \leq 24°$. 2490 reflections were collected of which 1762 were unique with $I > 2\sigma(I)$. Data were corrected for Lorentz and polarization but not for absorption. The structure was solved by Patterson methods and refined using the SHELX[90, 91] suite of programs. In the final least squares cycles all atoms were allowed to vibrate anisotropically. Hydrogen atoms were included at calculated positions except in the instance of the H51, H61 and H62 (attached to C5 and C6 respectively). These protons were located in an advanced Difference Fourier and refined at a distance of 0.96 Å from the relevant parent atoms.

Final residuals after 10 cycles of least squares were R = 0.0357, R_w = 0.0388, for a weighting scheme of $w = 2.5522/[\sigma^2(F) + 0.000893(F)^2]$. Max. final shift/esd was 0.000. The max. and min. residual densities were 0.31 and -0.21 e $Å^{-3}$ respectively.

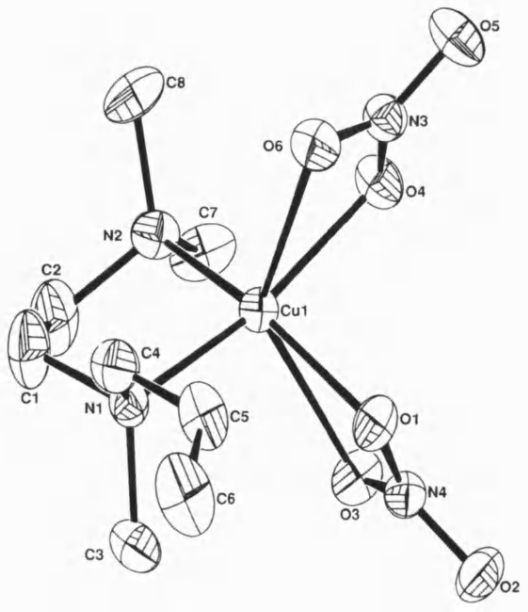

Bond Lengths (Å)

O(l)-Cu(l)	2.011(5)	C(3) -N(l)	1.479(6)	H(32)-C(3)	0.960
O(3)-Cu(1)	2.441(5)	C(4)-N(1)	1.510(7)	H(33)-C(3)	0.960
O(4) -Cu(l)	2.022(5)	C(2) -N(2)	1.491 (7)	H(41)-C(4)	0.960
O(6) -Cu(l)	2.402 (4)	C(7)-N(2)	1.478(6)	H(42)-C(4)	0.960
N(l)-Cu(l)	2.025(5)	C(8) -N(2)	1.496(6)	H(51)-C(5)	0.960(2)
N(2) -Cu(l)	1.991 (5)	C(2)-C(1)	1.424(8)	H(61)-C(6)	0.960 (2)
N(4)-O(1)	1.287(5)	C(5) -C(4)	1.474 (8)	H(62)-C(6)	0.960(2)
N(4)-O(2)	1.227 (5)	C(6)-C(5)	1.301 (8)	H(71)-C(7)	0.960
N(4)-O(3)	1.233(5)	H(11)-C(1)	0.960	H(72)-C(7)	0.960
N(3) -O(4)	1.299(5)	H(12)-C(1)	0.960	H(73)-C(7)	0.960
N(3)-O(5)	1.209(5)	H(21)-C(2)	0.960	H(81)-C(8)	0.960
N(3) -O(6)	1.240 (5)	H(22)-C(2)	0.960	H(82)-C(8)	0.960
C(l) -N(l)	1.505(7)	H(31)-C(3)	0.960	H(83)-C(8)	0.960

Bond Angles (°)

O(3) -Cu(l) -O(1)	56.8 (2)	C(7) -N(2)-C(2)	107.6(5)	H(33)-C(3)-N(1)	109.5(3)
O(4) -Cu(l) -O(1)	88.2 (2)	C(8)-N(2) -Cu(l)	112.8(3)	H(33)-C(3)-H(31)	109.5
O(4) -Cu(l) -O(3)	90.2 (2)	C(8) -N(2)-C(2)	114.4 (5)	H(33)-C(3) -H(32)	109.5
O(6) -Cu(l) -O(1)	87.3 (2)	C(8)-N(2) -C(7)	109.2(4)	H(41)-C(4) -N(l)	108.3(3)
O(6)-Cu(1)-O(3)	133.7(1)	O(5)-N(3)-O(4)	119.6(4)	H(42)-C(4)-N(1)	108.3(3)
O(6)-Cu(1)-O(4)	57.5(2)	O(6) -N(3)-O(4)	116.1 (4)	H(42)-C(4)-H(41)	109.5
N(l)-Cu(l) -O(1)	95.4 (2)	O(6) -N(3)-O(5)	124.3(4)	C(5)-C(4)-H(41)	108.3(3)
N(l) -Cu(l) -O(3)	104.5(2)	O(2)-N(4)-O(1)	119.2 (4)	C(5)-C(4)-H(42)	108.3(3)
N(1)-Cu (1)-O(4)	164 .4 (1)	O(3)-N(4)-O(1)	117.3(4)	H(51)-C(5)-C(4)	113.1(36)
N(1)-Cu(1)-O(6)	107 .4 (2)	O(3)-N(4)-O(2)	123.5(4)	C(6)-C(5)-H(51)	123.2(36)
N(2) -Cu(l) -O(1)	161.0 (1)	C(2) -C(l)-N(1)	112.2 (5)	H(61)-C(6)-C(5)	136.1(32)
N(2) -Cu(l) -O(3)	104.2 (2)	C(1)-C(2) -N(2)	111.3(5)	H(62)-C(6)-C(5)	114.7(32)
N(2)-Cu(1)-O(4)	92.8(2)	C(5)-C(4)-N(1)	114.3(4)	H(62)-C(6)-H(61)	108.1 (44)
N(2)-Cu(1)-O(6)	109.2(2)	C(6)-C(5)-C(4)	123.6(6)	H(71)-C(7) -N(2)	109.5(4)
N(2)-Cu(1)-N(1)	88.7(2)	H(ll)-C(1) -N(1)	108.8 (3)	H(72)-C(7)-N(2)	109.5(3)
N(4)-O(1)-Cu(1)	102.3(3)	H(12) -C(1)-N(1)	108.8(3)	H(72)-C(7)-H(71)	109.5
N(4) -O(3) -Cu(1)	83.5(3)	H(12)-C(1) -H(11)	109.5	H(73)-C(7)-N(2)	109.5(3)
N(3) -O(4) -Cu(1)	101.2 (3)	C(2)-C(1)-H(11)	108.8 (5)	H(73)-C(7)-H(71)	109.5
N(3)-O(6)-Cu(1)	85.0(3)	C(2)-C(1)-H(12)	108.8 (4)	H(73)-C(7)-H(72)	109.5
C(l)-N(l)-Cu(l)	103.7(4)	H(21)-C(2)-N(2)	109.0(4)	H(81)-C(8)-N(2)	109.5(3)
C(3)-N(1)-Cu(1)	113.1 (3)	H(21)-C(2)-C(1)	109.0(5)	H(82)-C(8)-N(2)	109.5(3)
C(3) -N(l) -C(l)	111.5(4)	H(22)-C(2)-N(2)	109.0(3)	H(82)-C(8)-H(81)	109.5
C(4) -N(l)-Cu{l)	111.1 (3)	H(22) -C(2) -C(l)	109.0(4)	H(83)-C(8)-N(2)	109.5(3)
C(4) -N(l) -C(l)	106.5(4)	H(22)-C(2)-H(21)	109.5	H(83)-C(8)-H(81)	109.5
C(4)-N(1) -C(3)	110.5(4)	H(31)-C(3)-N(1)	109.5(3)	H(83)-C(8)-H(82)	109.5
C(2)-N(2)-Cu(1)	104.0 (3)	H(32)-C(3)-N(1)	109.5(3)		
C(7)-N(2)-Cu(1)	108.5(4)	H(32)-C(3)-H(31)	109.5		

APPENDIX B

1. Determination of the Composition of **PL2**

- The overall formula of **CP1** was determined to be:

$$Me_3Si(OSiMe_2)_{172}(OSiMe(H))_{6.7}OSiMe_3$$

Therefore, from the excess of alkenylated ligand (**L15**) added, a maximum of 6.7 moles of **L15** can add to the polymer during the reaction. After the addition of **L15** the composition of **PL2** will be of the idealised form below:

$$Me_3Si(OSiMe_2)_{172}(OSiMe(H))_{6.7-z}(OSiMe(\mathbf{L15+H}))_zOSiMe_3$$

- Microanalysis of **PL2**, after purification to remove any excess alkenylated substrate (**L15**) and catalyst residue, gave the following C, H, N composition:

$$\%\ C = 36.8,\ \%H = 8.15,\ \%N = 1.83$$

Using the idealised structure of **PL2** above, the amount of ligand attached to the polymer (Z) was varied, and the theoretical amount of C, H and N calculated. The theoretical amount of nitrogen is calculated using the formula below, and the best theoretical matches to the experimental result above are listed in Table 17 below.

$$\%\ N = ((14.0067 \times 3) \times Z) / (M_w\ \mathbf{PL2}\ \text{calculated for the amount of substitution, Z})$$

Table 17: Theoretical Best-Fit C, H, N Analysis for PL2

Z	Mass of N in Polymer	M_w	%N	%C	%H
6.2	260.5	14524	1.79	37.2	8.16
6.3	264.7	14544	1.82	37.3	8.16
6.4	268.9	14563	1.85	37.3	8.16

- The attached NMR (NMR 1) shows no evidence of alkenylated substrate. All signals for **L15** and **CP1** protons are highlighted and labelled as per the diagram below.

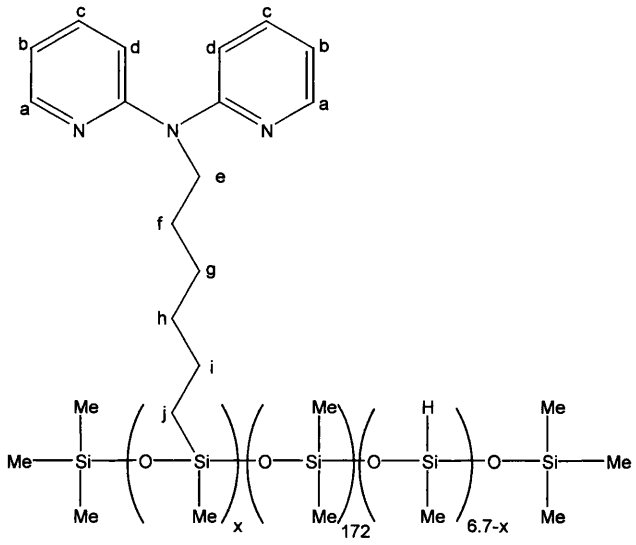

- The number of protons that each signal represents can be calculated using the method below.

Peak 1 - Number of Protons = 8 x Z

Peak 2 - Number of Protons = 2 x Z

Peak 3 - Number of Protons = 8 x Z

Peak 4 - Number of Protons = (2 x Z) + (3 x (6.7 - Z)) + (3 x Z) + (6 x 172) + (2 x 9), where (2 x Z) is the number of j protons, (3 x (6.7 - Z)) is the number of -OSi**Me**(H)- protons, (3 x Z) is the number of -OSi**Me**(L15+H)- protons, (6 x 172) is the number of -OSi$\mathbf{Me}_2$- protons, and (2 x 9) the number of –Si$\mathbf{Me}_3$ terminating group protons.

- The ratios of protons within each signal can be assessed using the integrals on NMR 1. The ratios are:

5.35 (Peak 1) : 1.00 (Peak 2) : 4.34 (Peak 3) : 89.9 (Peak 4)

Peak 3 and Peak 1 both have 8 x Z protons assigned to them, however the ratio is seen to be 5.35:4.34. This is due to Peak 1, which has an unquantifiable number of protons in it from $CHCl_3$ (peak at 7.27 ppm).

Using the theoretical best-fits from the C, H, N microanalysis, formulas and integral ratios above, a best fit can be identified and thus the composition of **PL2**. Table 18 highlights the theoretical number of protons for each peak.

Table 18: Theoretical Number of Protons for Amount of Substitution, Z, for Peaks 1-4

Z	Theoretical Number of Protons for Amount of Substitution, Z			
	Peak 1	Peak 2	Peak 3	Peak 4
6.2	49.6	12.4	49.6	1063.9
6.3	50.4	12.6	50.4	1063.8
6.4	52	13	52	1063.6

These theoretical values are compared to the actual values given in NMR 1 in Table 19, with the exception of Peak 1 for the reason identified above.

Table 19: Comparison of Theoretical and Actual Proton Ratios for PL2

Z	Ratio Peak 2 : Peak 4		Ratio Peak 3 : Peak 4	
	Theoretical	Actual	Theoretical	Actual
6.2	1 : 85.80	1 : 89.92	1 : 21.45	1 : 20.72
6.3	1 : 84.43	1 : 89.92	1 : 21.11	1 : 20.72
6.4	1 : 81.82	1 : 89.92	1 : 20.45	1 : 20.72

- Given the information contained in the tables above, a polymer with 6.3 of the 6.7 reactive Si-H sites (94%) substituted by **L15** is the best fit from both the microanalysis and NMR data collected.

This goodness of fit is exemplified by all the other polymers prepared in this study, and another example, **PL6**, is summarised below using the same method as outlined above. For polymers **PL5** and **PL8** the same basic method is used, however there is no nitrogen within the ligand on which to base the initial estimate of substitution. In these cases the NMR data are used to make this initial estimate, and then the theoretical microanalysis results for C and H, for the best-fit NMR results, are

compared to the actual data obtained in order to obtain the composition of the end product.

2. Determination of the Composition of **PL6**

- The average composition of **CP1** was determined to be:

$$Me_3Si(OSiMe_2)_{27.5}(OSiMe(H))_{3.5}OSiMe_3$$

Due to the amount of **L15** added to the reaction mixture, a maximum of 2 moles of **L15** can add to the polymer during the reaction. The excess of **L18** should ensure all remaining Si-H sites (1.5 per mol of polymer) are capped by **L18**. The composition of **PL6** will be of the idealised form below:

$$Me_3Si(OSiMe_2)_{27.5}(OSiMe(H))_{3.5-m-n}(OSiMe(\mathbf{L15+H}))_m(OSiMe(\mathbf{L18-H}))_nOSiMe_3$$

- Microanalysis of **PL6**, after purification to remove any excess ligand and catalyst residue, gave the following C, H, N composition:

$$\%\ C = 41.0, \%H = 3.1, \%N = 8.16$$

The theoretical amount of nitrogen is calculated using the formula below, and the best theoretical matches to the experimental result above are listed in Table 20 below.

$$\%\ N = ((14.0067 \times 3) \times m) / (M_w\ \mathbf{PL6}\ \text{calculated for the amount of substitution, Z})$$

Table 20: Theoretical Best-Fit C, H, N Analysis for PL6

m	n	Mass of N in Polymer	M_w	%N	%C	%H
2	1	84.0	2713	3.10	36.5	8.69

- NMR 2 shows no evidence of alkenylated substrate. All peaks for **L15**, **L18** and **CP1** protons are highlighted and labelled as per the diagram below.

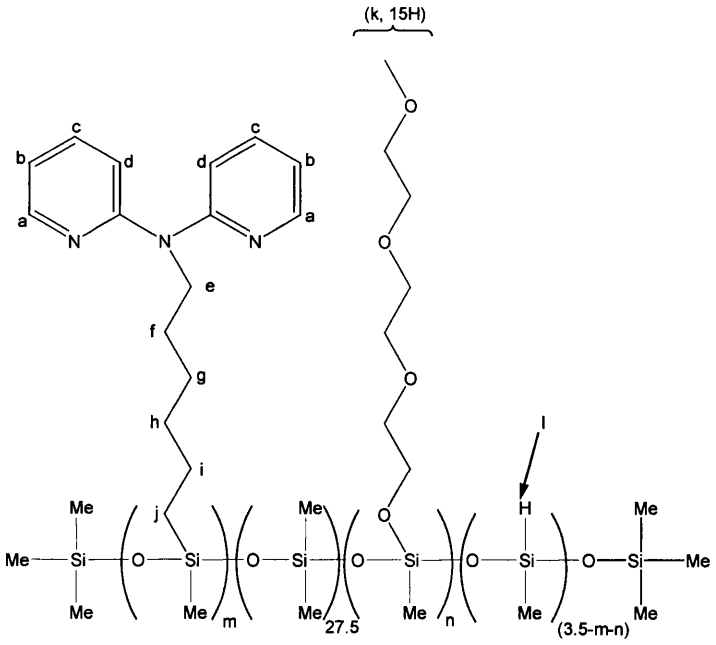

- The number of protons that each peak represents can be calculated using the method below.

Peak 1 - Number of Protons = 8 x m

Peak 2 - Number of Protons = (2 x m) + (15 x n) + (1 x (3.5 - m - n))

Peak 3 - Number of Protons =

(10 x m) + (3 x (3.5 - m - n)) + (3 x m) + (3 x n) + (6 x 27.5) + (2 x 9),

where (10 x m) is the number of f, g, h, i, and j protons, (3 x (3.5 - m - n)) is the number of -OSi**Me**(H)- protons, (3 x m) is the number of -OSi**Me**(L15+H)- protons, (3 x n) is the number of -OSi**Me**(L18-H)- protons, (6 x 27.5) is the number of -OSi$\mathbf{Me}_2$- protons, and (2 x 9) the number of –Si$\mathbf{Me}_3$ terminating group protons.

- The ratios of protons within each peak can be assessed using the integrals on NMR 2. The ratios are:

1.00 (Peak 1) : 1.16 (Peak 2) : 11.38 (Peak 3)

Using the theoretical best-fit from the C, H, N microanalysis, formulas and integral ratios above, a best fit can be identified and thus the composition of **PL6** defined. Table 21 highlights the theoretical number of protons for each peak.

Table 21: Theoretical Proton Ratios for PL6

M	n	Theoretical Number of Protons for Amount of Substitution, m and n		
		Peak 1	Peak 2	Peak 3
2	1	16	19	204.5

These theoretical values are compared to the actual values given in NMR 2 in Table 22.

Table 22: Comparison of Theoretical and Actual Proton Ratios for PL6

m	n	Ratio Peak 1 : Peak 2		Ratio Peak 1 : Peak 3		Ratio Peak 2 : Peak 3	
		Theory	Actual	Theory	Actual	Theory	Actual
2	1	1 : 1.16	1 : 1.22	1 : 11.38	1 : 12.8	1 : 9.81	1 : 10.5

- Minor changes in m and n cause the proton ratios to move radically. A polymer with 3 of the 3.5 reactive Si-H sites (86%) substituted by **L15** (2 sites, 57%) and **L18** (1 site, 29%) is the best fit from both the microanalysis and NMR data collected.

Figure 43: NMR 1

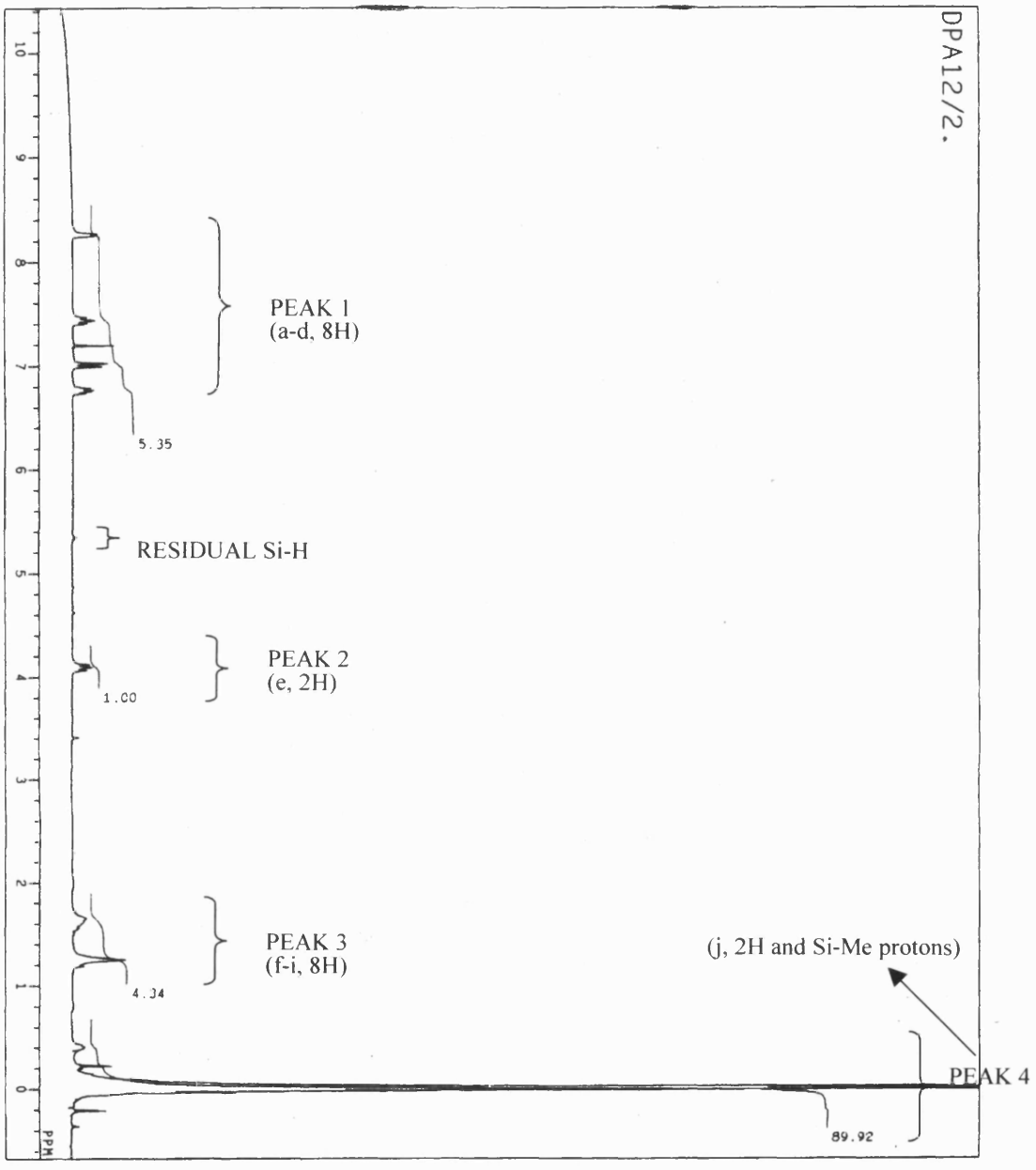

Figure 44: NMR 2